2016

Expression of Zinc Fingers and Homeoboxes 2 (Zhx2) and Zhx2 Target Genes in Multiple Tissues of Wild-Type and Zhx2 Knockout Mice

Minen Al-Kafajy
University of Kentucky, minen2006@gmail.com
Author ORCID Identifier:
http://orcid.org/0000-0003-3217-848X
Digital Object Identifier: https://doi.org/10.13023/ETD.2016.515

STUDENT AGREEMENT:

I represent that my thesis or dissertation and abstract are my original work. Proper attribution has been given to all outside sources. I understand that I am solely responsible for obtaining any needed copyright permissions. I have obtained needed written permission statement(s) from the owner(s) of each third-party copyrighted matter to be included in my work, allowing electronic distribution (if such use is not permitted by the fair use doctrine) which will be submitted to UKnowledge as Additional File.

I hereby grant to The University of Kentucky and its agents the irrevocable, non-exclusive, and royalty-free license to archive and make accessible my work in whole or in part in all forms of media, now or hereafter known. I agree that the document mentioned above may be made available immediately for worldwide access unless an embargo applies.

I retain all other ownership rights to the copyright of my work. I also retain the right to use in future works (such as articles or books) all or part of my work. I understand that I am free to register the copyright to my work.

REVIEW, APPROVAL AND ACCEPTANCE

The document mentioned above has been reviewed and accepted by the student's advisor, on behalf of the advisory committee, and by the Director of Graduate Studies (DGS), on behalf of the program; we verify that this is the final, approved version of the student's thesis including all changes required by the advisory committee. The undersigned agree to abide by the statements above.

Minen Al-Kafajy, Student

Dr. Brett T. Spear, Major Professor

Dr. Ken Fields, Director of Graduate Studies

EXPRESSION OF ZINC FINGERS AND HOMEOBOXES 2 (ZHX2) AND ZHX2 TARGET GENES IN MULTIPLE TISSUES OF WILD-TYPE AND ZHX2 KNOCKOUT MICE

DISSERTATION

A dissertation submitted in partial fulfillment of the requirements
for the degree of Doctor of Philosophy in the
College of Medicine at the University of Kentucky
By

Minen Al-Kafajy

Lexington, KY

Director Dr. Brett T. Spear, Professor of
Microbiology, Immunology and Molecular Genetics

Lexington, Kentucky

ABSTRACT OF DISSERTATION

EXPRESSION OF ZINC FINGERS AND HOMEOBOXES 2 (ZHX2) AND ZHX2 TARGET GENES IN MULTIPLE TISSUES OF WILD-TYPE AND ZHX2 KNOCKOUT MICE

The Spear lab has had a long-standing interest in gene regulation in the liver during development and disease. Several years ago, these studies identified a novel transcriptional regulator called Zinc fingers and homeoboxes 2 (Zhx2), which is a member of a small family that includes Zhx1 and Zhx3. All Zhx proteins contain two amino-terminal C2-H2 zinc fingers and four or five carboxy-terminal homeodomains. Previous studies indicate that Zhx proteins can form homodimers and heterodimers with each other.

Zhx2 regulates numerous hepatic genes, including *alpha-fetoprotein* (*AFP*) and *H19*. Genes controlling lipid and cholesterol homeostasis are also regulated by Zhx2. More recently, our lab has found that a number of *Cytochrome P450* (*Cyp*) genes and *Major urinary protein* (*Mup*) genes are also targets of Zhx2. The BALB/cJ mouse substrain contains a natural hypomorphic mutation in *Zhx2*, and the aforementioned targets are dysregulated in the livers of adult BALB/cJ mice. Recently, our lab developed mice that contain a floxed allele of *Zhx2*. By crossing these mice with transgenic mice that express the Cre recombinase in all tissues or in hepatocytes, we can knock-out Zhx2 expression in all tissues or solely in the liver, respectively.

Much of the research in the Spear lab has focused on the role of Zhx2 in liver gene expression during development and several models of liver disease. However, we have found that Zhx2 is ubiquitously expressed in all adult mouse tissues. The first part of my

project has utilized whole-body Zhx2 knock-out mice to investigate the role of Zhx2 in various tissues, including kidney, brain, small intestine, liver, salivary and lacrimal glands. These studies indicate that some, but not all, previously identified Zhx2 targets are also regulated by Zhx2 in non-liver tissues. I have also carefully evaluated whether the absence of Zhx2 results in increased perinatal lethality and/or altered postnatal growth. These studies suggest that postnatal growth of male Zhx2 knock-out mice is delayed compared to wild-type Zhx2 littermates.

My second project examined subcellular localization of Zhx proteins. To accomplish this, GFP-Zhx fusion proteins were expressed in transfected cells. Zhx1 and Zhx2 localized to the nucleus whereas transfected Zhx3-GFP proteins were found in both the nucleus and cytoplasm. Moreover, when Zhx3-GFP was co-transfected with Zhx2, Zhx3-GFP was found strictly in the nucleus. This data suggests that interactions between Zhx proteins could alter protein localization. I employed bioinformatics tools to predict the 3D structures of Zhx1, Zhx2, and Zhx3 monomers, homodimers, and heterodimers.

KEYWORDS: Zhx2, Gene regulation, Bioinformatics, Protein structure, Knock-out mice.

Minen Al-Kafajy
Student's Signature

12/9/16
Date

EXPRESSION OF ZINC FINGERS AND HOMEOBOXES 2 (ZHX2) AND ZHX2 TARGET GENES IN MULTIPLE TISSUES OF WILD-TYPE AND ZHX2 KNOCKOUT MICE

By

Minen Al-Kafajy

Dr. Brett T. Spear, Ph.D
Director of Dissertation

Dr. Ken Fields, Ph.D
Director of Graduate Studies

12/9/16
Date

ACKNOWLEDGMENTS

I would like to thank my mentor Dr. Brett T. Spear, PhD for providing me with the opportunity to work in his lab, and guiding me during the course of my graduate career. I am honored to have Dr. Martha Peterson, PhD, Dr. Michael Kilgore, PhD, Dr. Joe McGillis, PhD and Dr. Subbarao Bondada, PhD on my committee, with much of appreciation for their valuable inputs and insightful suggestions to improve my research. I would like to thank Dr. Nancy Webb, PhD for her willingness to serve as an outside examiner. I am extremely grateful for Dr. Patricia Bond, PhD in the graduate school for the encouragement that she has provided throughout my study period.

I would like to acknowledge the Higher Committee for Education Development (HCED) in Iraq for their financial support during my course work at the University of Kentucky, which would have not been possible without their assistantship. I am extremely grateful for the Microbiology department for providing me with an excellent education and training.

This work would not have been achieved without the support and encouragement from my mother Layla. Finally, I would like to thank my lovely children Ali and Jenna for their patience and encouragement during my PhD career.

TABLE OF CONTENTS

LIST OF TABLES

LIST OF FIGURES

CHAPTER 1

Introduction

Liver

The liver is the largest internal organ in mammals and performs multiple activities, including numerous metabolic functions, energy and glycogen storage [1]. The liver synthesizes numerous serum transporter proteins, such as albumin and transthyretin, as well as clotting factors. Furthermore, the liver eliminates toxic compounds by detoxification (i.e., ammonia) or excretion via bile acids (i.e., bilirubin). Energy storage is one of many essential liver functions and is accomplished, in part, by hepatocytes that engulf, synthesize, esterify, oxidize and export fatty acids [2]. The fetal liver is the site of embryonic hematopoiesis [3]. The liver is the main site for the synthesis and storage of triglycerides, an important energy source and major component of cellular membranes. Triglycerides are only one type of lipid synthesized in the liver. Others include lipoproteins such as very low density lipoprotein (VLDL), low density lipoproteins (LDL) and high density lipoproteins (HDL), which transport phospholipids and cholesterol [2]. Although grouped together, each form has unique metabolic properties. Variation in normal VLDL, LDL and HDL serum levels are strongly correlated with cardiovascular disease (CVD) [4]. Due to the huge clinical impact of CVD, there is considerable interest in the regulation of hepatic genes that control lipid homeostasis. Numerous transcription factors, including Peroxisome proliferator activated receptors (PPARα, β, γ1, and γ2), sterol regulatory element binding protein-1c (SREBP-1c), hepatic nuclear factors (HNF-4α and γ), retinoid X receptor (RXRα), liver X receptor (LXRα) ultimately regulate liver lipid homeostasis [5].

The liver has a distinctive structure that allows it to carry out its functions. Hepatocytes, which carry out a majority of liver functions and comprise roughly 60% of liver cells and 90% of liver volume, are arranged in small repeating hexagonal structures termed lobules [6]. Each of the six corners of this lobule contains a portal triad, comprised of the hepatic artery, portal vein, and bile duct. Oxygen- and nutrient-rich blood enters the

lobule via the hepatic artery and portal vein, respectively. The blood exists via the central vein, located at the center of the lobule. Trafficking of compounds occurs as the blood passes by hepatocytes [7]. An interesting aspect of liver biology requires this unique architecture. Certain liver functions take place in hepatocytes surrounding the portal triad (periportal hepatocytes) whereas other functions occur solely in hepatocytes surrounding the central vein (pericentral hepatocytes, a phenomenon termed zonal gene regulation or metabolic zonation. This separation of function allows the liver to carry out opposing metabolic activities. [1], [6], [8].

Since the liver receives blood with nutrient and possibly microbes from the gut and is therefore continually exposed to pathogens, it is considered an important immunological organ. Besides mediating metabolism, hepatocytes can initiate liver immunological tolerance. Although naïve T-lymphocytes in non-lymphoid organs generally do not interact with resident cells, hepatocytes, with their cytoplasmic extensions, and liver sinusoidal endothelial cells (LSEC) can interact with resident and circulating naïve CD+8 T-cell filopodia [9]. Furthermore, in inflammatory conditions, mouse hepatocytes might function as antigen presenting cells (APCs) via MHC class II proteins to activate CD4+ T-cells [10]. Kupffer cells, another type of non-parenchymal cell, are resident liver macrophages that reside mainly in the sinusoid periportal regions of the liver [11]. Kupffer cells can prevent inflammation by inhibiting pathogen growth and eliminating excess dietary materials [12]. Furthermore, the liver contains a considerable number of resident natural killer (NK) cells, also known as pit cells, that sensitize and kill the tumor cells and thus serve as an innate immune monitoring mechanism in the liver [13].

The adult liver is largely a quiescent organ with a very low level of cellular proliferation. However, one of the unique and marvelous liver features is the ability to rebuild itself after damage, a phenomenon termed liver regeneration. In situations of modest injury, it is thought that normally quiescent hepatocytes can proliferate to restore liver mass. Repeated or more severe injury leads to the activation of a small population of bipotent stem cells, termed oval cells, that reside in the canals of Hering surrounding the portal triad [14]. Oval cells can give rise to hepatocytes and bile duct epithelial cells and are critical for normal regeneration [15]. Moreover, liver stellate cells, which store vitamin

A [16], secrete growth factors and cytokines necessary for liver function [7]. Stellate cells, also called lipocytes or vitamin A storing cells [16], are non-parenchymal cells that comprise about 15% of liver cells and reside in the subendothelial space. Upon repeated injury and through stimulation with TGF-beta or other cytokines, stellate cells differentiate into activated collagen-producing fibroblasts and contribute significantly to liver fibrosis. Liver fibrosis as well as other chronic liver diseases are characterized by accumulated extracellular matrix protein. Progressive fibrosis can lead to liver cirrhosis, liver cancer, and liver failure. Due to the importance of liver disease in the United States, scientists are trying to develop effective anti-fibrotic drugs to treat liver disease [17].

Some liver proteins must be synthesized at all times, whereas other proteins are required during specific developmental time points or in response to various stimuli. Since changes in proteins occur primarily at the transcriptional level, there is considerable interest in liver gene regulation. Genes encoding alpha-fetoprotein (AFP), and the long non-coding RNA H19 are highly active in the fetal liver but are silenced after birth, and provide an experimental system to investigate postnatal gene repression in the liver.

Alpha-Fetoprotein (AFP)

The AFP gene, which encodes a 65 kDa glycosylated serum transport protein, is a member of the albumin gene family that is located on chromosome (Chr) five or four in mice and humans, respectively [18]. This small gene family contains albumin (Alb), Alpha-albumin (AFM), Vitamin D-binding protein (DBP) [19], and alpha-fetoprotein related gene (Arg) [20]. AFP, along with the other albumin family members, is expressed mainly in the liver although AFP is also expressed abundantly in the extraembryonic yolk sac [21]. AFP and Alb are expressed early in the fetal liver, whereas DBP is activated later in the fetal liver; AFM and Arg are activated after birth. AFP is the only albumin family member that turns off after birth since Alb continues to be highly expressed in the adult liver. [22, 23]. AFP assist in mammals fetal development [24]. AFP is the most abundantly expressed gene in the fetal liver but exhibits a dramatic (10^5-fold) decrease in expression after birth [18]. While normally off in the adult liver, the AFP gene is reactivated during liver regeneration and often in hepatocellular carcinoma (HCC). Since AFP can be readily detected in the

blood, its reactivation during HCC makes AFP an important cancer marker [25]. Moreover, AFP has been used as gestational marker during pregnancy as elevated maternal AFP levels may indicated neural tube defects in the developing fetus [26]. Furthermore, maternal serum AFP can be used as a test for Downs syndrome through the first trimester of pregnancy [27]. The mechanisms that govern changes in AFP expression during development and disease are not fully understood.

H19

The H19 gene is located on Chr 7 and Chr 11 in mice and humans, respectively. H19 is among the first long non-coding RNA (lncRNA) to be discovered; these classes of RNAs are transcribed by RNA polymerase II and polyadenylated but do not encode a protein and therefore function as a noncoding RNA. Another unique feature of H19 is that it is imprinted, i.e., an autosomal gene that is expressed solely from the maternal- or paternal-derived chromosome. In the case of H19, only the maternal H19 allele is expressed. H19 is expressed abundantly in multiple fetal tissues such as liver, heart, skeletal muscles and gut. H19 is repressed after birth in the liver [28, 29] and kidney [30] but continues to be expressed in the adult skeletal muscle and the heart. H19 encodes for the micro-RNAs miR-675 3p and miR-675 5p, both of which play a role in skeletal muscle differentiation and regeneration [31].

H19 expression is localized in the fetal ureteric bud branches and epithelial elements of kidney metanephros. Pregnant mice exposed to a high glucose diabetogenic diet leads to decreased fetal kidney H19 expression [30]. Furthermore, H19 is hypermethylated and silenced in kidneys of Wilm's tumor protein and frequently activated in HCC [29]. These data suggest that H19 might play role in normal liver and kidney function.

Methionine adenosyltransferase (Mat) genes

Mat2a is a member of Mat gene family that also includes Mat1a. Mat2a gene is expressed in the fetal liver, but is gradually silenced after birth and replaced by the related Mat1a, which is expressed in the mature liver. The Mat genes have been a point of scientific

interest after Kinsell *et al* in 1947 noticed that liver cirrhosis patients have lower methionine metabolism [32], [33].

Adults human and mouse Mat1a, in the liver, encodes for the methionine adenosyl transferase enzymes MATI and MATIII, while Mat2a, in the kidney, code for MatII [34] [35]. MATI, II and III control cellular levels of S-adenosyl methionine (SAMe, also called AdoMet), derived from methionine. Since SAMe is the sole methyl donor for DNA methylation, these MAT enzymes are important in epigenetic gene regulation. Mat1a can function as a source of propylamine that is important in polyamine biosynthesis [33], [34].

MATI, MATIII and SAMe levels are reduced in non-alcoholic fatty liver disease (NAFLD). Mat1a knock out mice exhibit altered lipid homeostasis due to the severe reduction in MATI, MATIII and SAMe levels [36]. A second group independently reported that Mat1a knock out mice are more prone to develop fatty liver at twelve weeks old and had suffered oxidative stress and liver steatosis at two years of age [33]. Moreover, Mat1a knockout mouse developed liver tumors after treatment with the hepatotoxin carbon tetrachloride (CCl_4) [37]. The importance of Mat1a is not limited to the hepatic tissue, SAMe is found in the kidney, brain and skeletal muscles [38]. Additionally, SAMe levels are dramatically reduced in HepG2 and Huh7 human hepatoma cell lines and human HCC [35]. Worth notable that Mat2a is expressed in the fetal liver, switch off after birth, and reactivated in liver regeneration and HCC [39].

Zinc fingers and homeoboxes 2 (Zhx2)

As mentioned previously, AFP is expressed in the fetal liver and silenced at birth. Consistent with this, serum AFP levels also decrease dramatically within the first month after birth. However, serum AFP levels in adult BALB/cJ mice are 5-20 fold higher than other mice strains, including the closely related BALB/cBOM and BALB/cBy substrains [40]. Further studies indicated that this was an autosomal recessive trait governed by a locus on mouse Chromosome 15 that was called Alpha-fetoprotein regulator 1 (Afr1) [41]. Adult liver AFP mRNA levels are also elevated in BALB/cJ mice, suggesting that this increase was due to a change in gene expression. In addition, the H19 and Glypican 3

(Gpc3) genes also appear to be targets of Afr1 since they are also expressed in the fetal liver, silenced at birth, and elevated in adult liver of BALB/cJ mice [42]. Interestingly, AFP, H19 and Gpc3 are frequently activated in HCC.

Using a positional cloning strategy, the Spear and Peterson labs identified Zhx2 as the gene responsible for the Afr1 phenotype. The Zhx2 gene in BALB/cJ mice contains a natural hypomorphic mutation induced by the insertion of an endogenous retroviral element into the first Zhx2 intron that dramatically reduces, but does not eliminate, Zhx2 expression. Expression of a Zhx2 transgene in the livers of BALB/cJ mice restored normal postnatal silencing of AFP, H19 and Gpc3, confirming that the Zhx2 mutation was responsible for continued expression of these genes in adult BALB/cJ liver [43].

The Zhx2 gene contains four exons with the entire protein coding region found in exon 3. The mouse and human Zhx2 proteins are 836 and 837amino acids in length, respectively and are 87% identical [44]. Zhx2 has two amino-terminal C2-H2 zinc fingers (ZFs) and four carboxy-terminal homeodomains (HDs) [6]. The ZFs may be involved in nucleic acid binding or protein-protein interactions whereas the HDs likely function as DNA binding sites [45]. It has been hypothesized that Zhx2 functions as a transcriptional repressor [46] [47]. However, recent studies suggest that Zhx2 positively regulates elongation of very long chain fatty acids like 3 (Elovl3) [48] and Major urinary proteins (MUPs) in the liver [Chapter 3 and Spear unpublished data].

Zhx2 belongs to a small gene family that also includes Zhx1 and Zhx3, although Zhx2 has a predicted proline-rich region adjacent to HD2,which is hypothesized to be involved in DNA binding [6].

Zhx1

The Zhx1 and Zhx2 genes are closely linked on mouse Chr 15 and human Chr 8, which raises the possibility that a genetic duplication created both genes. Zhx1 was identified for the first time in 1996 by immunoscreening of a bone marrow stromal cell line. Zhx2 consists of 873 amino acids [49]. Moreover, Zhx1 has been detected in a yeast 2-hybrid search for proteins that have a potential to bind the activation domain A subunit

of NF-YA [46, 50]. NF-YA is an ubiquitous transcription factor that bind to specific genes promoters and activate their transcription [51]. Zhx1 has two C2H2 zinc fingers on the amino-terminal end and five homeodomains (HD)s on the carboxy-terminal end. Northern blot analysis indicates that Zhx1 is ubiquitously expressed with highest expression in the brain, moderate expression in the testis, kidney, and liver and very low expression in the skeletal muscle and heart [49]. It has been reported that ZHX1 functions as a transcriptional repressor [52], and ZHX1 and NF-YA are thought to govern transcription of genes critical for cell growth and differentiation [46].

Zhx3

Zhx2 and Zhx1 are proposed to heterodimerize in the cytoplasm with Zhx3, another member of Zinc finger and homeodomain family. Zhx3 is located on human chromosome 20 and mouse chromosome 2. Zhx3 was discovered in a yeast 2-hybrid screen for Zhx1-interacting proteins. Zhx3 is ubiquitously expressed and codes for a 956 amino acid protein that can homodimerize or heterodimerize with NF-YA [47]. Human ZHX3 is a predicted 104.7 kDa protein with a 5.68 PI [47].

It has been hypothesized that Zhx3 functions as an important regulator in podocytes. Translocation of Zhx3 from the cytoplasm to the nucleus has been observed in rat and human podocytes and correlates with expression of the Wilms tumor (WT) gene that is crucial for normal kidney function and a marker for kidney tumor and focal sclerosis disease. Downregulating ZHX3 correlates with WT1 downregulation and increased levels of nuclear ZHX1 and ZHX2 in the kidney [53].

Northern blot of various tissues has revealed that human ZHX3 is highly expressed in the testis and kidney. It is also expressed moderately in the skeletal muscles and at low but detectable levels in the heart, brain, placenta, lung, liver, pancreas, spleen, thymus, prostate, ovary, small intestine, colon and nearly negligible level in the leucocytes [47].

Kidney

The kidney is a glandular organ consisting of sieves to purify the urine. The kidney keeps the body hydrated by controlling electrolytes, water, sodium, renin, and vasoactive eicosanoids. The kidney carries out several metabolic functions and helps maintain blood pressure [54] via filtrating and reabsorbing molecules [55]. The kidney consists of hundreds of thousands of structural unites termed nephrons. Every nephron unit consists of one glomerulus which is a sieve structure with pores allowing molecules with a molecular mass <50 kDa to be excreted to the urine and the highest mass molecules reabsorbed back to the plasma [56].

Zhx2 role in cancer

One million individuals are diagnosed with HCC every year worldwide [57]. HCC is characterized by poor prognosis in its advanced stages and is the third most fatal and the fifth most widespread cancer [58]. HCC early-stage diagnosed patients are usually treated by liver resection or transplantation. Unfortunately, HCC is usually diagnosed at the advanced stages; subsequently, the only treatment option left is using chemotherapy such as doxorubicin and cisplatin. Regrettably, advanced HCC stages are highly resistant to these drugs [59]. HCC is induced by a number of altered genetic and epigenetics pathways including p53, PTEN, PI3K, AKT, mTOR, Ras, Raf, MAPK and miRNAs [60-62]. Moreover, the palindromic group GPC (5'-CG-3') ZHX2 promoter have been observed to be hypermethylated in HCC tumor as compared to neighboring non-tumor region and HepG2 cell line using methylation sensitive restriction finger printing (MSRF) [63]. This suggests that methylation-dependent silencing of Zhx2 is associated with HCC.

Even though the roles of Zhx2 in hepatocellular carcinoma (HCC) have not been well addressed yet, preliminary data, along with previous publication, have shown ZHX2 as a potent regulator of HCC proliferation in vitro and in vivo by inhibiting hexokinase II, cdc25C and AFP [43, 46, 64]. ZHX2 transcriptional repressor activity has been hypothesized to be linked to the presence of a proline-rich region in HD1 and a dimerization domain located between amino acids 263 and 446 [46]. Zhx2 reduces HCC cell proliferation and growth of xenograft tumors in nude mice by downregulating Cyclins

A and E expression. Knocking down ZHX2 in the SMMC7721 cell line has shown an increased cell proliferation rate. However, knocking down Cyclin A and E was partially able to reduce the proliferation, suggesting that ZHX2 might positively regulate tumor suppressor genes or negatively regulate oncogenes [65].

Zhx2 in cardiovascular disease

BALB/cJ mice exhibit a cardioprotective trait called *Hyplip2*, which is characterized by low cholesterol and lipoprotein levels and small plaque lesion size when placed on a high fat diet as compared to the other mouse strains. Transgenic studies performed by Dr. Jake Lusis in collaboration with our lab have identified Zhx2 as the gene responsible for the *Hyplip-2* trait [66]. In addition, BALB/cJ mice have high tendency to have increased fatty liver and liver damage when placed on a high fat diet. This study indicates that Zhx2 is essential for liver lipid trafficking [Clinkenbeard Thesis, 2011].

Cardiovascular disease (CVD) and non-alcoholic fatty liver disease (NAFLD) are rising complications in the United States and western countries [67]. NAFLD is a metabolic disorder characterized by the accumulation of lipoprotein triglycerols (TAGs) in hepatocytes. Long-term consequences of NAFLD include advance staged steatohepatitis, cirrhosis and in rare cases can lead to hepatocellular carcinoma [68]. The primary cause of mortality in patients is when NAFLD progresses to non-alcoholic steatohepatitis (NASH) and ultimately to HCC, even in the absence of cirrhosis if NASH patient has insulin resistance [69]. Notably, insulin-resistant adipocytes will release more fatty acids into the circulation and eventually will cause CVD [70]. Numerous genes have been examined for their link to atherosclerosis in GWAS study, one of those genes located on chromosome 8q24 was proposed to be related to carotid intima media thickness. This genetic locus is occupied by Zhx2 [67]. A second independent GWAS study also identified Zhx2 as a candidate of carotid intima media thickness and plaque (CIMT) marker in Caucasians [71]. Unfortunately, the mechanism by which Zhx2 correlates with CIMT has not been characterized, but the relationship with lipid homeostasis is intriguing.

Earlier studies and data from our lab indicate that Zhx2 is important for lipid homeostasis and regulates critical metabolic genes [72] [Creasy Thesis, 2015]. Zhx2

upregulates Elovl3 and represses Lipoprotein lipase (Lpl), which control liver lipid metabolism [48]. Liver-specific Zhx2 knock out mice ($Zhx2^{\Delta hep}$) have elevated Lpl and decreased Elovl3 compared to wild type mice. Unexpectedly, this study did not detect differences in weight gain between $Zhx2^{\Delta hep}$ and $Zhx2^{wt}$ mice [Creasy Thesis, 2015]. In conclusion, there is a correlation between Zhx2, cardiovascular disease, liver disease, and lipid homeostasis.

Zhx2 role in normal brain function

The brain consists of a complex of neuronal and non-neuronal support cells that carry on delicate and unique functions such as feeling, intelligence, memory and social behavior. The mouse brain is comprised of seven main parts, including the olfactory bulb, cerebral cortex, hippocampus, midbrain, cerebellum, medulla and hypothalamus [73]. The mouse brain has an amazing and complex gene expression pattern that enables regions of the brain to interact and carry out its numerous functions [74].

Zhx2 has been reported to contribute to neural progenitor differentiation in the developing cerebral cortex via binding to the cytoplasmic domain of Ephrin-B. Ephrin-B, a member of type I transmembrane proteins family that includes B1, B2 and B3 which bind to the tyrosine kinase of ephrin B receptor (EphB) [75]. Zhx2 is expressed in the ventricular (VZ) and subventricular (SVZ) zone of the mouse cortex where neuronal progenitor cells reside. Ephrin-B is localized within the same location in the cortex with Zhx2. Overexpression of Zhx2 in *vitro* cultured cortical neural progenitors caused reduction in the number of neuronal and basal progenitor cells [76]. Taken together, these data suggest that Zhx2 functions as a repressor of neuronal differentiation in the cortex.

DNA sequence analysis of Native American and British patients suffering from asymmetric Parkinson disease, revealed mutations in ZHX2 along with other genes regulated by miR-4277 [77]. Moreover, ZHX2 is upregulated in the dorsal root ganglia (DRG) of rat after intraplantar complete Freunds' adjuvant (CFA) treatment [78]. GWAS studies for Autism Spectrum Disorder (ASD) patients has shown an association with

inherited copy number variation (CNV) of the ZHX2 locus [79]. Taken together these data provide further evidence that Zhx2 might be required for normal brain function.

Major urinary proteins (Mups)

Psychiatric disorder studies have utilized BALB/cJ mice as an experimental model system, since they exhibit behavioral anomalies compared to C57BL/6J mice [80]. For example, BALB/cJ mice have a small brain size [81]. Moreover, BALB/cJ male mice are more aggressive than BALB/c and its substrains, including BALB/cH and BALB/cBYJ. BALB/cJ mice have decreased level of urinary Mup proteins compared to the closely related BALB/cBy strain [82]; studies from our laboratory indicate that this is due to the natural Zhx2 mutation in BALB/cJ mice. Quantitative trait locus mapping identified three loci that control aggressive behavior in BALB/cJ male mice, including one that maps near the D15Mit46 microsatellite that resides close to Zhx2 gene [83]. These data raise the possibility that Zhx2, possibly through its control or Mup expression, might have a role in mice social behavior.

Mups belong to a gene family comprised of roughly 20 genes and 20 pseudogenes that are highly related and tightly linked on mouse chromosome 4. Mups are expressed at low levels at birth, but their expression increased gradually and reaches a stable level several months after birth [84] [Jiang et al, submitted]. Mup proteins are acidic with low molecular weight (20 kDa) and are structurally similar [85]. The liver is the major site of Mup synthesis; Mups are the most abundantly expressed genes in the adult mouse liver and comprise 5-10 % and 1-2% of total mRNA in male and female liver, respectively [86]. Mups circulate in the blood to be secreted via the kidney to the urine, where they are the most abundant proteins [87]. Male rat liver, but not female liver, expresses α2μ-globulin as the rat version of major urinary protein via 20 closely related genes and also excreted to the urine [88].

Mups are hypothesized to possess two functions. Mups are members of the lipocalin family and as such have been proposed to function as pheromones (odorants) transporters. Pheromones are compounds produced by one animal and target to other animals as a way

to communicate. The lipocalin protein tertiary structure includes eight beta sheets organized in a β-barrel with one open end. Both the amino (N) and the carboxy (C) terminal ends have α-helices [89], which give Mups a hydrophobic pocket (glove) that enables Mups to bind pheromone ligands [90]. The pheromones will be sensed by neurons located in the vomeronasal organ (VNO) and main olfactory epithelium (MOE), the chemosensory structures of the nasal cavity, so the animal can smell and communicate with other members of the same species. Lipocalins can bind pheromones and stabilize their scent in nature [91]. The second proposed function of MUPs are to act as pheromones themselves [92].

Group I Mups (old name of liver Mups) were reported to be produced in the liver and their mRNAs levels are 30% higher in lean mice as compared to the obese (ob/ob) mice. The ob/ob mice RNA level can be partially increased if the animal is treated with rosiglitazone, an antidiabetic drug that target insulin sensors. On the other hand, circulating group I Mups are reduced in genetically diabetic obese mice. In conclusion, animal nutrition influences Mup RNAs and proteins levels [93].

Steroid hormones also play a role in determining Mup RNA and protein levels. Mups are sexually dimorphic in the liver as males express more MUPs than females. Lacrimal glands (LG), another site of Mup expression, are similar to the liver in that males express Mups at higher levels than females. One percent of lacrimal gland mRNAs are Mups [94]. Although, Mups are sexually dimorphic in the liver and lacrimal glands, there is no sexual dimorphism in the submaxillary, sublingual, and parotid gland (salivary glands; SG) between male and female. Female Mups are responsive to hormonal regulation; treating females with testosterone or thyroxin or growth factor will elevate Mup RNA and protein levels to almost equal to males, although this response is not observed in hypophysectomized female mice, indicating the importance of the pituitary gland in sexual dimorphic Mup expression [95]. The transfer of castrated male mice as intruders to a cage of different male mice will not initiate a fight, as the intruder will not excrete aggressiveness pheromones [92]. *Little* mice have a natural mutation in their growth hormone (GH) gene that leads to dwarfism and other developmental delays. Interestingly,

little mice have low Mup levels which can be restored by GH treatment [96]. These findings demonstrate the importance of hormones in regulating MUPs.

One challenge in studying Mups is the irregular terminology that has been used by different groups. For example MUPI, MUPII, MUPIII are terms used to describe liver MUPs, while MUPIV and MUPV are referred to MUPs that have been synthesized in the lacrimal and submaxillary gland, respectively [97]. On the other hand, isolated urinary Mups were initially called MUP1, 2 & 3 [98] [85]. The new nomenclature is based on cloning of Mup genes of C57BL/6J mice that can be separated into two classes. Class A Mups include Mup1, Mup2, Mup18, Mup24, Mup25, Mup26 and 5 Class A pseudogenes. Class B Mups (refered to as MupU in this dissertation) consist of Mups 3-17 and are >97% identical and also include a number of pseudogenes. Mups 3, 8, 17, 24 and 25 are expressed in the liver, while MUPs 1, 3, 18, 24 and 26 are expressed in the submaxillary glands. Mup1 and Mup18 are also called MUPIV and MUPV, respectively [99].

Although functional Mup genes are not present in human, menstrual synchrony is an example of a pheromone-induced involuntary change in women. Specific compounds resembling pheromones, synthesized by female axillary glands, can enhance the production of luteinizing hormone of the recipient women and change their cycle time. Similar observation have also been detected in females rats [100]. Humans have chemoreceptive structures containing bipolar neurons that resemble VNO in mice, located in the base of nasal cavity to sense pheromones [101]. Curiously, Mups prompt female mouse ovulation through triggering nerves in the VNO [102]. For these reasons, our lab has an interest in studying the expression and function of Mups.

Salivary and lacrimal glands

The salivary glands (SG), which are exocrine glands, are a crucial organ in oral health that synthesize saliva, mucous and serous [103]. Saliva performs numerous functions such as buffering and neutralizing mouth bacterial acid, lubricating, supplementing teeth with essential mineral since it contains calcium, phosphate and proteins. Impairment in saliva production (hyposalivation) can cause dental disease and

mouth mucosal membrane abnormalities [104]. Salivary gland malfunctions can be induced by Sjogren's Syndrome, certain medications, salivary gland tumors, stones that block the SG ductal system or radiotherapy [103, 105, 106]. Rodents (mice and rats) resemble human salivary glands by comprising of three ocular pairs termed parotid, submandibular and sublingual glands, the last two of which are blanketed by a common fascia and separated by connective tissue. Although, human parotid glands are similar to mice in having pure serous acini (singular acinus) bordered by myoepithelial cells, they are different in that humans have adipocytes that are absent in mice. Submandibular glands are composed of serous and mucous acinar cells in human and only serous cells in mice. Sublingual glands are unique in structure by having mucous cells in the middle surrounded by serous cells [103]. Rodent salivary glands secret saliva into the glandular bodies at the bottom of the oral cavity via excretory channel lining by ductal cells, which are the predominant salivary glands cells along with the acinar cells. Acinar cells synthesize proteins and primary saliva [107].

In contrast, lacrimal glands (LGs) are binary almond-shaped glands that secret tears to the cornea to facilitate vision. LGs distorted by age or disease such as Sjogrens' syndrome, an autoimmune disease, can lead to dry-eye disease (DED) [108]. Dartt 1989 has stated that LGs mainly consist of secretory acinar cells which compromised 80% of the total forming cells, however, LGs also contain ductal and myoepithelial cells. LGs defend the eye via producing the antibacterial substances such as lysozyme and lactoferrin. Moreover, LGs maintain eye health by synthesizing and excreting growth factor α (GF α) [109]. Stimulation of LG secretion can be initiated by eye afferent sensory nerves and growth factors [110].

Small intestine

Duodenum, jejunum and ileum are grouped in the term small intestine, while caecum, colon and rectum comprise the large intestine. Both form a tube covered by a single columnar epithelium layer. The small intestine (SI), along with the large intestine and the stomach form the gastrointestinal tract that mainly digests and absorbs nutrition. The small intestine is unique within the gastrointestinal tract by exclusively having villi.

Villi are finger-like extensions located on the inner side of the small intestine and are crucial for food digestion and absorption. The small intestine is comprised of three layers organized from the inside cavity to the outside termed the mucosa, propria and muscularis mucosa. The main cells in the small intestine are neuroendocrine cells, Paneth cells, goblet cells, dendritic cells, eosinophil and the adsorptive enterocytes [111]. Crohn's disease and ulcerative colitis are two well-known types of small intestine disease [112].

CHAPTER 2

Materials and Methods:

Mice:

Following our lab approved protocol of the Institutional Animal Care and Use Committee (IACUC), mice were maintained in the Division of Laboratory Animal Research facility (DLAR), and kept in micro-isolator cages. The mice were provided with food and water ad libitum and were on a 14-10 hr light-dark cycle.

Generation of whole body Zhx2 knock out mice ($Zhx2^{ko}$):

The KnockOut Mouse Project (KOMP) at the University of California at Davis generated C57Bl/6 mice having Zhx2 exon 3 floxed with loxP site. Exon 3 is the only protein-coding exon of the Zhx2 gene. These mice were maintained on a C57BL/6 background. Floxed mice were bred to Actin-cre transgenic mice (E2α-cre, Jackson Laboratory # 003724) to obtain mice which had deleted Zhx2 in all cells, including germ cells. Mice with the deleted Zhx2 exon 3 (Zhx2-) were bred to mice with wild-type Zhx2 (Zhx2+) to obtain Zhx2+/- offspring. F1 intercrosses were performed to obtain Zhx2+/+ (referred to as $Zhx2^{wt}$), Zhx2+/- ($Zhx2^{het}$) and Zhx2-/- ($Zhx2^{ko}$).

Genotyping:

1. Each mouse pup, around 13-days old was given an ear tag for identification; the ear punch, along with approximately 1mm tail snip cut were placed in 1.5 ml Eppendorf tube.
2. Genotyping was accomplished by quick DNA extraction assay as described by Jackson lab (www.jax.org) with a few modifications.
3. 100 µl of 50 mM NaOH was added to ear punch and the tail piece.
4. The mixture was heated at 95 ºC for 10 min in dry bath.
5. 25 µl of 50mM Tris-HCL pH 5.5 was added to the tubes.
6. The remaining material was pelleted via centrifugation at 12,000 RPM for 5 min.

7. Four µl of the DNA (supernatant) was mixed with 6 µl of the primers (table 2.1) and 10 µl of 2x my tag red mix (bioline # 25043).
8. The mixture was placed in semi-quantitative RT-PCR thermocycler machine and underwent the following protocol: 1 cycle of initial denaturation at 95ºC for 1 min, followed by 35 cycles of denaturation at 95 ºC for 15s, annealing 52 ºC for 15s, and extension at 72 ºC for 10s.
9. In 0.5 ml tube, 10 µl of the PCR product was mixed with 3 µl of 6x loading dye (Fermentas).
10. The mixture was vortexed and separated on 1% w/v agarose (SeaKem) gel, along with 100 bp ladder. The bands were visualized by UV light and the picture was captured using images software.

Mice euthanizing and tissue collection:

150 mice (males and females) were retained on normal diet for 60 days with weekly weight measurements. On day 60, 25 males (6 $Zhx2^{wt}$, 13 $Zhx2^{het}$, 6 $Zhx2^{ko}$) and 24 females (7 $Zhx2^{wt}$, 10 $Zhx2^{het}$, 7 $Zhx2^{ko}$) were food-fasted for 5hrs (9:00 am-2:00 pm); however, they had access to water. Mice were euthanized using CO_2 and dissected to collect liver, kidney, small intestine, brain, salivary gland, lacrimal glands and spleen. The tissues were quickly frozen in dry ice and stored at -80 ºC for subsequent RNA isolation. The left side of the brain was placed in OCT media, quickly frozen in liquid nitrogen and kept at -80 ºC for future immunohistochemistry staining.

Tissue homogenization and RNA extraction:

Principle:

RNAzol contains phenol and guanidine that bind with high affinity to DNA, proteins, polysaccharides, facilitating the isolation of RNA of high purity.

Procedures:

1. Frozen mice tissues were obtained from -80 ºC freezer and placed in dry ice to avoid tissue thawing during the homogenization.
2. RNA was extracted using 1ml of cold RNAzol (Molecular research center # RN190), that was added to approximately 50 mg of the tissue kept in 1.5 micro centrifuge tubes.
3. The tissue was homogenized manually on ice using plastic douncer for (5-15 min) depending on the tissue type. The plastic douncer was cleaned and autoclaved after each sample.
4. Since the brain has more fat than other tissue, preparing high quality brain RNA was difficult. To overcome this problem, brain homogenate was placed in dry ice to freeze the fats into a white-yellowish layer on the tube sides. Quickly, the aliquots were transferred to different tubes to remove fats.
5. 0.4 ml of sterile ddH_2O was added to the samples, each tube was mixed vigorously by hand for 30 seconds, vortexed, then all the samples were stored for 15 min at 4ºC.
6. The samples were spun down at 12,000 RPM in microcentrifuge tubes for 15 mins. Approximately 1ml of supernatant was added to 1ml isopropanol, mixed together, vortexed and stored at 4ºC for 15-30 mins.
7. Following centrifugation as before, the supernatant was decanted and the RNA pellets were washed twice with 95% ethanol. Pellets were slightly air dried for no more than 10 mins to avoid over drying and resuspended in 30-50 µl of DNAase/ RNAase free sterile ddH_2O proportional to the pellet size.
8. The RNA purity and concentration were determined using spectrophotometer (Nanodrop) at 260 nm. A260/280 ratio was around 2 was used to confirm the purity of RNA samples.

cDNA synthesis:

Principle:

Reverse transcriptase via random primer scheme will generate cDNAs from the RNA template.

Procedure:

1. 10x RT buffer, 25x dNTP (100mM), 10xRT random primers, Multiscribe TM reverse transcriptase, RNase inhibitor and nuclease free H_2O were added in this order to the individual thermal tubes. All these reagents were provided by the high capacity cDNA reverse transcription kit purchased from Thermofisher scientific (# 4368813).
2. 1µg of RNA was added to the thermal tubes and reverse transcribed into 20 µl of cDNAs after placed in the thermal cycler (PCR) at 25 ºC for 10 min, 37 ºC for 120 min, 85 ºC for 5 min, then hold at 4 ºC until being transferred to -20 ºC fridge for long term storage.

Real-Time qPCR (RT-qPCR)

Gene sequences were obtained from Ensemble (useast.ensemble.org) or the NCBI website and entered into Primer Quest Tool (Integrated DNA technologies; IDT) to blast and design primers and predict the perfect melting temperature. Caution was taken in designing primers to rule out homology to other genes. 1µl of cDNA was amplified via RT-qPCR (Bio-Rad; Hercules, CA) following the manufacturer's protocol after being mixed with 2x SYBR green PCR supermix (Bio-Rad # 720001784) and appropriate primers (Table 2.2). The ribosomal L30 protein mRNA (L30) was used to normalize most of the samples since it was the most stable reference gene. Aliquots were analyzed and quantified using CFX96 touch^{Tm} real-time PCR detection system, evaluated and normalized to the control (L30) by CFX manager software (Bio-Rad) or Excel (Microsoft). All tissue analysis experiments were done in duplicate.

Cloning:

Oligonucleotides obtained from IDT were used to clone each of mouse Zhx1, Zhx2 and Zhx3 in pcDNA. In order to tag Zhx1, Zhx2 and Zhx3 DNAs with GFP sequence, the

cDNA of each of these genes were subcloned from pcDNA into GFP using appropriate restriction enzymes. The constructs were verified via DNA sequencing (ACGT, Inc.).

Ligation:

The following equation was used to estimate the amount of the vector and the insert:

$$\left\{\frac{\text{200 ng of the vector x X kb of the insert}}{\text{Y kb of the vector}}\right\} \text{ x } 3/1 = Z$$

X= The insert length (kb)

Y= The vector length (kb)

Z= The total insert mass required for the ligation

1. The appropriate amounts of vector and insert, based in the calculation shown above, were added to Eppendorf tube to a total volume of 3.5 µl.
2. 5 µl of 2x Rapid ligation buffer (c671A- Promega) was added to the reaction.
3. 1 µl of T4 DNA ligase (M180 Promega) was used to ligate either the cohesive or blunt ended of 5'-phosphatase and the 3'-hydroxyl groups of the two independents DNA strands.
4. 0.5 µl of nuclease free ddH_2O was added to the tube.

Transformation

1. An aliquot of JM109 *E. coli* bacteria was removed from the -80 ºC freezer and thawed on ice.
2. In 1.5 ml Eppendorf tube, 100 µl of the cells was added and followed by 10 µl of the plasmid (ligation product see above) and mixed.
3. The mixture was incubated for 30 min on ice.
4. The cells were heat shocked at 45 ºC for 45 seconds.
5. The tubes were placed on ice for 2 min.

6. 900 µl of SOC media was added and tubes were placed in a shaker at 37 ºC for 1 hour.
7. During the 1 hour incubation, ampicillin plates were removed from the cold room (Combs building) and placed in 37 ºC incubator.
8. After 1 hour, the cells were centrifuged at 12,000 RPM for 1 min.
9. The supernatant was discarded and the cells were resuspended with the remaining media.
10. The ampicillin plates were quickly passed over the flame to get rid of the extra water on the agar and the lid surfaces.
11. Metal loop was placed at 45 angle over the flames until it turned red, then cooled down at the plates edges. The loop was used to culture the cells over the plates.
12. The plates were incubated overnight at 37 ºC for colonies to grow.
13. The plates were stored in the 4 ºC fridge for up to 3 months.

Mini-preparation:

Reagents:

1. Solution I: 50 mM sucrose, 25 mM Tris pH 8, 10 mM EDTA
2. Freshly made Solution II: 20 µl of 10 N NaOH, 100 µl 1% SDS and 0.9 ml of H2O

Procedure:

1. In 5 ml tubes, 1.5 ml of autoclaved LB media were added.
2. Random colonies were picked up from the ampicillin plates and added to the LB media.
3. The tubes were placed overnight in the shaker at 37 ºC.
4. Aliquot of the cells suspension was transferred to the 1.5 ml Eppendorf tubes and cells were pelleted at 14,000 RPM for 1 min.
5. The supernatant was aspirated and the cells were resuspended in 100 µl of cold (4ºC) plasmid preparation Solution I and mixed by inversion, vortexing and pipetting.

6. 200 µl of freshly made solution II were added to the tubes and mixed gently by inversion approximately for 40 seconds.
7. 130 µl of 3M of potassium acetate (KoAc) was added and mixed via inversion until white precipitate was observed.
8. In the hood, 150 µl chloroform: IAA were added and samples were shaken vigorously for 30 seconds.
9. The mixture was centrifuged at 14,000 RPM for 3 min. In this step white interface was appeared.
10. Using toothpick, the white precipitate was removed. Then, carefully, the lower organic phase was pipetted and discarded.
11. 1 ml of 100 % ethanol was added to the aqueous phase and vortexed for 30 seconds.
12. Sample was centrifuged for 3 min at 14,000 RPM. Supernatant was decanted, leaving small but visible white pellet.
13. 100 µl of ddH2O was added to the DNA and vortexed to dissolve the DNA.
14. 100 µl of 7.5 M NH4OAC (4 ºC) was added and mixed very well.
15. Centrifugation at 14,000 RPM for 3 min was used to precipitate the pellet.
16. The supernatant was removed and 95% ethanol was added to the pellet, mixed and spun for 1 min at 14,000 RPM.
17. The supernatant was discarded, the pellet was slightly air dried and resuspended in 50 µl ddH2O.
18. After verifying the DNA concentration and purity using spectrophotometer at 260 nm, the DNA was digested with restriction enzymes and send to ACGT for sequencing to confirm the constructs. After confirmation, large-scale plasmid preps were obtained using Maxi-prep.

Maxi-prep:

1. 400 ml of LB media supplemented with ampicillin (50 µg/ml) was used to grow bacteria overnight at 37 ºC while shaking.
2. The next day, the bacteria were centrifuged at 4 ºC, 5000 RPM for 20 min. Qiagen Maxi purification kit was used to purify the plasmid according to manufacturer's instructions.

3. UV Spectrophotometry at 260 nm was used to determine DNA purity and concentration.

Cell Culture:

Primary hepatocytes and liver perfusion:

Principal:

In order to study the events under conditions that mimic the normal liver, primary hepatocytes were isolated from adult liver using the following protocol

Reagents:

1.**Perfusion buffer I**: 40 ml of 1x Hanks' Balanced Salt Solution (HBSS) without Ca++, Mg++ was supplemented with EGTA (100 uM made by adding 20 µl in 40 ml).

2. **Perfusion buffer II**: 40 ml of 1xHBSS (with Ca++, Mg++) was supplemented with phenol red 10 mg/L natural red (7:1000) dilution and (0.02 g) of collagenase (Sigma type IV collagenase #C-5138) was added 30 min before perfusing the mouse liver. The solutions were mixed and filtered into new sterile 50 ml tubes.

Procedure was performed as described in Froh *et al* 2003 [113], with few modification:

The VWR pump was primed at 10 RPM (Cat#54856-070), using the VWR silicone tube (Cat# 60985 .125x,25x63 wall) and sterile phosphate buffer saline (PBS).

1. The perfusion I and perfusion II (freshly made) were prewarmed in the water bath at 37 ºC.
2. 8-10 weeks $Zhx2^{wt}$ mouse was weighed and anesthetized with Avertin that consist of 2,2,2-Tribromoethanol 97% (Aldrich # T48402-5G) plus 2-methyl-2-butanol (Aldrich # 240486), via single intraperitoneal injections in amount proportional to the mouse weight (20 µl/ one-gram weight) during the procedure.
3. The mouse was examined for non-responsiveness to physical stimuli.

4. Vertical incision was made after the animal median to open the abdominal cavity.
5. Needle was inserted in the mouse portal vein. This was a tedious step, because the needle could easily move. Therefore, the needle was manually held in place until the end of the perfusion.
6. The inferior vena cava was cut immediately after starting the perfusion.
7. After the liver was perfused via perfusion I at speed 3 ml/ min, the mouse liver was enlarged and changed its color as clue for successful perfusion. 10 min later, the liver was perfused using perfusion II 5-6 ml/min for no more than 5 min.
8. The liver was tested for successful digestion using blunt end of the scissor to press on the liver lobes.
9. Then, the liver was removed from the mouse and placed in a sterile 60 mm petri dish with 10 ml cold DMEM media.
10. Caution was taken to avoid cells lysis by performing the following steps at 4ºC unless otherwise noted.
11. In the hood, the liver capsule was torn by forceps and gently aspirated up and down by a large pore pipette to break the tissue and release the cells.
12. 100 µm cell strainer was used to filter the cells into sterile 50 ml tube. The undigested and connective tissues were discarded.
13. Then, the liver suspension was centrifuged at 25,000 RPM for 3 min using cold centrifuge.
14. The supernatant, contained non parenchymal cells (Kupffer and stellate cells), were collected and frozen at -80ºC until time of assay, while the pellet contained mainly hepatocytes (parenchymal cells) was re-suspended in 30 ml cold DMEM (HI Glucose Penn/Srept) and washed by centrifugation at 25,000 RPM for 3 min.
15. After repeating washing steps for 2 more times, 100 µl of the primary hepatocytes were removed and diluted by adding 800 µl PBS and 100 µl of 0.5% Trypan blue stock. 10 µl of the mixture were examined under the microscope to estimate the cells number and viability. The viable cells will not take the blue color while the dead cells will appear as blue cells under the microscope.
16. Approximately $2x10^5$ were seeded on coated six wells plates for 24hr, then treated per experiments.

Primary hepatocytes and cell lines culture:

Cryopreserved human hepatoma (Hep3B), human cervical cancer (HeLa) and human embryonic kidney cells (HEK293) cells lines were obtained from American Type Culture Collection (ATCC) (Manassas, VA), aliquoted, stored at liquid nitrogen. To establish cultures, a single aliquot of frozen cells was thawed. In a T25 flask, the cells were cultured in either Dulbecco's minimal eagle's media (DMEM, media tech, Corning Cellgro or life Technologies) supplemented with 10% fetal bovine serum (FBS) (Fisher #03-600-511), 1% L-glutamine and 1% Pen-Strep (Gibco) for HEK-293 cells, HeLa and primary hepatocytes or in RPMI 1640 (RPMI 1640) with 10% FBS for Hep3B cells. All the media, trypsin and the phosphate buffer saline (PBS) were preheated to 37ºC before use. Caution was taken to avoid cells contamination by performing all the cells handling in clean hood inside the tissue culture facility. All cells were maintained in an incubator set at 37 ºC and 5% CO_2.

Transient transfections:

Autoclaved coverslips were placed into 12 well sterile plates. Cultured cells were trypsinized, resuspended in media, counted with 20x objective and $2x10^5$ cells per well were seeded in the top of the coverslip. Then, the plate was shaken right-left, up-down to gain even cells distribution on the coverslip. After 24 hrs later, cells were at ~70-80% confluency. Cells were transfected using TurboFect (Thermoscientific #R0533) following manufacturer's instructions except primary hepatocytes were transfected with lipofectamine2000 (Life Technologies #1683449/11668-019). DNA (µg) to transfection reagent (µl) ratio was either 1:2 for Zhx1-GFP, Zhx3-GFP, Zhx2 or 0.5:2 for GFP and Zhx2. However, a 2:5 ratio was used to transfect the primary hepatocytes with all the plasmids in this study. Each plasmid alone was mixed with serum free media in Eppendorf tube and added to the wells. All the transfection assays were performed in duplicate and repeated at least four times. After the cells were incubated with plasmids for 48hrs, cells were fixed (except the primary hepatocytes; see below).

Cells fixation was performed as described in a protocol from Dr. Vivek Rangnekars' lab (University of Kentucky, Lexington, KY) with several modifications:

All the following steps were performed in the hood and at room temperature unless otherwise noted.

1. The media was aspirated; the cells were rinsed once with warm 1x PBS to removed unattached cells.
2. In the hood, cells attached to the coverslips were fixed by gently pipetting 500-600 µl of 5% formaldehyde on the wells edges and incubated for 2-5 min.
3. Formaldehyde was aspirated and the cells were washed twice via gently pipetting warm 1x PBS.
4. The wells were slightly air-dried.
5. Glass slides were previously washed with detergent, wiped with 70% ethanol and Labeled.
6. 2 µl of DAPI H-1000 supplemented with anti-fade mounting medium (Vector Laboratories, Burlingame, Canada) was placed on the labeled slide.
7. Since DAPI is light-sensitive; subsequent steps were carried out away from direct light.
8. The coverslip was carefully picked up from the wells and inverted gently on the top of the DAPI drop with caution to avoid making bubbles.
9. The coverslip edges were mounted using colorless nail polish and air dried for 10 min.
10. The slides were frozen at -20 ºC until being examined using fluorescent microscope (Olympus 1x70). Pictures were captured and analyzed using pro-capture 7 software.

Prediction of the proteins 3 dimensional structures and binding sites:

Full length mouse Zhx1, Zhx2 and Zhx3 proteins sequences were obtained from NCBI server (https://www.ncbi.nlm.nih.gov), and were entered in the I-TASSER website http://zhanglab.ccmb.med.umich.edu/I-TASSER/) [114]. I-TASSER is maintained by the

Zhang lab University of Michigan (Ann Arbor, Michigan). I-TASSER was used to predict 5 simulations of each of Zhx1, Zhx2 and Zhx3 proteins tertiary structures organized from the highest to the lowest scores. The highest score model of each protein was visualized by PyMOL software (The PyMOL Molecular Graphics System, Version 1.8 Schrödinger, LLC) and entered into the ZDOCK server to predict the homodimer and heterodimer forms and the predicted protein domains. ZDOCK is endorsed and certified by Zhiping Weng's lab (ZLAB) at the University of Massachusetts medical school (Worcester, Massachusetts) [115].

Statistical analysis:

GraphPad prism version 7 software for Windows, La Jolla California USA, www.graphpad.com, was used to average and plot the data groups in this study with standard deviation. In addition to performing student t-test between two groups, prism was used ANOVA to analyze three or more groups followed by multiple comparison using Tukey's test. Chi-square analysis was employed to compare the mouse survival percentages compared to the expected results. Significant data denoted by star as the following: $0.01 \leq *p < 0.05$; $0.001 \leq **p < 0.01$; $***p < 0.001$.

Table 2. 1 Genotyping mice primer sequences

Gene	Sequence Forward	Reverse
Zhx2	GGACCGAATCTCACTATTTAACTCA	AGGCTGGCAGTGGGTTAGAAA
		ACAACGGGTTCTTCTGTTAGTCC

Table 2.2. Quantitative real time polymerase reaction (PCR) primer sequences

Gene	Forward	Reverse
Zhx1	ACACTTGGGAACCCCCACGACA	AGTGTCATCAGGATTAGTTGGGCCC
Zhx2	AGGCCGGCCAAGCCTAGACA	TGAGGTGGCCCACAGCCACT
Zhx3	CCAAGTGCTCCTGAGGCCAGC	AGCATCCCAGACTGGCCGGT
L30	ATGGTGGCCGCAAAGAAGACGAA	CCTCAAAGCTGGACAGTTGTTGGCA
Sfrs	CTCGCACAGAGTACAGACTTAT	TTGCGTCCCTTGTGAGCATCT
Afp	ATCAGTGTCTGCTGGCACGCA	GGCTGGGGCATACATGAAGGGG
H19	GGAGAGGACAGAAGGGCAGT	GGAGAGGACAGAAGGGCAGT
Cyp2a4	GGAAGACGAACGGTGCTTTC	TTCCCAGCATCATTCTAAGA
Mat1a	GGCTGAAATTCCTCAAGGAGTCA	GGGCAAAGAGGGAGATAGCG
Stat5a	CGCTGGACTCCATGCTTCTC	GACGTGGGCTCCTTACACTGA
Hnf4a	GGAAGCTGTCCAAAATGAGCG	ATGTCGCCATTGATCCCAGAG
Stat5b	GGACTCCGTCCTTGATACCG	TCCATCGTGTCTTCCAGATCG
Wt	ATGACCTCCCAGCTTGAATG	GTTCTCACTCTCATACCCTGTG
Shp	TCTGGAGCCTTGAGCTGT	AGGGCTCCAAGACTTCACAC
Lmx1b	GCAAACAAGACTACCAACAGC	AGCAGAAACAGCCCAAGTG
Mup1	AGAAGCTACTTCCAAGGGACAG	TGTCAGAGGCCAGGAGAATAGA
MupU	CAGAAGAAGCTAGTTCTACGGG	GAGGCCAGGATAATAGTATGCC
Mup18	TGACCTATCCAATGCCAATCG	ACAGAACTTGTCACCCCATG
Mup24	GTGCTGCTGCTGTGTTTGGG	TGTCAGTGGCCAGCATAATAGTA
Mup25	GCTTCTGCTCCTGTGTTTGGA	CATCAGAGGCTT CAGCAATAGAA
Mup26	GAGTGCACCGAAATGACTTTG	TCCCCATCTTTTTCGTTAATGAGA
Mcpt2	GCAGTCCCACAACATCAAAAT	CAGGTAATAGGAGATTCGGGTG

CHAPTER 3:

Expression of Zhx2 target genes in multiple adult tissues of Zhx2+ and Zhx2- mice

Previous studies in our laboratory examined the expression of Zhx2 target genes in the liver using different mouse models. These studies initially used BALB/cJ mice, which have a hypomorphic Zhx2 mutation that results in elevated AFP expression in the adult liver [43]. This mutation is specific to BALB/cJ since Zhx2 is expressed normally in the highly related strains BALB/c/BOM and BALB/cBy [40]. When placed on a high fat diet, BALB/cJ mice have lower serum lipid levels and reduced atherosclerotic plaques compared to other mouse strains; a trait that has been mapped to a locus called *Hyperlipidemia 2* (*Hyplip2*) [116]. In collaboration with the lab of Jake Lusis, we have shown that the Hyplip2 phenotype in BALB/cJ mice is due to the Zhx2 mutation [48]. In contrast to the cardiovascular phenotype, BALB/cJ mice have increased liver lipid accumulation and liver damage compared to other mouse strains when placed on a high fat diet [Creasy, Clinkenbeard and Spear, unpublished]. These data indicate that Zhx2 is hepatoprotective in mice on a high fat diet. [48].

In studies with BALB/c and BALB/cJ mice, our lab identified Cyp8B1 [Clinkenbeard Thesis, 2012], lipoprotein lipase (Lpl) and Elongation of very long chain fatty acids like 3 (Elovl3) [Ren Thesis, 2012] as targets of Zhx2 in the liver. Using liver-specific Zhx2 knock-out mice $Zhx2^{\Delta hep}$ that were developed in our lab, we found that Zhx2 also regulates sex-biased expression of Cytochrome p450 steroid 15α-hydroxylase (Cyp2a4). These studies suggest cross-talk between Zhx2 and methionine adenosyltransferase 1a (Mat1a), and Hepatocyte nuclear factor 4a (Hnf4a) and signal transducer and activator of transcription 5a and 5b (Stat5a and Stat5b) [Creasy Thesis, 2015]. To date, most of the research on Zhx2 has focused on the liver since many Zhx2 target genes are expressed primarily in this organ. However, Zhx2 is expressed in multiple tissues, suggesting that Zhx2 might regulate genes in tissues other than the liver. The major focus of this Chapter is to analyze expression of Zhx2 and the highly related Zhx1 and Zhx3 genes in multiple tissues and the expression of potential Zhx2 target genes in whole-body Zhx2 knock-out ($Zhx2^{ko)}$ mice.

Numerous hepatic genes exhibit sex-biased expression and are controlled by pituitary hormones, including growth hormone (GH), Luteinizing hormone (LH) and follicle stimulating hormone (FSH) [117]. Examples include the Cytochrome P-450 (Cyp) enzymes, a large family comprised of 57 genes and 58 pseudogene in humans [118] and 102 genes and 88 pseudogenes in mice [119]. Cyps are expressed in many organs but expressed at the highest level in the liver. Cyps are clinically important since they metabolize a number of pharmaceutical drugs. Many Cyps, which metabolize drugs and non-xenobiotics [118], are expressed differently in males and females. For example, females express Cyp2A4 [120] while males express Cyp2d9 in the liver. Cyp2A4 is also expressed in the kidney and lungs [121]. Human kidneys express other CYPs, including CYP2B6 and CYP3A5, the latter has clinical importance since it metabolizes certain tyrosine kinase inhibitors such as dasatinib [55].

Beside metabolizing xenobiotics, CYP4A catalyzes the ω-hydroxylation of excess long chain fatty acids, producing dicarboxylic acid [122]. Moreover, CYP4A is important for renal vascular and tubular function and controls blood pressure by forming hydroxyeicosatetraenoic acis (20-HETE). In C57BL/6 mice, Cyp4a12a is expressed four-fold higher in males than in females. In contrast, Cyp4a10 and Cyp4a14 are highly expressed in females. Males and female kidneys do not appear to express Cyp4a12b [123]. Besides the liver and kidney, some mouse Cyps are expressed in the duodenum and jejunum [121]. Using Zhx2$^{\Delta hep}$ mice, our lab demonstrated that sexually dimorphic Cyp2a4 expression was regulated by Zhx2. Specifically, low Cyp2a4 expression in adult male liver is controlled, at least in part, by Zhx2 since expression of this Cyp increases in the male liver of Zhx2$^{\Delta hep}$ male mice [Creasy Thesis, 2015]. These studies led us to consider whether Zhx2 might control expression of Cyps and other genes in the kidney and small intestine of males and female mice.

As mentioned earlier, studies in our lab suggest a possible relationship between Zhx2 and Stat5 proteins. Two Stat5 isoforms (Stat5a and Stat5b) exist in the liver, both of which are controlled by growth hormone. Stat5a regulates liver metabolism and inflammatory gene expression in female mouse liver but does not play a role in the male mouse liver [124]. Stat5b controls genes in the male mouse liver and knocking it out causes

a developmental delay [124]. Interestingly, elevated levels of Janus kinase 2 (Jak2), Stat1, Stat3, Stat5a and Stat5b have been observed in hyperglycemic diabetic rat kidney [125]. These data have led us to consider whether Zhx2 could regulate Stat5 in the liver, kidney, brain and small intestine.

Several investigators have studied Zhx1, Zhx2 and Zhx3 in various organs such as liver, brain, kidney and blood [43], [65],[126], [76], [127]. Independent investigations have revealed two genes, Wilms tumor (Wt) and Lim homeobox transcription factor 1 beta (Lmx1b), to be inversely correlated with Zhx2 in *in vitro* experiments [53].

Wilms tumor (Wt1), a transcription factor, is expressed highly and specifically in kidney podocytes. Wt1 is a zinc finger protein that plays a role in transcriptional and posttranscriptional events. It is important for normal kidney function [53] and has been correlated with hematological disorders [128]. Mutations in Wt1 in the mouse germline results in embryonic lethality due to development of Wilms tumor and abnormalities in kidney, genital system, mesothelium, heart and lungs [129]. Interestingly, Wt1 is expressed in the fetal liver but silenced after birth. However, its expression is increased in liver fibrosis, hepatitis and cirrhosis. Moreover, an inverse correlation exists between Wt1 and HNF4a in the liver [130]. Given that, Zhx2 is involved in repressing several genes that are usually expressed in the fetal liver and shut down after birth and that Zhx2 is ubiquitously expressed [43], I hypothesized that expression of Wt1 could be altered in $Zhx2^{ko}$ liver and kidney in comparison to $Zhx2^{wt}$ mice.

The *Lmx1b* gene is involved in the normal development of brain, limbs, eyes, and kidney. Mouse studies indicate that vertebrate dorsal-ventral pattering is driven by Lmx1b, in partnership with Wnt signaling. Lmx1b knock-out mice have dorsal skin on their paws with ventral skin on both dorsal and ventral sides; this is due to the lack of Lmx1b that is usually expressed in the dorsal mice mesenchyme [131]. In human, mutated LMX1B causes developmental defects in a disease termed nail-patella syndrome [132]. Podocyte-specific Lmx1b knock-out mice have scattered actin cytoskeleton in podocytes [132]. Lmx1b is moderately downregulated after Wt1 downregulation in the Puromycin aminonucleoside nephrosis (PAN) plus Passive Heymann nephritis (PHN) rat model [126].

Shp is the orphan nuclear receptor encoded by the *Nrob2* gene. It belongs to the nuclear receptor family but does not possess a DNA binding domain and therefore must interact with other nuclear receptors but does contain at least one putative ligand binding domain. Shp functions as a repressor of numerous liver functions such as bile acid, cholesterol, lipid and glucose metabolism [133]. SHP usually functions as a repressor in the liver by heterodimerizing with nuclear receptors and block their interactions with co-activators and enhancing binding with co-repressors. For example, glutathione-S-transferase pull-down experiments have shown that SHP can bind and repress the liver X receptor (LXR) [134].

Using *in situ* hybridization, the *SHP* gene has been localized to chromosome 1p36.1 in humans and chromosome 4 in mice. Human and mouse *SHP* genes are 77% conserved and contain two exons spanning 1.8 and 1.2 kilobase (Kb), respectively. In human, SHP is expressed in the fetal liver and fetal adrenal gland [135], and adult liver [136], spleen and small intestine [135]. Since H19 in the liver is repressed by Zhx2 [43] and by Shp [136], I hypothesized that a correlation could be exist between Zhx2 and Shp.

In summary, analysis of gene expression patterns in multiple organs of whole-body Zhx2 knock-out mice might shed light on the role of Zhx2 in regulating genes that influence behavior, cancer and cardiovascular disease. Examination of several known targets of Zhx2 expressions in hepatic and non-hepatic tissue will provide a better understanding of Zhx2 function.

Results

AFP levels are increased in the adult liver of whole body $Zhx2^{ko}$ mice:

Our lab previously identified AFP and H19 as targets of Zhx2 in the liver due to the observation that BALB/cJ mice have increased AFP and H19 in the adult liver and decreased Zhx2. Introducing a liver-specific Zhx2 transgene into BALB/cJ mice results in normal AFP and H19 silencing after birth [43]. Therefore, to validate the use of whole body $Zhx2^{ko}$ mice for my studies, I first analyzed hepatic expression of AFP and H19 in male and female adult liver of $Zhx2^{wt}$ and $Zhx2^{ko}$ mice. First, RT-qPCR conformed the absence of Zhx2 in $Zhx2^{ko}$ liver (Figure 3.1). Consistent with BALB/cJ mouse data, AFP levels are significantly increased ($p=0.04$). Although not statistically significant due to small sample number, H19 mRNA levels were increased in liver of $Zhx2^{ko}$ mice compared to $Zhx2^{wt}$ mice ($p=0.06$; Figure 3.1). Increasing the mouse sample size would likely result in the H19 difference to reach significance. This expression of AFP and H19 mRNA levels validate the use of $Zhx2^{ko}$ mice as a model to examine Zhx2 target gene expressions.

Zhx1 is expressed in multiple organs of male and female $Zhx2^{wt}$ mice:

We used RT-qPCR to evaluate Zhx1 mRNA levels in the kidney, small intestine (SI), salivary gland (SG) and lacrimal gland (LG) of age matched male and female $Zhx2^{wt}$ mice. In males, Zhx1 mRNA levels were found to be the highest in the kidney and lowest in the SG and LG; Zhx1 levels in the SI were slightly higher than the SG (Figure 3.2 A). In females, Zhx1 expression was higher in SI compared to the kidney and SG (Figure 3.2 B). In fact, females have significantly higher Zhx1 mRNA levels than males in the SI. These results raise the question whether Zhx1 is a female-biased gene in SI (Figure 3.2 C).

Zhx2 is ubiquitously expressed in adult male and female $Zhx2^{wt}$ mice:

Utilizing Northern blot analysis, our lab previously demonstrated that Zhx2 is ubiquitously expressed in the brain, thymus, heart, lung, liver, spleen, gut, kidney, muscles and testis [43]. I used RT-qPCR to confirm these results in five organs of adult $Zhx2^{wt}$ male and female mice. In males, the highest Zhx2 expression was detected in the kidney and SI.

Liver Zhx2 expression levels were low and almost equal to that seen in brain. The lowest expression was detected in the SG and LG (Figure 3.3 A). The highest Zhx2 expression level of female mice were observed in the SI and it is slightly higher than SI expression in male. Female Zhx2 expression in the liver, kidney and brain show similar expression levels, while the lowest Zhx2 levels were in the SG (Figure 3.3 B). In conclusion, although not statistically significant, male kidney has slightly higher Zhx2 levels than the female kidney, while SI Zhx2 levels are slightly higher in females than in males (Figure 3.3 C).

Zhx3 is expressed in several organs of Zhx2^{wt} mice:

In order to quantify and compare the expression level of Zhx3 in various mice organs, I performed RT-qPCR analysis in several male and female organs. Zhx3 was expressed at substantially higher levels in the kidney of male mice compared to the SI, SG and LG (Figure 3.4A). Females kidney exhibited higher Zhx3 levels than SI (Figure 3.4B). Zhx3 mRNA levels were almost equal between male and female kidney and small intestine (Figure 3.4C).

Mups are candidate Zhx2 targets in the liver:

Our lab previously demonstrated that BALB/cJ mice have a hypomorpic mutation in the Zhx2 gene. To test whether BALB/cByJ and BALB/c substrains have normal Zhx2 genes, I used RT-qPCR to analyze gene expression in the adult livers of these 3 closely related substrains. My analysis indicates that Zhx2 is expressed normally in BALB/cByJ and BALB/c mice, while BALB/cJ mice, as expected, express very low Zhx2 levels. Consistent with this, adult liver AFP and H19 mRNA levels were low in mice that express Zhx2. MUP24, which we have found to be positively regulated by Zhx2, is lower in BALB/cJ mice compared to the other two groups (Figure 3.5).

Mups are upregulated in the SG of Zhx2^{ko} male mice:

Several groups have examined expression of Mups in the liver, SG and LG [86, 87, 95, 97]. BALB/cJ mice secrete low Mup levels [82], which are known to influence male behavior such as aggression. Genetic analysis has identified one locus that regulates this

behavior, at least in part, near the D15Mit46 microsatellite marker [83]. Zhx2 is also close to this marker. Preliminary data has shown that Zhx2 is a positive regulator of Mup expression in the liver [Spear unpublished data]. Since several Mups are also expressed in the SG, we examined Mup expression in the SG of $Zhx2^{wt}$ and $Zhx2^{ko}$ mice.

Mup1 and Mup18 are expressed in the SG [97]. Therefore, I performed RT-qPCR to analyze expression of these Mups in the longitudinal half of mouse SG that consists of parotid, submandibular and sublingual gland. I confirmed that Zhx2 is absent in SG of $Zhx2^{ko}$ male mice. Notably, I found that Mup1, Mup18, Mup24 and class B Mups (MupU) were increased in the absence of Zhx2. No difference was observed for Mup25 (Figure 3.6). This inverse relationship between Zhx2 and Mup expression in SG was quite surprising since Mups are positivity regulated by Zhx2 in the liver.

MUPs are upregulated in the $Zhx2^{ko}$ female mice SG:

A significant negative correlation was observed between Zhx2 and Mup1 and Mup18 but not Mup24 or Mup25 in the female salivary gland (Figure 3.7). Expression of Mup1, Mup18 and Mup25 are nearly equal in male and female SG, while Mup24 expression is higher in female SG; Class B Mups were not tested in female. This data suggests the lack of sexual dimorphism of Mup expression in the SG (Figure 3.8) as compared to a big difference in Mup expression between male and female liver (Figure 3.15 B).

The absence or the presence of Zhx2 does not alter the gene expression of Zhx1, Zhx3 and H19 in the mice SG:

I considered whether the absence of Zhx2 would alter the expression of the highly related Zhx1 and Zhx3 genes in SG. However, Zhx1 and Zhx3 mRNA levels did not change in $Zhx2^{ko}$ SG in either male or female mice. It is worth noting that Zhx1 and Zhx3 were expressed at higher levels than Zhx2 in SG of both male (Figure 3.9) and female (Figure 3.10) mice. There is no gender bias in the expression of Zhx1 (Figure 3.2 C) and Zhx2 (Figure 3.3C) in SG. Previous studies have shown that H19 levels increase in the absence of Zhx2 in the adult liver. However, H19 levels showed a slight but not significant increase

in SG of both male (Figure 3.9) and female mice (Figure 3.10). Curiously, H19 mRNA levels were elevated in SG of the pleomorphic adenomas in PLG1 transgenic mice [137] and are often elevated in HCC.

A trend towards a negative correlation between Zhx2 and MUP1 expression in male lacrimal glands (LG):

Since Mup1 is abundantly expressed in the LG [95], I examined Mup1 expression in $Zhx2^{ko}$ and $Zhx2^{wt}$ mice. While Mup1 levels increased slightly in $Zhx2^{ko}$ LG, this change was not significant ($p= 0.07$). The mRNA levels of class B Mups, Mup18, Mup24 as well as Zhx1 and Zhx3 did not show any difference between $Zhx2^{ko}$ and $Zhx2^{wt}$ mice (Figure 3.11). In summary, I found that Mup1, Mup18, class B Mups, and, to a lesser extent, Mup24, are expressed in male LG; of these, Mup1 is the most abundantly expressed. In contrast, Mup18 is the most abundant Mup in SG (Figure 3.12). Other Mups have not been investigated. My data is consistent with previous studies showing that MupIV, which is likely Mup1 [99], is the most abundant Mup in lacrimal glands [97]. As with the SG, we have found that Zhx1 and Zhx3 are expressed at higher levels than Zhx2 in LG; expression of these two Zhx genes do not change in $Zhx2^{ko}$ mice (Figure 3.11).

Mups are not regulated by Zhx2 in the male liver:

My data indicate that several Mup genes are negatively regulated by Zhx2 in SG. In contrast, previous studies in our lab indicate that Mups are positively regulated by Zhx2 in the liver. Consistent with this result, I found that Mup expression is lower in adult BALB/cJ liver compared to BALB/c and BALB/cByJ (Figure 3.5). Therefore, I examined Mup expression in $Zhx2^{ko}$ and $Zhx2^{wt}$ mice (Figure 3.13). In contrast to my studies in BALB substrains and previous studies in knock-out mice (Jiang, submitted), I found no difference in Mup expression between $Zhx2^{ko}$ and $Zhx2^{wt}$ mice. Consistent with previous studies, I found that class B Mups (MupU) are the most abundant liver Mups, with Mup24, Mup25 and Mup26 also being highly expressed (Figure 3.13).

Mat1a mRNA levels are decreased in adult male Zhx2^{ko} mouse liver:

Most of our knowledge about Zhx2 comes from studies in BALB/cJ mice, which have a natural mutation in Zhx2. For instance, BALB/cJ male mice have increased production of Cyp2a4 [138]. Moreover, Kate Creasy, a former student in our lab found that expression of Mat1a, Stat5a and Stat5b genes were decreased in hepatocyte-specific Zhx2^{ko} (Zhx2$^{\Delta hep}$) mice [Creasy Thesis, 2015]. This led me to test whether Cyp2a4, Mat1a, Stat5a and Stat5b were altered in Zhx2^{ko} mice. I did not observe a significant change in Cyp2a4, Stat5a or Stat5b expression. However, I did observe a significant decrease in Mat1a mRNA levels in Zhx2^{ko} liver (Figure 3.14). Shp is a critical factor in liver lipid homeostasis and it negatively correlates with Cyp8B1 expression [139], a negative correlation exists between Shp and Cyp8B1in cholestasis [140], Cyp8B1 was correlated with Zhx2 in BALB/cJ mice [Clinkendeard Thesis, 2012]. Therefore, I investigated Shp mRNA levels in Zhx2^{ko} male liver. I found no change in Shp levels, indicating that Shp is not a target of Zhx2 in male liver (Figure 3.14).

The *Emr1* gene encodes a 160 KD macrophage-specific cell surface glycoprotein [141]. A correlation between elevated H19 and increased hepatic macrophage numbers has been reported [136]. Since Zhx2 negatively regulates H19 [43], I tested whether Emr1 levels would increase in livers of Zhx2^{ko} mice. However, Emr1 mRNA levels were not altered in liver of Zhx2^{ko} as compared to Zhx2^{wt} mice (Figure 3.14).

Hepatocyte nuclear factor 4 alpha (HNF4α) is an important liver-enriched transcription factor [142]. HNF4 mRNA is highly expressed in the liver, kidney, brown and white adipose, muscle, stomach, tongue, duodenum, jejunum, ileum, colon and gall bladder [143]. Zhx2$^{\Delta hep}$ mice liver exhibited a significant positive correlation between Zhx2 and Hnf4α [Creasy Thesis, 2015]. However, I found no change in HNF4α in Zhx2^{ko} liver (Figure 3.14).

Mup24 is positively regulated by Zhx2 in the adult female liver:

Class B Mups (MupU) and Mup24 were expressed at higher levels than Mup1 and Mup18 in adult female liver (Figure 3.15A). Mup24 was significantly decreased in Zhx2^{ko}

female liver, whereas none of the other Mups changed in the absence of Zhx2. Mups are expressed at higher levels in the male liver than in female liver. My data also indicates that class B Mups (MupU) and Mup24 were higher in male liver than in female liver (Figure 3.15B)

Zhx2 is positively correlated with Mat1a and inversely with Shp, lipid metabolism genes, in the female mice livers:

As described in Figure 3.14, we analyzed several different hepatic genes in $Zhx2^{wt}$ mice $Zhx2^{ko}$ mice. We also analyzed these same genes in female livers to see if their expression changed in the absence of Zhx2. As expected, Zhx2 mRNA levels were significantly reduced in $Zhx2^{ko}$ female liver. Mat1a levels exhibited a significant decrease, Shp levels exhibited a trend toward a negative regulation in the absence of Zhx2, whereas all other genes were not affected by the loss of Zhx2 (Figure 3.16)

Analysis of candidate Zhx2 targets in the kidney:

Several reports indicate that expression of Zhx proteins are altered in rodent models of kidney disease [126]. We were interested in analyzing Zhx target genes, as well as Zhx1 and Zhx3, in $Zhx2^{ko}$ mice. While Zhx2 levels were dramatically reduced in $Zhx2^{ko}$ mice, as expected, we did not see any changes in the other genes that were analyzed (Figure 3.17). These include Mup24, H19 and AFP, which are known targets of Zhx2 in the liver. Zhx1 and Zhx3 are expressed much higher than Zhx2 in the kidney, but do not change in the absence of Zhx2. We were particularly interested in Wt1 and Lmx1b due to their important role in kidney development and disease. However, I found no correlation between Zhx2, Wt1 and Lmx1b (Figure 3.17). Similar results were observed in female mice except Stat5b which has shown a trend towards a positive correlation with Zhx2 status (Figure 3.18).

Zhx2 control gene expression in the brain:

I was interested to examine whether expression of Zhx2 and Zhx2 target genes is altered in the brain. I was particularly interested in Mat1a, Shp, and Cyp2a4. Although

previous northern blot studies indicated that Mups were not expressed in the brain or other organs, [95] [86], preliminary RT-qPCR studies from our lab indicated that Mups were expressed in the brain [Data not shown]. Levels of Cyp2a4, Mat1a, Shp, Mup1, class B Mups (MupU), Mup18, Mup24, Mup25 and Mup26 mRNA in the brain of $Zhx2^{wt}$ and $Zhx2^{ko}$ mice were analyzed by RT-qPCR. Mups were expressed at very low levels in the brain compared to liver. Mup 24, Mup25 and class B Mups (MupU) were decreased in the absence of Zhx2, although none of these differences were statistically significant. None of the other genes tested were affected by the absence of Zhx2, although Shp showed a modest but insignificant decline (Figure 3.19). Similar studies were performed in female brain samples. The fact that females Mup mRNA levels were lower than males is expected, since it has been documented that females express lower level of MUPs than males [99] [95]. However, none of the candidate Zhx2 target genes exhibited significant differences in expression in $Zhx2^{ko}$ mice (Figure 3.20).

Expression of Zhx genes and Zhx2 target genes in small intestine:

A number of Zhx2 target genes, including AFP and H19, are expressed at low but detectable levels in the small intestine (SI). Previous northern analysis suggested that these targets were not affected by Zhx2 in this tissue. Since RT-qPCR is a more sensitive measure of gene expression, I decided to analyze Zhx2 and Zhx2 targets, as well as other Zhx genes, in the small intestine. Despite the dramatic decline of Zhx2 mRNA levels in $Zhx2^{ko}$ mice, none of the other genes analyzed, including AFP and H19, showed a change in expression in the absence of Zhx2. I also found that Zhx1 and Zhx3, whose levels were much higher than Zhx2, did not exhibit any compensatory change in $Zhx2^{ko}$ mice. Mast cell protease 2 (Mcpt2) is an enzyme secreted by Mast cells and is usually activated in allergy or parasite infection. Previous studies reported that Mcpt2 is not secreted in the SI. However, BALB/cJ mice will secret Mcpt2 after helminth infection [144]. Therefore, I tested whether Mcpt2 expression would be higher in $Zhx2^{ko}$ SI as compared to $Zhx2^{wt}$ mice. However, I observed no correlation between Zhx2 and Mcpt2 (Figure 3.21).

I also analyzed Zhx2 and Zhx2 target genes in SI of adult female mice. Despite the dramatic decline in Zhx2 mRNA levels in $Zhx2^{ko}$ SI, no significant change in AFP, H19,

or Cyp2a4 was observed. As was observed in male mice, SI expression of Zhx1, which is much higher than Zhx2, was not affected by the absence of Zhx2 (Figure 3.22).

Discussion:

One goal of my dissertation is to understand how Zhx2 regulates target gene expression. In particular, since much of the previous work in our lab has focused on the liver, I analyzed expression of Zhx2 and Zhx2 target genes in tissues other than the liver. These studies utilized $Zhx2^{ko}$ mice that have been generated in our lab. This is the first report utilizing $Zhx2^{ko}$ mice as previous studies utilized BALB/cJ mice [Clinkenbeard Thesis, 2012] and $Zhx2^{\Delta hep}$ mice [Creasy Thesis, 2015]. I demonstrated increased hepatic AFP and H19 expression in $Zhx2^{ko}$ mice as compared to age-matched $Zhx2^{wt}$ mice. These data are consistent with our previous findings which indicated that Zhx2 is required for postnatal silencing of AFP and H19 expression in the liver [43]. Moreover, my finding validates $Zhx2^{ko}$ mice as a good model to study Zhx2 regulation of target genes in multiple organs.

Since Zhx2 is closely related to Zhx1 and Zhx3 [145], we analyzed expression of these genes in various tissues. We found that both genes were ubiquitously expressed but, similarly to Zhx2, their expression varies between tissues. The fact that male Zhx1 expression was highest in the kidney was not surprising since Zhx1 has been implicated in normal kidney podocyte function. Other studies also found Zhx1 to be expressed at higher levels in kidney than in small intestine [47]. In contrast to males, my data indicates that the highest Zhx1 expression in females occurred in the SI. The human protein atlas database indicates that the highest Zhx1 mRNA levels are found in the gastrointestinal track, although this study did not signify sex (http://www.proteinatlas.org/ENSG00000165156-ZHX1/tissue). There is no published information regarding Zhx1 expression in the small intestine.

We did not test Zhx1 in the brain, but other investigators used Northern blot analysis to show that Zhx1 is highly expressed in the brain, with lower expression found in the liver and kidney and undetectable levels in the heart and muscle [145] [49].

Interestingly, human ZHX1 was observed in all organs tested with the highest level in the heart, skeletal muscle and pancreas. However, other studies indicate that Zhx1 is moderately expressed in the brain, kidney and placenta with lower levels in the lung and the liver [50]. In conclusion, further studies may be needed to further examine Zhx1 expression in numerous organs.

Altered cellular localization of Zhx2, as well as Zhx1 and Zhx3, has been observed in Passive Heymann nephritis (PHN) and Puromycin amino nucleoside nephrosis (PAN), two rat models of kidney disease [126]. These data raise the possibility that Zhx2 could play a role in normal kidney function. My data showing that Zhx2 is expressed at higher levels in the male kidney than other organs is consistent with this possibility. In contrast, Zhx2 mRNA levels are highest in the female small intestine. My data is consistent with our previous Northern blot analysis showing Zhx2 to be highest in the kidney, although it is in contrast to our earlier data showing brain Zhx2 mRNA levels to be higher than the liver [43]. I believe that real time qPCR is more accurate than Northern blot. Also, my data is similar to some of the data in the human protein atlas, although they did not state the sex of the samples. This database showed that Zhx2 mRNA is comparable between kidney and small intestine, but also noted that SG express high Zhx2 levels (http://www.proteinatlas.org/ENSG00000178764-ZHX2/tissue). It is possible that these differences are due to variations in gene expression between men and women. Previous studies from our lab suggest that Zhx2 regulates sex-biased differences of hepatic Cyp enzymes and may cross-talk with Stat5a and Stat5b [Creasy Thesis, 2015], which are controlled by circulating growth hormone [146]. Zhx2 regulates Mup expression in the SG and LG (this Chapter) and in the liver [Jiang and Spear, submitted] and Mups are regulated by hormones [95].

I was not surprised to find the highest Zhx3 mRNA levels in the kidney compared to the small intestine in both sexes and to SG and LG glands males. Other investigators reported that Zhx3 regulates Wt1, an important podocytes gene, and correlated with nephrotic syndrome disease [53]. In support of this, Northern blot analysis showed human ZHX3 to be highly expressed in the kidney [47]. These data are consistent with human protein atlas that showed ZHX3 to be expressed in the kidney at twice the levels seen in

the small intestine. This data raises the possibility that Zhx3 could play a critical role in the kidney.

Overall, my data indicates that Zhx1 and Zhx3 are expressed at higher levels than Zhx2 in all the organs that I tested. Although there is no published data describing the function of Zhx1, Zhx2 or Zhx3 in the SI, SG and LG, my results suggest that Zhx1 and Zhx3 may be more important than Zhx2 and support further investigation of these Zhx proteins in multiple organs, including the liver.

Although Mup genes are not found in humans, there are reasons to study these genes. Mups are highly expressed in mouse liver and other glands; therefore, studying Mups could reveal important clues about gene regulation in these organs. In addition, behavior and physiological processes in humans, especially woman, are influenced by pheromones. Menstrual synchrony is a phenomenon in which pheromones from one woman can alter the ovulation cycle time of other females. The same phenomenon has also been reported in rats [100].

I focused on analyzing of Mup1 and Mup18 in the salivary glands since Logan *et al* found these two genes to be expressed in this tissue [99]. My data are novel in showing that Mup18 is the highest expressed Mup in the SG. Mup1 and class B Mups are the second and third highest expressed Mups in this tissue, respectively. My data showing Class B Mup expression in SG is in support with Logan *et al* that documented that MUP3(Class 3 MUP) is expressed in the submaxillary glands. In SG, Mup18 expression is greater than Mup1. Unfortunately, I have not tested class B Mups in female salivary gland, but this should be done in future studies. High Mup24 levels in the SG of females but not males was surprising since it has been reported to be expressed in male C57BL/6J liver and submaxillary glands [99]. A more careful developmental analysis of Mup expression in the salivary gland may be warranted since Mup RNA production has been reported to start at one weeks of age in mice, increase over time but decrease at six months of age [95]. A time course study in liver found that Mup24 is activated after birth and gradually increases up to a high level on day 56, a pattern similar to Zhx2 and opposite to AFP [Jiang and Spear, submitted].

Mup expression in the salivary gland is not sexually dimorphic, which strongly suggests a lack of hormonal regulation of Mups in this tissue. My data are consistent with previous Northern blot data showing male biased Mup expression in the liver and lacrimal gland but not in submaxillary glands [95]. Future studies should analyze Mup expression changes in the absence of Zhx2 in the lacrimal gland.

Prior to my studies, little was known regarding the role of Zhx2 in non-hepatic tissue, including SG and LG. My data revealed a novel significant negative correlation between Zhx2 expression and Mup1, Mup24 Mup18 and class B Mups in males and Mup1 and Mup18 in females. This is in contrast to what is observed in the liver. These findings support a model in which higher Mup expression in SG of male BALB/cJ mice could explain their high aggression [82]. Further studies should further test this possibility.

Mup expression in mouse submaxillary gland begins one week after birth and is free from hormonal regulation. Shaw *et al* 1982 [95] treated hypophysectomized mice with testosterone, thyroxin and growth hormone. Surprisingly, none of these hormones influenced Mup expression in the submaxillary glands, which are a component of the SG that was studied in this Chapter.

Zhx1 and Zhx3 levels were not altered in SG of $Zhx2^{ko}$ mice, indicating that there were no compensatory changes in the expression of these related genes when Zhx2 was no longer expressed. This is similar to what was seen with Stat5 genes, which are more than 90% similar. Stat5a could not compensate for Stat5b in Stat5b knockout mouse liver [124].

While Mups are expressed at highest levels in the liver, these genes are also expressed in LG and SG although the liver and these glands expressed different Mup genes. Since Zhx2 positively regulates Mup expression in the liver, I hypothesized that Mups were also be positively regulated by Zhx2 in SG and LG. However, I was surprised to find that Mups appeared to be negatively regulated by Zhx2 in these tissues. In male SG, Mup1, Mup18 and class B Mups (MupU) increase in the absence of Zhx2. For class B Mups and Mup18, this difference was significant. Mup24, which is liver-specific, is expressed at very low levels in $Zhx2^{wt}$ mice but increased in $Zhx2^{ko}$ mice. A similar pattern is seen in female

SG; Mup1 and Mup18 are expressed at higher levels in Zhx2^{ko} SG than in Zhx2^{wt} SG. In contrast to SG, we did not see any change in Mup expression in the LG of Zhx2^{ko} mice. The fact that LG is under hormonal regulation while SG is not might explain the difference in gene expression. Although I have not analyzed the females LG samples, I would expect them to express less Mups since previous Northern blot analysis showed Mups to be expressed 5-fold higher in the LG of male mice compared to female mice [95]. Experiments in hypophysectomized mice showed that lacrimal gland Mup expression can be restored by testosterone only [95]. My RT-qPCR data is consistent with previous northern blot studies showing that Mup1 is most abundantly expressed in LG, while Mup18 is the major Mup in SG [97].

It is known that Mups control a number of behaviors in mice. In addition, Zhx2 has been associated with certain mouse behaviors, including male-on-male aggression. My data propose that the correlation of Mups in SG and LG with Zhx2 might help explain these associations since Mups mediate mice communication.

Most studies on Zhx2 have been performed in the liver, and it is clear that Zhx2 has an important role in controlling target genes in this organ. Since Zhx2 controls H19 in the liver [43] and it was found that livers with elevated H19 had in influx of macrophages [136], I considered whether the lack of Zhx2 could induce macrophage accumulation in the liver. To test this, I analyzed expression of Emr1, a macrophage marker. However, I found no change in Emr1 expression in Zhx2^{ko} livers compared to the liver of Zhx2^{wt} mice. Perhaps immunohistological staining with macrophage-specific antibodies of Zhx2^{ko} and Zhx2^{wt} livers could reveal differences in macrophage accumulation.

I analyzed the expression of several liver genes in male and female Zhx2^{ko} mice that were previously tested in hepatocyte-specific (Zhx2$^{\Delta hep}$) mice [Creasy Thesis, 2016]. I found no significant change in expression of Cyp2a4, Mups, Hnf4, Shp, Stat5a or Stat5b. Hnf4 is a critical regulator of genes involved in numerous, essential liver functions including bile acid, lipid metabolism, gluconeogenesis, amino acid and blood coagulation factors. Hnf4 null mice die prenatally due to the development of sever hepatomegaly and steatosis [147]. Our lab previously found that Cyp2a4 levels were increased in the adult

male liver of Zhx2$^{\Delta het}$ mice, but I saw no significant change in adult male liver of Zhx2^{ko} mice. There must be differences in how these genes are regulated in the liver depending on whether Zhx2 is absent in all liver cells or just hepatocytes. However, I did find a significant decrease in Mat1a in both male and female liver in Zhx2^{ko} mice. Previous studies by our collaborator in China indicate that nuclear Zhx2 protein levels are decreased in HCC. It is also known that Mat1a is reduced in NAFLD, NASH [36], liver steatosis [33] and HCC [37]. These data suggest a possible link between Zhx1 and Mat1a in HCC.

My data supports previous studies indicating that class B Mups, Mup24, Mup25 and Mup26 are highly expressed in male liver. I cannot explain why I did not see a decrease in Mup expressioin in the absence of Zhx2, since previous studies in our lab showed that Mup levels are dramatically reduced in the absence of Zhx2, except my studies have utilized different mice.

In adult female liver, my data indicates that Mup24 levels were significantly lower in the absence of Zhx2. It is not known why we saw a difference in Mup expression in female mice but not male mice when Zhx2 was deleted.

I was particularly interested in the kidney, since previous studies showed changes in Zhx protein expression in several models of kidney disease. I found that Zhx1 and Zhx3 were expressed at much higher levels than Zhx2 in the kidney. This might explain why levels of these two genes did not change in Zhx2^{ko} kidney. Despite the similarities in Zhx proteins, we do not yet know the extent to which their functions overlap. ChIP-seq might shed some light on possible overlapping targets of different Zhx proteins. Also, staining Zhx2^{ko} mice kidney with Zhx1 and Zhx3 antibodies, could help determine if their cellular localization have been altered in absence of Zhx2. It has been reported that elevated Zhx1 and Zhx2 podocyte nuclear expression is observed in a proteinuric rat model. In other models of kidney disease (PAN plus PHN rat model) Zhx2 and Zhx3 were marginally increased and Zhx1 was downregulated [126]. This is partially supported by my data as I observed marginal increases in Zhx1 and Zhx3 gene expression in Zhx2^{ko} male kidney. The same group demonstrated Zhx proteins were redistributed to the nucleus during disease.

Although known Zhx2 targets were not altered in Zhx2^{ko} kidney, we cannot rule out the possibility that Zhx2 influences progression of kidney disease. A more comprehensive study would be needed to test this possibility. I should note, however, that Wt1 and Lmx1b mRNA levels did not change in Zhx2^{ko} kidney. A change in expression of these genes, which are important in kidney development and function [126], would justify further studies of Zhx2 and kidney function. If we want to assess the kidney function of Zhx2^{ko} mice, we might test podocyte protein-tyrosine phosphatase (GLEPP1) because this gene will be decreased when there is defect in the kidney function. Anasarca is another sign of kidney disease when humans or animals accumulate fluid under the skin. This phenotype has not been seen in the Zhx2^{ko} mice, presumably, because severe Anasarca rats die very early in life [126]. So we might carefully examine Zhx2^{ko} mice in early ages and test blood and urine proteins to investigate if they will develop any sign of Anasarca.

I observed changes in Mup expression in SG and LG; previous studies indicate that Mups are regulated by growth hormone [95]. Previous studies from our lab indicated that Cyp2a4 is regulated by Zhx2 in the liver [Creasy Thesis, 2015] and by growth hormone [124]. Therefore, it seems logical that Stat5 and Cyps could be altered in different tissues in Zhx2^{ko} mice. However, for the most part this was not the case. Our data showing Cyp2a4 expression in the male kidney with a level slightly higher than in female kidney is consistent with previous results [148] [121]. In conclusion, expression of Cyp2a4, Stat5a, H19, Shp, Mat1a, Mup24, H19 and AFP in the male and female kidney did not change in the absence of Zhx2. I did notice a trend in Stat5b in Zhx2^{ko} mice, but this was not significant. Since this trend was seen with other genes, it is possible that analysis of more mice may reveal significant differences in gene expression in the presence or absence of Zhx2.

I expected to see changes in Mup expression in the brain in the absence of Zhx2. While Mups were reduced in Zhx2^{ko} brain samples, these differences were not significant. Since Mups influence behavior and previous studies suggest that Zhx2 might influence mouse behavior, it might be worthwhile to explore Zhx2 and Mups in the brain in greater detail. The expression of Cyp2a4 and Mat1a in the brain were low but not affected by Zhx2. Nightly expression of Mat2a in rat pineal gland is 5-6 fold higher than daytime, and rat

brain pinealocytes are the major producer of Mat2a mRNA in the brain [149]. Rat kidney and pineal gland are the only two organs expressing Mat2a. It may be more appropriate to monitor Mat2a in the brain, kidney and the liver during darkness.

We did not observe any changes in Zhx2 target genes in the small intestine of $Zhx2^{ko}$ mice. We were particularly interested in Mcpt2 since this gene is expressed differently in BALB/cJ mice, but we did not observe changes in Mcpt2 expression in small intestine between $Zhx2^{ko}$ and $Zhx2^{wt}$ mice [144]. It might be worthwhile to stain the small intestine with mast cell markers to test if the induction of mast cells was altered in the presence or absence of Zhx2. My findings that Mat1a is expressed at high levels in the liver and very low in the kidney, brain and small intestine is consistent with previous studies [34]. My finding that Cyp2a4 is expressed at very low levels in the SI is also consistent with previous reports in human and mice [121].

In conclusion, I have evaluated expression of Zhx genes and a number of candidate Zhx2 genes in various tissues of $Zhx2^{wt}$ and $Zhx2^{ko}$ mice. We did observe some significant changes in Mup expression in SG and LG of $Zhx2^{ko}$ mice. However, for the most part, many Zhx2 targets were not altered in organs of $Zhx2^{ko}$ mice, although trends were noted for many genes. It is possible that analysis of a greater number of animals may be needed for differences to reach significance. Even if the data are not significant, this does not rule out the possibility that changes in Zhx2 might influence disease processes in various models of tissue damage. It is also interesting that Zhx1 and Zhx3 are normally expressed at higher levels than Zhx2 in most tissues. This might explain why we did not see compensatory changes in expression of Zhx1 and Zhx3 in $Zhx2^{ko}$ mice. These data raise the possibility that Zhx1 and Zhx3 might be important for the development and function of different organs. To test these possibilities, more studies will be needed. My data has revealed new insight into potential role of Zhx2 in different organs are provide the framework for future studies.

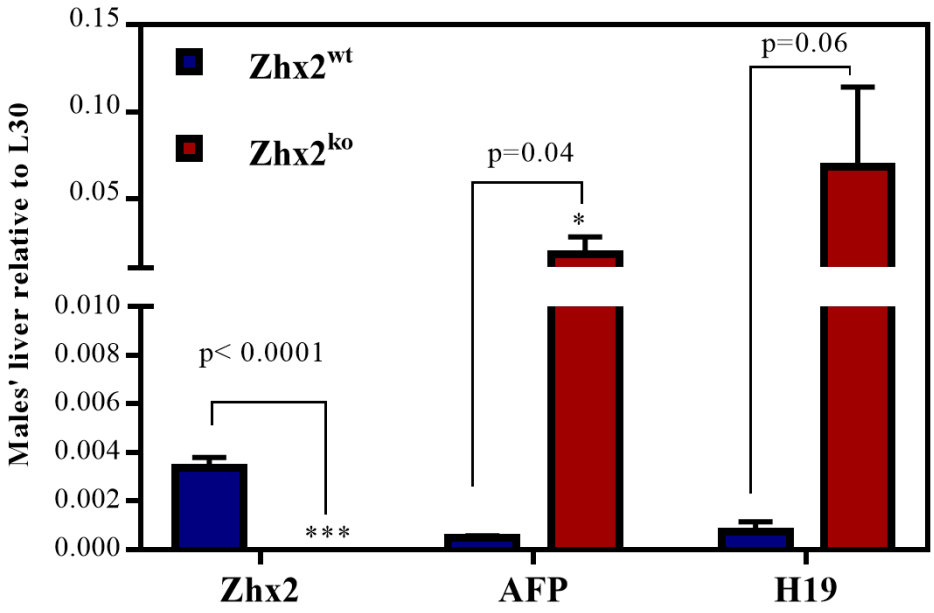

Figure 3.1 Hepatic Zhx2 mRNA levels are reduced and AFP and H19 mRNA levels are increased in the livers of Zhx2^{ko} mice. RT-qPCR was used to analyze total liver mRNAs from Zhx2^{wt} n=3 and Zhx2^{ko} mice n=3 cohorts. Zhx2 is dramatically reduced in the Zhx2^{ko} cohort (p=0.0001). AFP and H19 were elevated in adult mice Zhx2^{ko}. Data shown are relative to L30. *p≤0.05, ***p ≤0.0001.

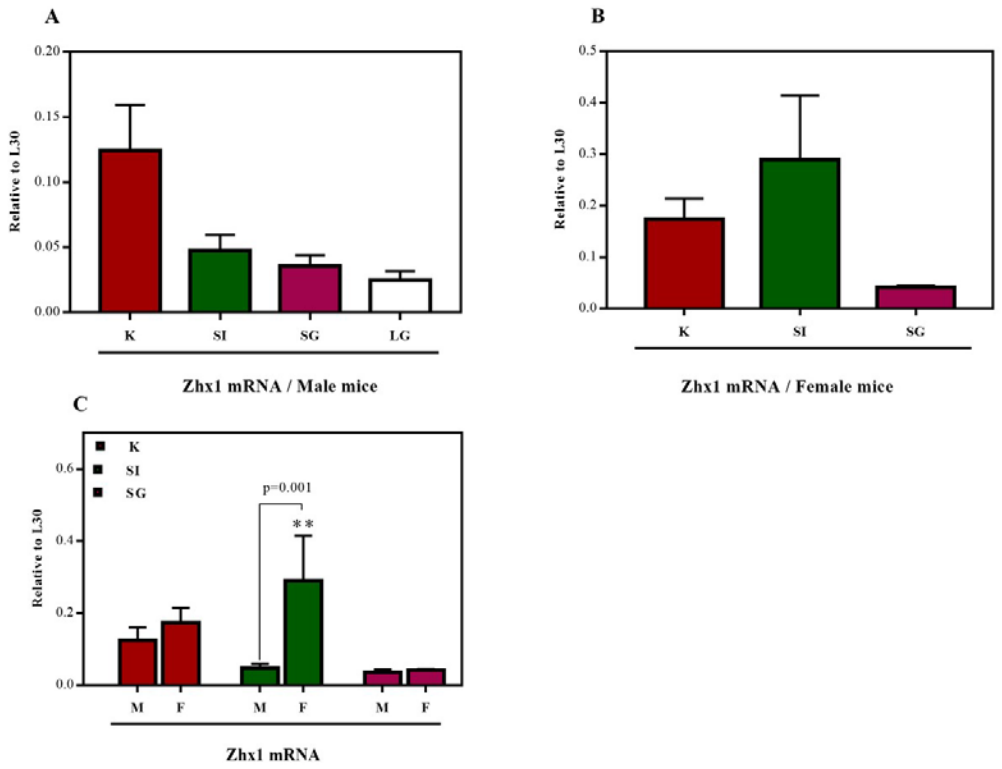

Figure 3.2 Zhx1 is ubiquitously expressed in adults Zhx2^{wt} mice. Zhx1 is highly expressed in the male adult mice kidney (K) as compared to the small intestine (SI), salivary glands (SG) and lacrimal gland (LG) (A). Females SI exhibited higher Zhx1 expression as compared to kidney and SG (B). Zhx1 expression in the SI exhibited females-biased expression. Data shown are relative to L30. Each Colum represents 3 mice. ** $p \leq 0.001$.

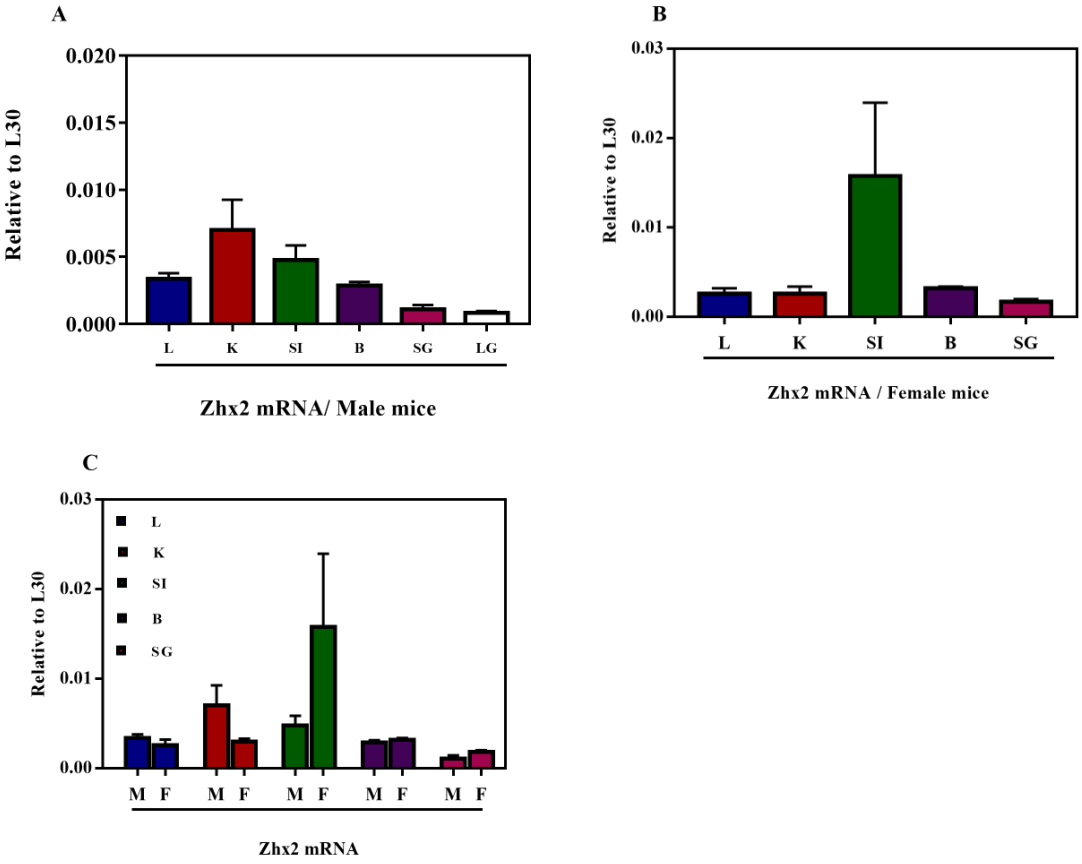

Figure 3.3 The highest Zhx2 mRNA levels are found in male kidney and female small intestine of adult Zhx2^{wt} mice. RT-qPCR was used to analyze Zhx2 expression in the kidney, small intestine (SI), liver, brain (B), salivary (SG) and (LG) lacrimal glands of males Zhx2^{wt} mice with the highest expression detected in the kidney (A). In female mice, the highest Zhx2 levels were found in the SI (B). Although not statistically significant, higher Zhx2 expression was found in the SI of female mice and the kidney of male mice (C). Data shown are relative to L30. Each Colum represents 3 mice. Tukey's analysis was employed to perform multifunctional analysis.

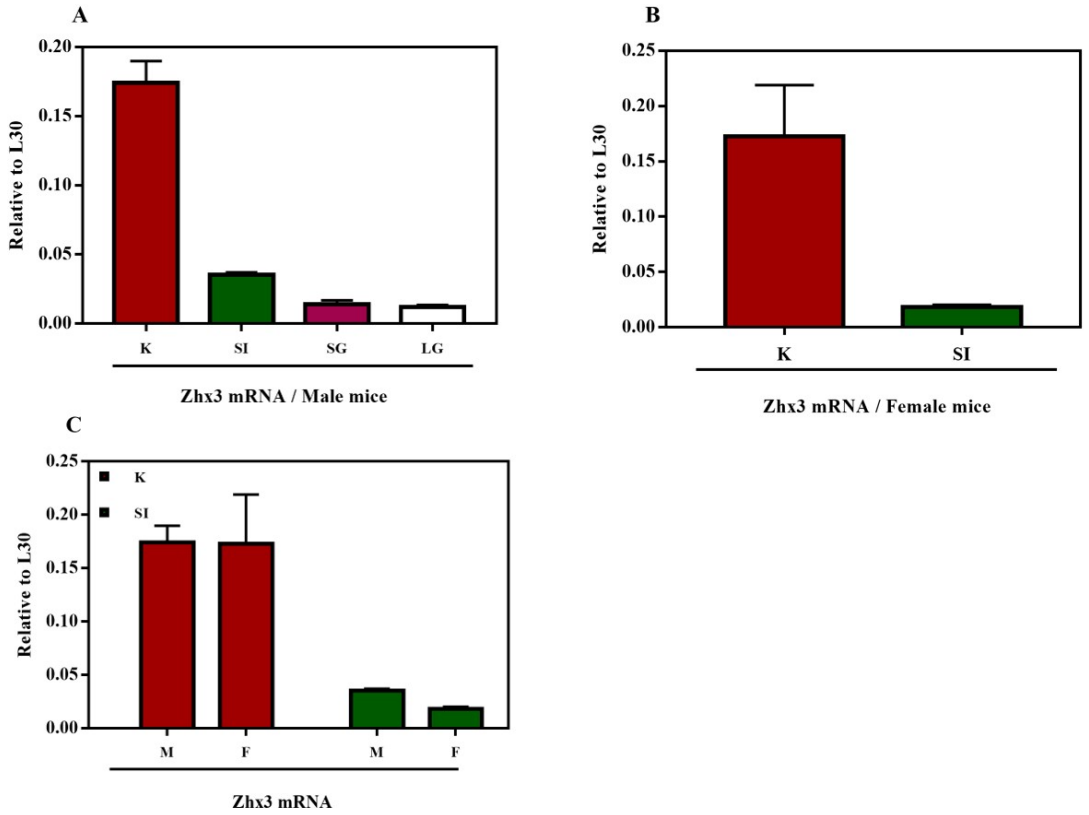

Figure 3.4 Zhx3 mRNA is expressed at equal levels in male and female Zhx2^{wt} kidney and SI. RT-qPCR was used to analyze Zhx3 expression in multiple male and female mice organs. Male kidney RNA levels are higher than other organs (A). In female mice, Zhx3 is expressed at higher levels in kidney than the SI (B). There is no sex difference in Zhx3 expression in the kidneys or SI (C). Data shown are relative to L30. Each Colum represents 3 mice.

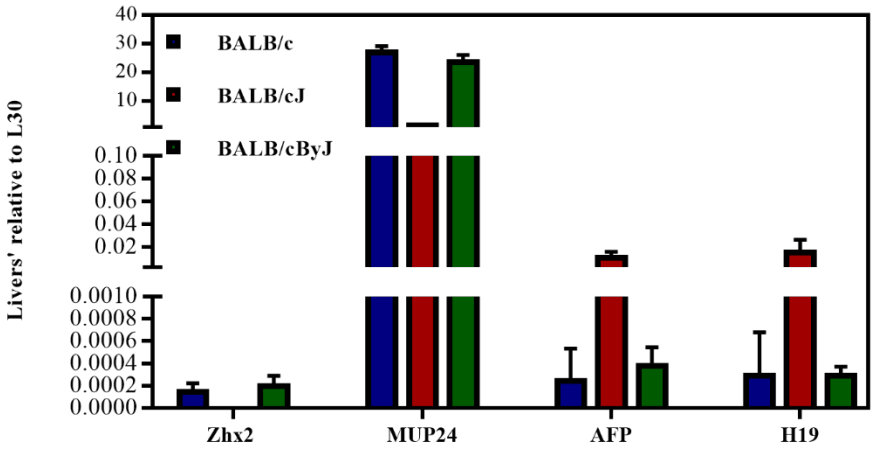

Figure 3.5 Zhx2 and Zhx2 targets are properly regulated in BALB/c and BALB/cByJ mice. Adult liver RNA from BALB/c, BALB/cJ and BALB/cByJ mice was analyzed by RT-qPCR. Data indicate that Zhx2 expression was reduced, while AFP and H19 mRNA levels were elevated in BALB/cJ mice compared to the closely related strains BALB/c and BALB/cByJ. MUP24 expression was reduced in BALB/cJ liver, consistent with it being positively regulated by Zhx2. Data shown are relative to L30. Each Colum represent 2 mice.

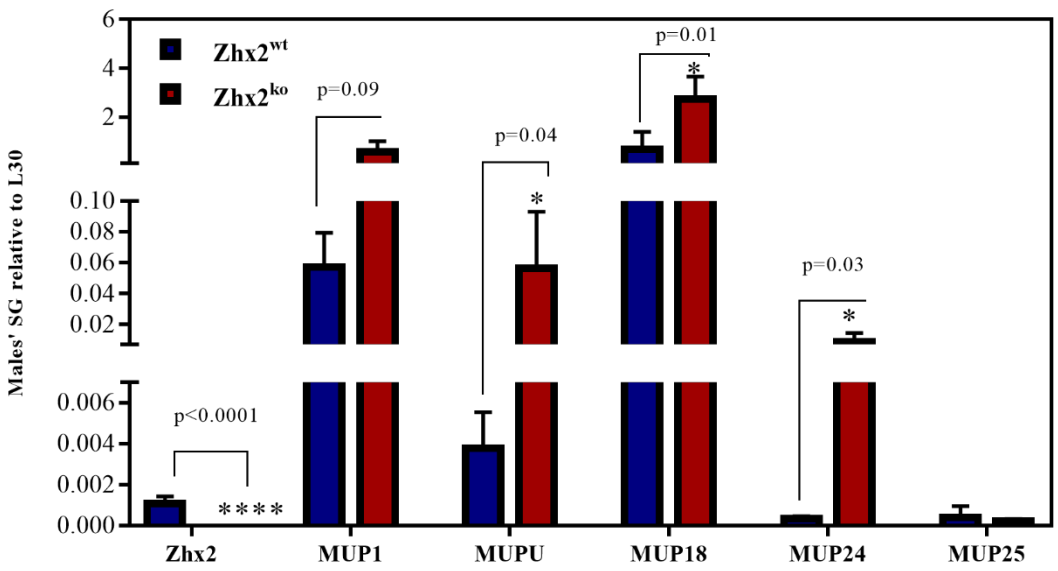

Figure 3.6 Expression of Mup genes are inversely correlated with Zhx2 expression in male SG. Total RNA from adult male Zhx2^{wt} and Zhx2^{ko} SG was analyzed by RT-qPCR Mup18, Mup 24, and class B Mups (MupU) were significantly increased in the absence of Zhx2; Mup1 also increased but this difference was not significant. Mup25 levels showed no change. Data shown are relative to L30. Each Colum represents 6 mice. *p≤0.05, ****p≤0.0001.

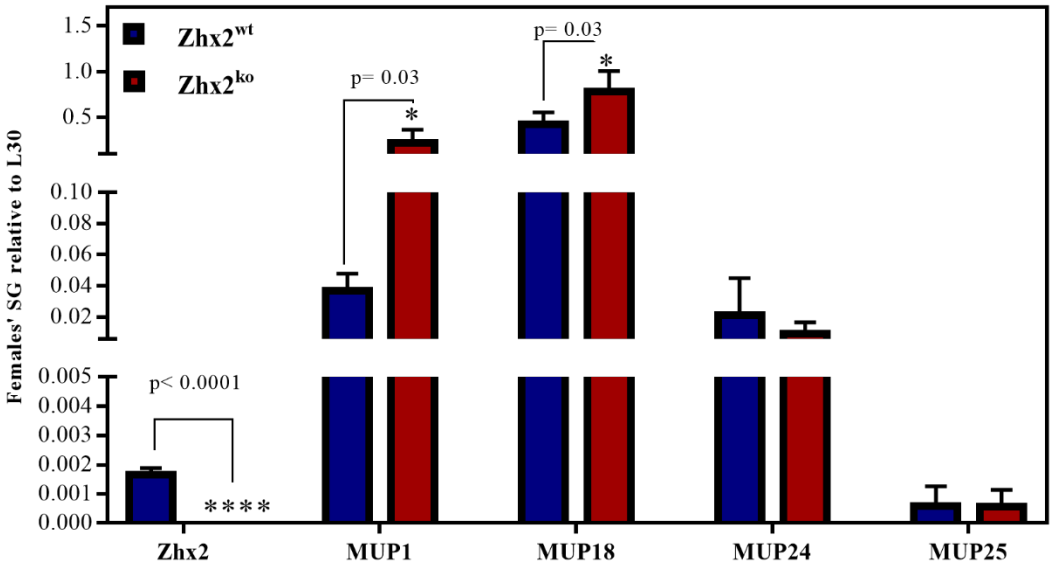

Figure 3.7 Mup1 and Mup18 are regulated by Zhx2 in female SG. SGs RNA was examined by RT-qPCR to quantify the difference between $Zhx2^{wt}$ and $Zhx2^{ko}$ littermates. Mup1 and Mup18 are significantly decreased in $Zhx2^{ko}$ mice whereas Mup24 and Mup25 are the same in both groups. Data shown are relative to L30. Each column represents 6 mice. * ≤0.05; ****p≤0.0001.

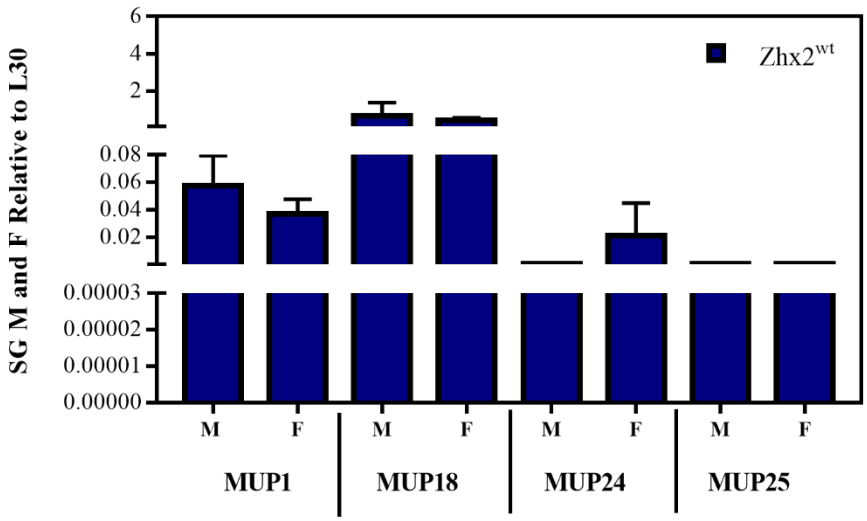

Figure 3.8 The lack of SG sexual dimorphism of MUP1 and MUP18, MUP24 and MUP25 expression. Analysis using RT-qPCR of SG mRNA of males and females demonstrated that Mups are expressed in comparable levels in both sexes. Data shown are relative to L30. Each Column represents 6 mice.

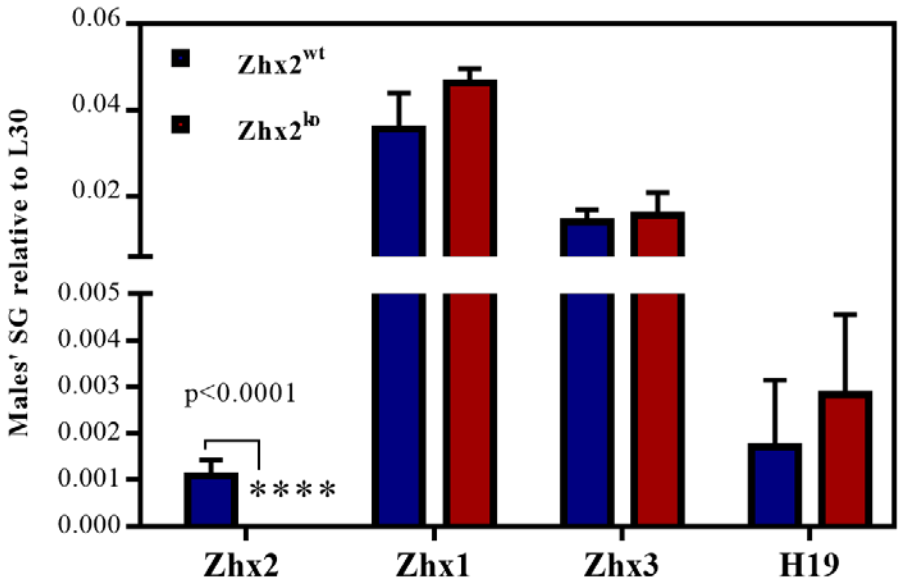

Figure 3.9 The absence of Zhx2 does not alter Zhx1, Zhx3 or H19 levels in male SG. RNA was examined by RT-qPCR to quantify differences between $Zhx2^{wt}$ and $Zhx2^{ko}$ littermate. Zhx1, Zhx3 and H19 did not exhibit significant changes when Zhx2 was absent. Zhx1 and Zhx3 are expressed at higher levels than Zhx2 in the female SG. Data shown are relative to L30. Each Colum represents 6 mice. ****$p \leq 0.0001$.

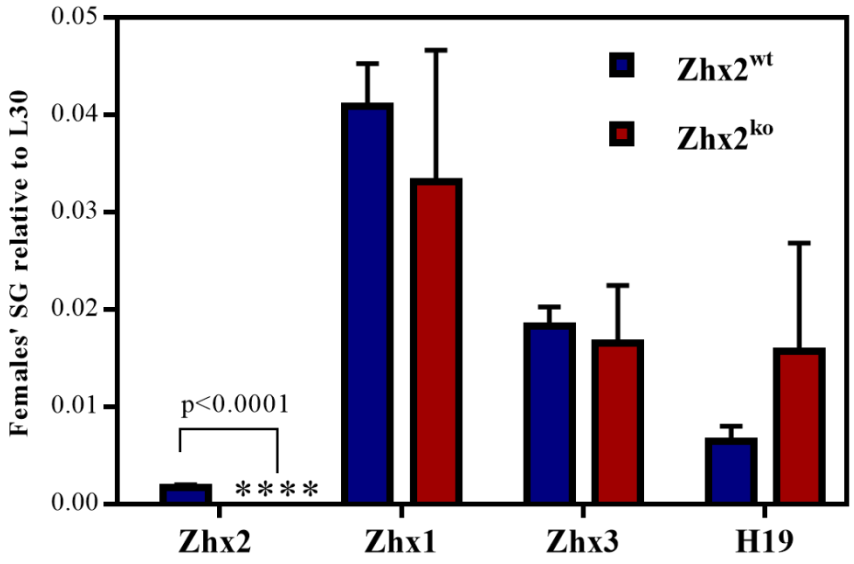

Figure 3.10 The absence of Zhx2 does not alter Zhx1, Zhx3 or H19 levels in female SG. RNA was examined by RT-qPCR to quantify differences between $Zhx2^{wt}$ and $Zhx2^{ko}$ littermate. Zhx1, Zhx3 and H19 did not exhibit significant changes when Zhx2 was absent. Zhx1 and Zhx3 are expressed at higher levels than Zhx2 in the female SG. Data shown are relative to L30. Each column represents 6 mice. ****$p \leq 0.0001$.

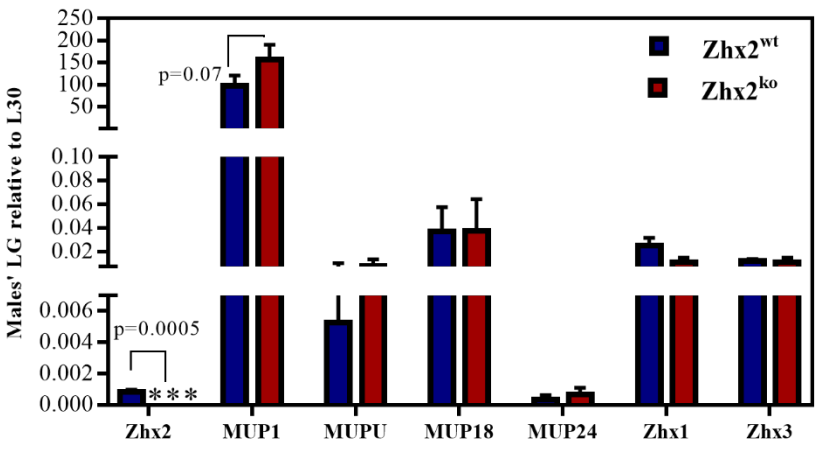

Figure 3.11 Expression of Mups are not altered in the absence of Zhx2 in male LG. Analysis by RT-qPCR indicated that LG Zhx2 mRNA levels decreased dramatically in Zhx2^{ko} mice. While Mup1 and class B Mup mRNA levels increased in the absence of Zhx2, these differences were not significant. Zhx1 and Zhx3 mRNA levels were not altered in male Zhx2^{ko} LGs. Data shown are relative to L30. Each Column represents 3 mice.

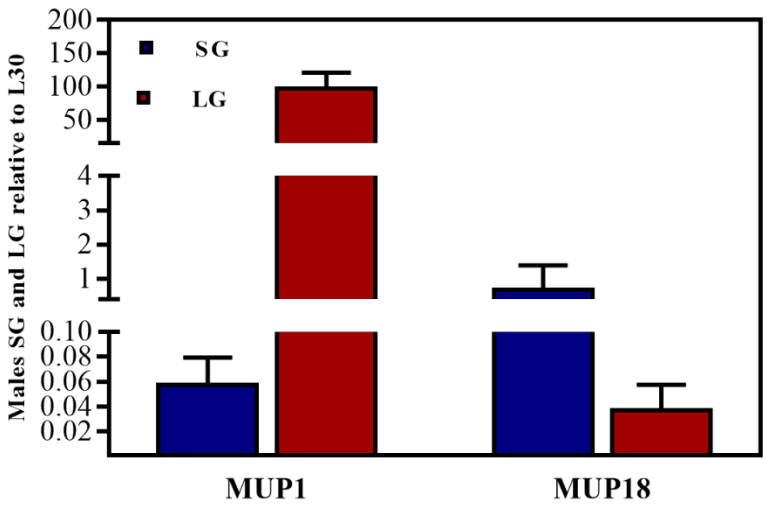

Figure 3.12 MUP1 is the most abundant Mup in LG whereas Mup18 is the most abundant Mup in SG, as determined by RT-qPCR. Data shown are relative to L30. Each Column represents 3 mice.

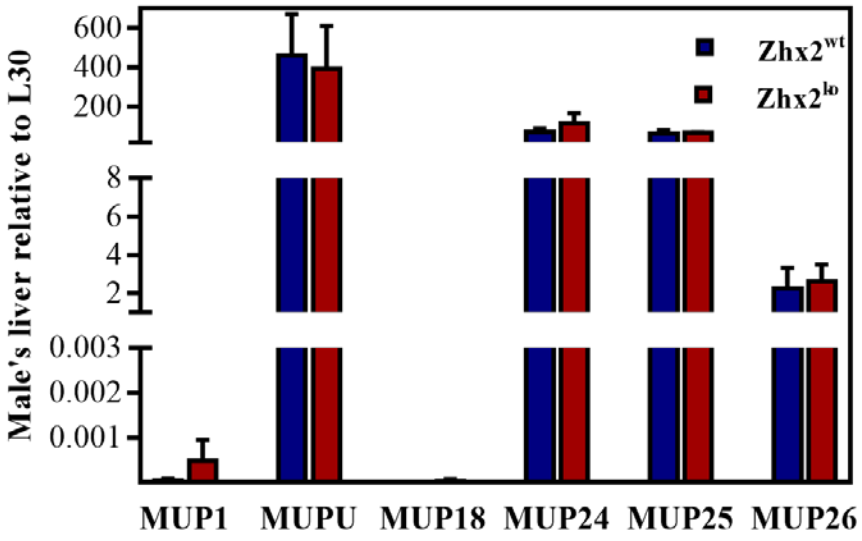

Figure 3.13 Expression of several Mup genes is not altered in liver of male Zhx2^{ko} mice. Expression of Mups was analyzed by RT-qPCR. Class B Mups (MupU), Mup24, Mup25 and Mup26 are expressed at high levels in male liver. As expected, Mup1 and Mup18, which are expressed in SG and LG, are expressed at very low levels in the liver. None of these Mups appear to be regulated by Zhx2. Data shown are relative to L30. Each Column represents 3 mice.

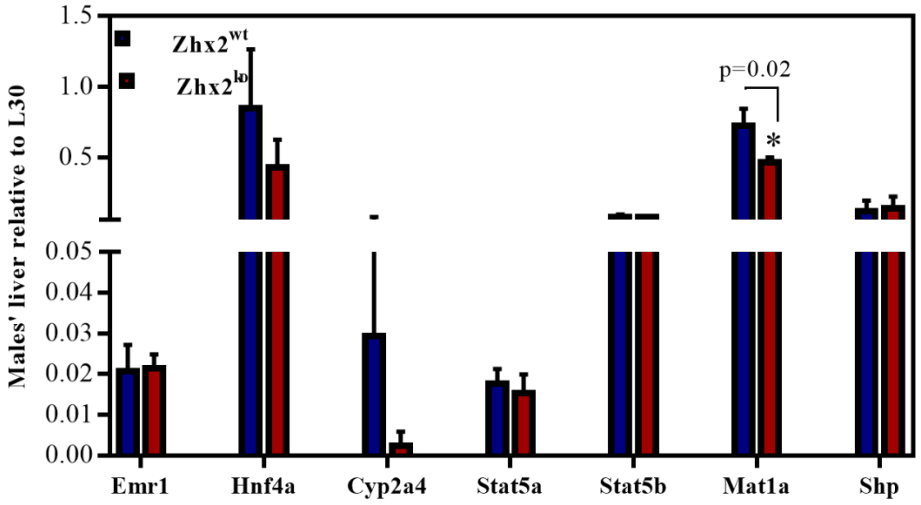

Figure 3.14 Mat1a levels decrease in adult liver of male Zhx2^{ko} mice. Cyp2a4, Stat5a, Stat5b, Shp, Emr1, or Hnf4α levels were not significantly different between Zhx2^{wt} and Zhx2^{ko} livers. Mat1a RNA expression is significantly reduced in Zhx2^{ko} male mice liver. Data shown are relative to L30. Each Column represents 3 mice. *p≤0.05

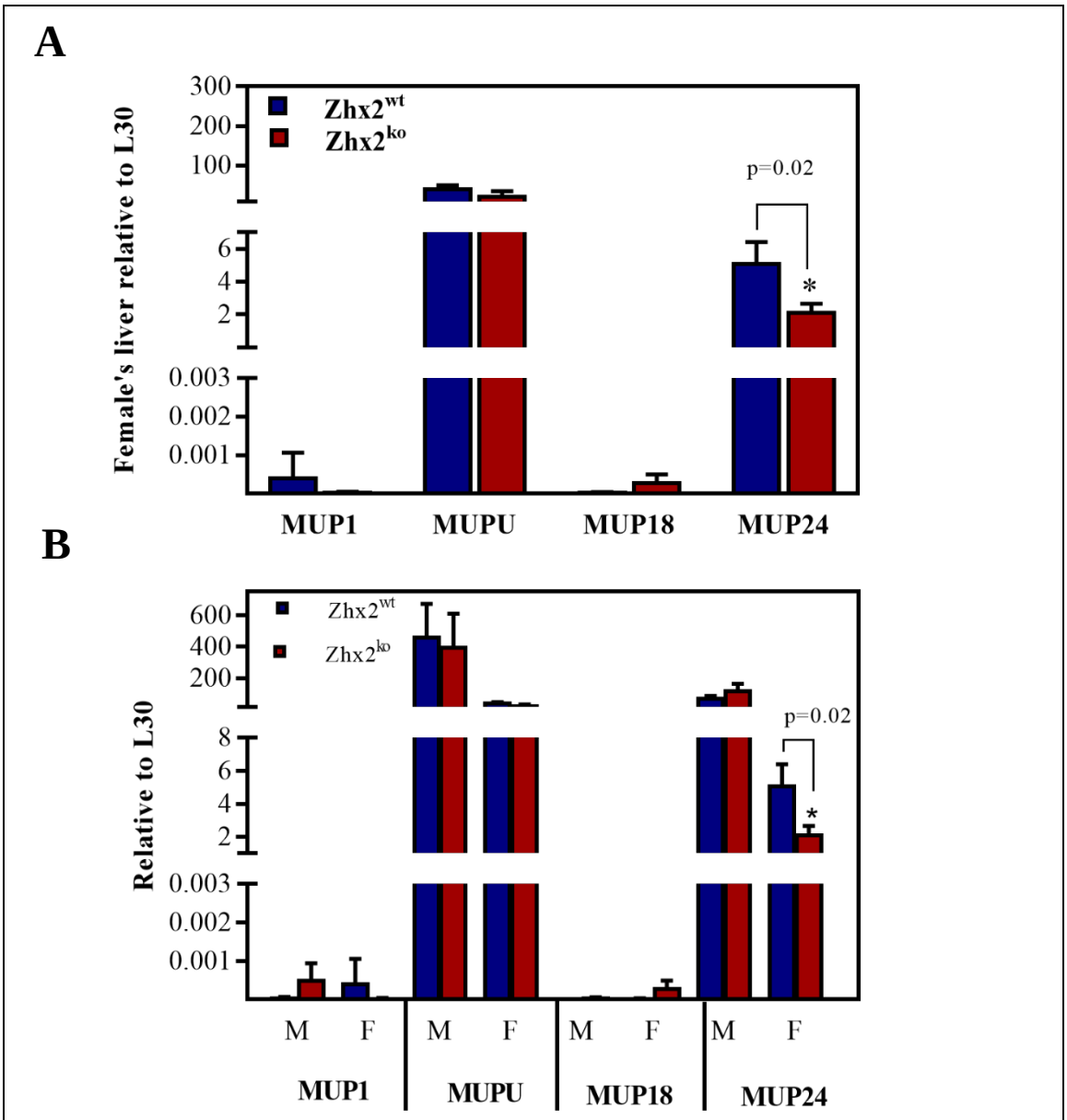

Figure 3.15 Mup24 mRNA levels are reduced in adult female liver in Zhx2^{ko} mice. MUP24, but not Mup1 Mup18, or class B Mups, was significantly decreased in Zhx2^{ko} mice (A). Mup 24 and class B Mups are expressed at higher level in male liver than in female liver. (B). Data shown are relative to L30. Each Column represents 3 mice.

*p≤0.05.

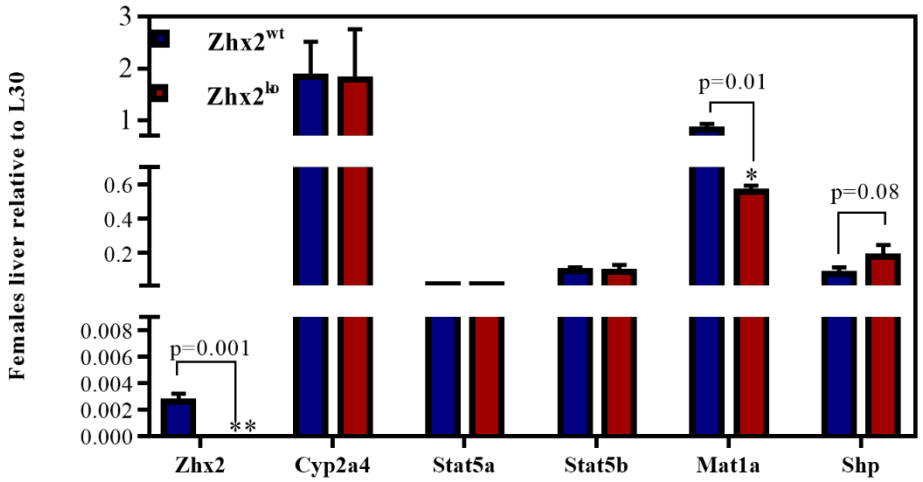

Figure 3.16 Zhx2 regulates Mat1a in the female mice liver. Expression of Cyp2a4, Stat5a, Stat5b, Mat1a and Shp were analyzed in the total RNA of female mice liver using RT-qPCR. Mat1a, but none of the other genes tested, changed in the absence of Zhx2. Data shown are relative to L30. Each Column represents 3 mice. *p=0.01.

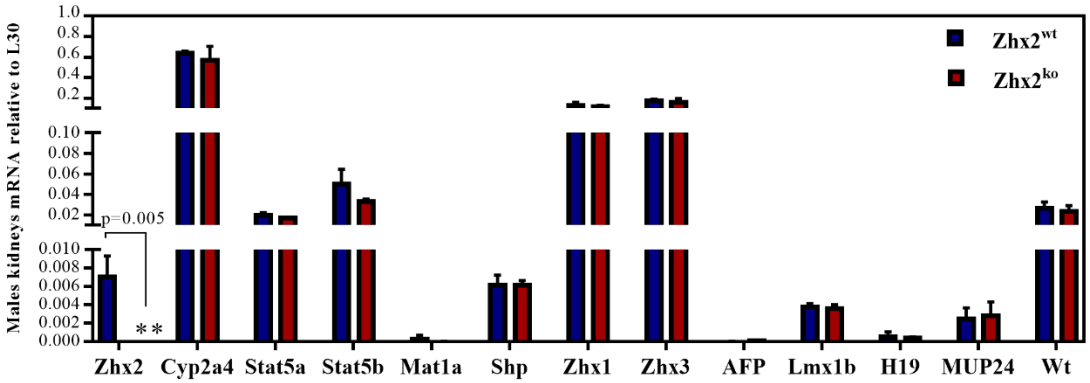

Figure 3.17 Expression of Zhx2 and candidate Zhx2 target genes in the male kidney. Zhx2 is expressed in the kidney but at levels that are lower than Zhx1 and Zhx3. The kidney genes Wt1 and Lmx1b are not altered in the absence of Zhx2. A number of other genes, including several that are known to be regulated by Zhx2 in the liver, are not altered in the absence of Zhx2 in the kidney. Data shown are relative to L30. Each Column represents 3 mice. ** $p \leq 0.005$.

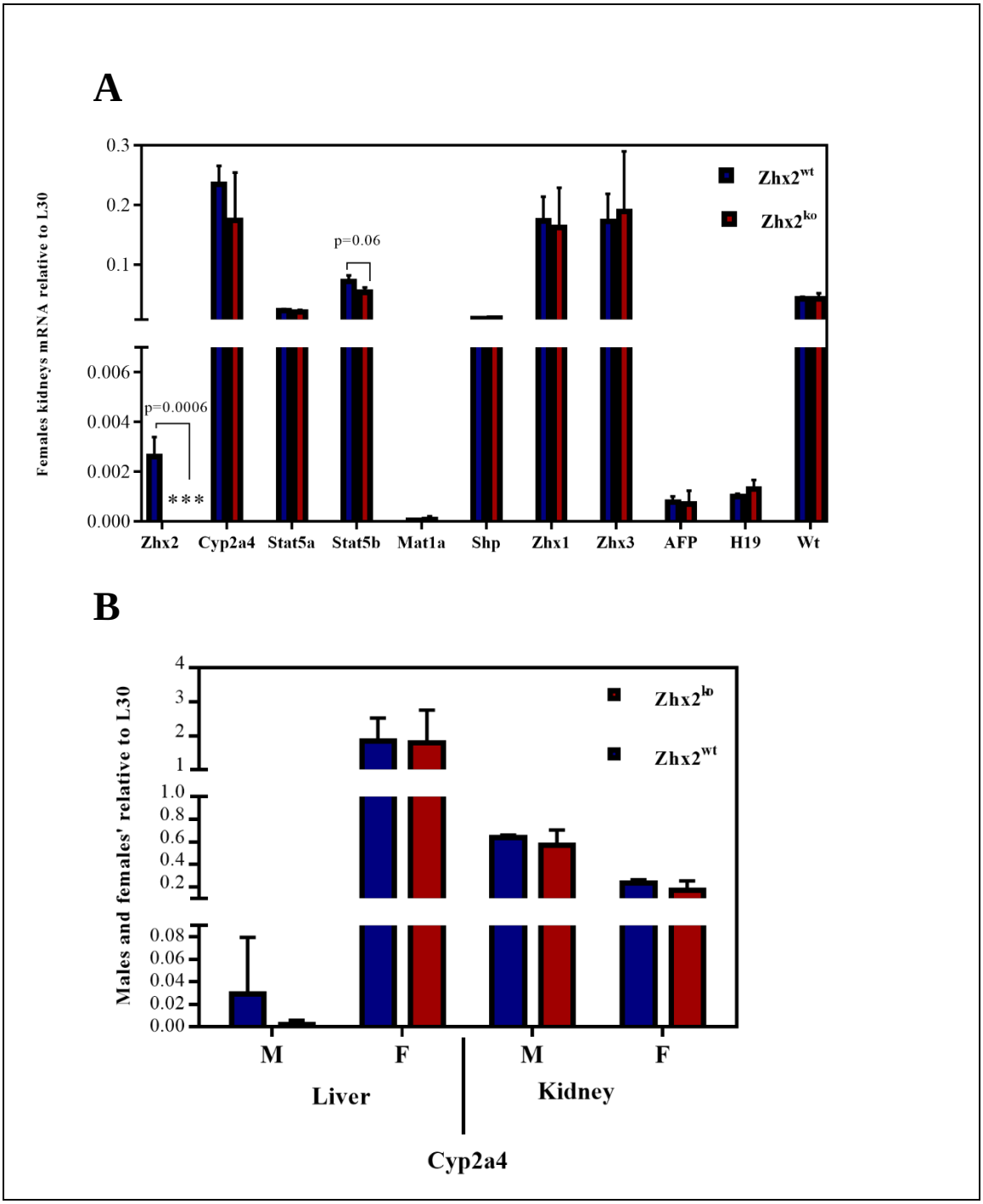
A
Females kidneys mRNA relative to L30
0.3
0.2
0.1
0.006
0.004
0.002
0.000
p=0.06
p=0.0006
***
Zhx2wt
Zhx2ko
Zhx2
Cyp2a4
Stat5a
Stat5b
Mat1a
Shp
Zhx1
Zhx3
AFP
H19
Wt
B
Males and females' relative to L30
4
3
2
1
1.0
0.8
0.6
0.4
0.2
0.08
0.06
0.04
0.02
0.00
Zhx2ko
Zhx2wt
M
F
M
F
Liver
Kidney
Cyp2a4

Figure 3.18 A positive trend was observed between Zhx2 and Stat5b in the females' kidney. RT-qPCR analysis of female adult kidney indicates that candidate Zhx2 target genes are not altered in the absence of Zhx2. Stat5b showed a modest decline in $Zhx2^{ko}$ kidneys but this was not significant (A). Although, Cyp2a4 is female-biased in the liver, Cyp2a4 levels in the kidney are comparable between male and female (B). Data shown are relative to L30. Each Column represents 3 mice. *** $p \leq 0.001$.

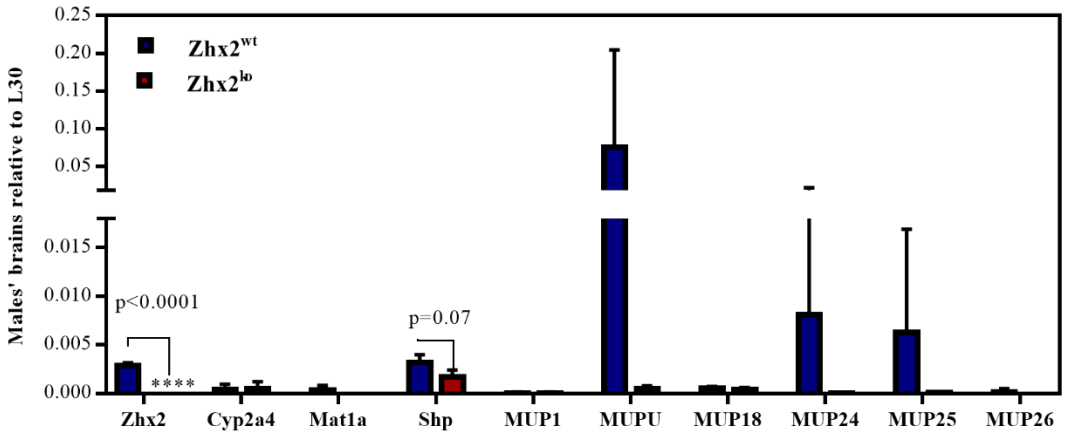

Figure 3.19 Candidate Zhx2 target genes are not altered in adult male Zhx2^{ko} brain. Total adult male mouse brain mRNAs were analyzed by RT-qPCR. Although Zhx2 was dramatically reduced in knock-out mice, none of the other genes tested exhibited a significant change. Data shown are relative to L30. Each Column represents 3 mice. ****p≤0.0001.

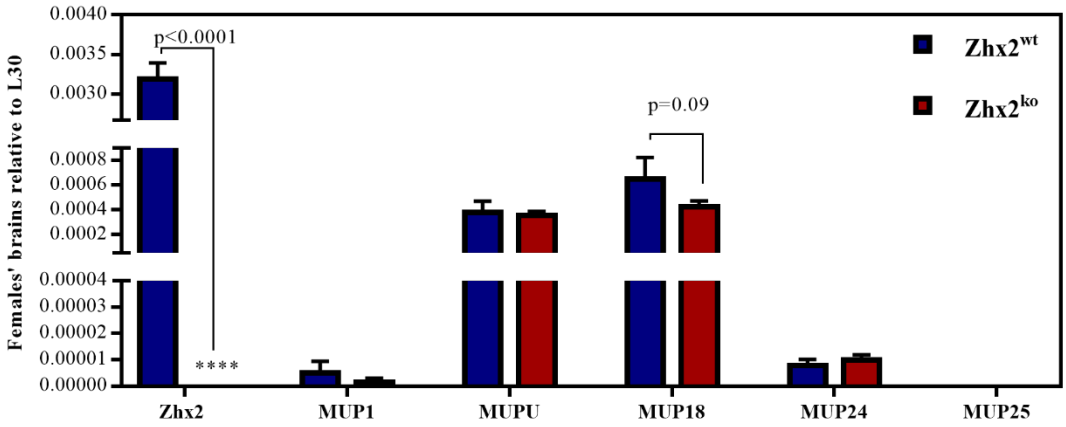

Figure 3.20: Candidate Zhx2 target genes are not altered in adult female Zhx2^{ko} brain. Total adult female mouse brain mRNAs were analyzed by RT-qPCR. Although Zhx2 was dramatically reduced in knock-out mice, none of the other genes tested exhibited a significant change. Data shown are relative to L30. Each Column represents 3 mice. ****p≤0.0001.

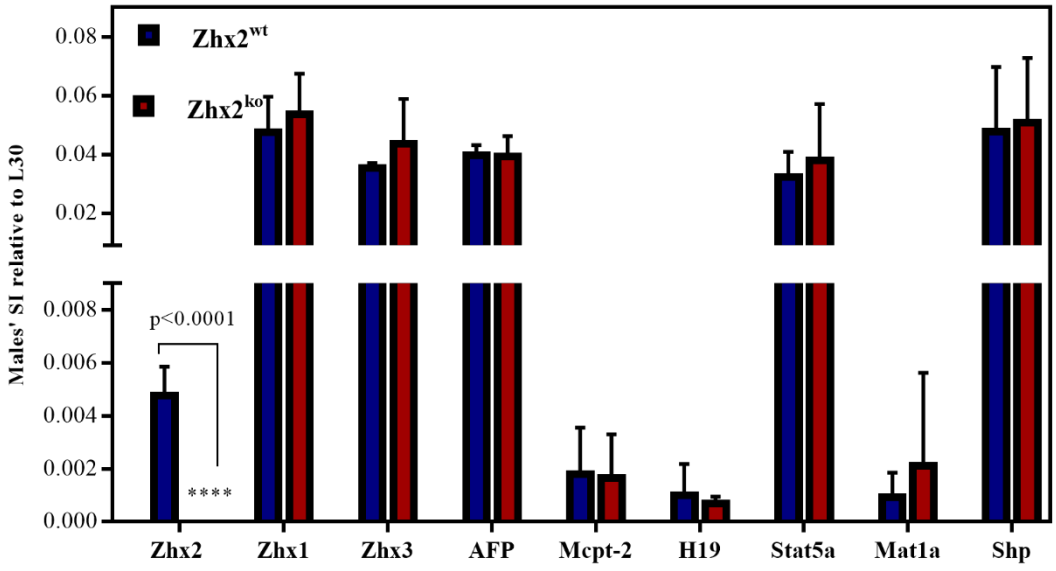

Figure 3.21 Zhx2 target gene expression is not altered in adult male Zhx2^{ko} small intestine. RT-qPCR of total RNA of males SI of Zhx2, Zhx1, Zhx3 and Zhx2 target genes is shown. Data shown are relative to L30. Each Column represents 3 mice.****p≤0.0001.

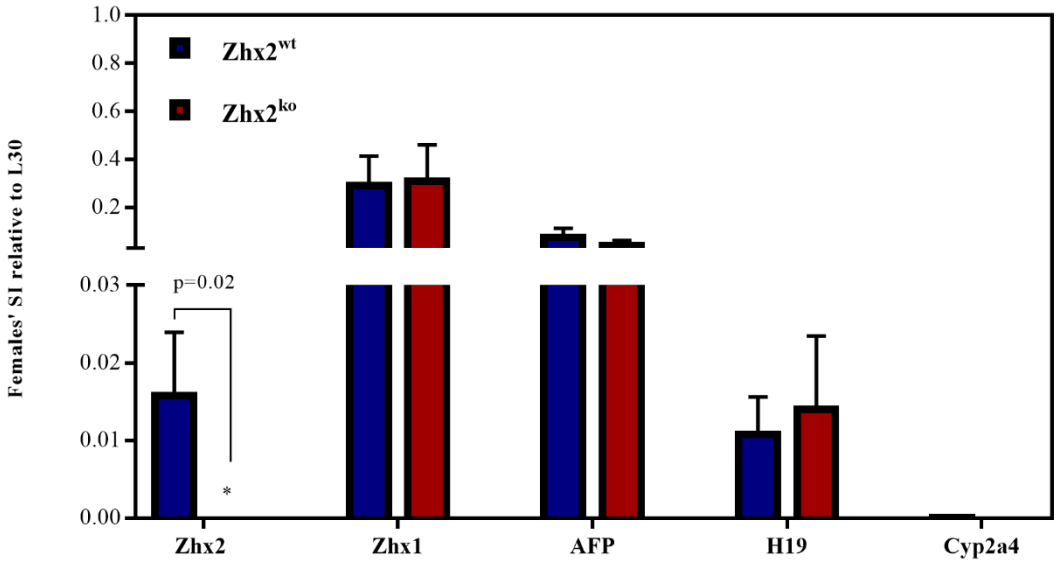

Figure 3.22 Zhx2 target gene expression is not altered in adult female Zhx2^{ko} small intestine. RT-qPCR of total RNA of males SI of Zhx2, Zhx1, Zhx3 and Zhx2 target genes is shown. Data shown are relative to L30. Each Column represents 3 mice. *p≤0.05.

CHAPTER 4

The effect of Zhx2 in postnatal mouse survival

Introduction

Embryonic and postnatal lethality is often seen in knock-out mice. We have observed viable Zhx2 knock-out mice, so we know that the absence of Zhx2 is compatible with life. However, it seemed that postnatal survival of Zhx^{ko} mice might be decreased. Therefore, I performed a careful analysis of postnatal survival and body weight increase of mice that are wild-type, heterozygous or homozygous for deleted Zhx2 allele.

Results:

Postnatal survival of male $Zhx2^{ko}$ mice is reduced:

Matings were set up between mice that were heterozygous for the Zhx2 allele (Zhx2+/-). Cages were monitored carefully to identify litters on the day that they were to be born. Mice were monitored for two months, at which time they were euthanized and DNA was prepared. I also prepared DNA from any mice that died during the two months period. I calculated the number of mice at birth, postnatal day 13 (p13), p20, p33, p44 p50 and p60. I then calculated the percentage of Zhx2+/+ ($Zhx2^{wt}$), Zhx2+/- ($Zhx2^{het}$) and Zhx2-/- ($Zhx2^{ko}$) mice [Data not shown]. Of the three mice cohorts in the study at day 60, we expected to get 25% $Zhx2^{ko}$, 25% $Zhx2^{wt}$ and 50% $Zhx2^{het}$ mice according to Mendelian principles. At p60, the number of surviving male $Zhx2^{ko}$ mice was reduced to 15.9%, which is 9.1% less than expected (Table 4.1). These data suggest that postnatal death of $Zhx2^{ko}$ mice occurs in males but not females.

Weekly measurement indicated a comparable weight gain of $Zhx2^{wt}$, $Zhx2^{het}$ and $Zhx2^{ko}$ mice cohorts which have been fed normal diet (ND):

Previous studies indicated that BALB/cJ mice gained more weight than BALB/c and BALB/cJ+Zhx2 over an eight weeks period when maintained on a high-fat diet. [Clinkenbeard Thesis, 2012]. I therefore weighed the male and female $Zhx2^{wt}$, $Zhx2^{het}$ and

$Zhx2^{ko}$ over a 60 day period when maintained on a regular chow diet. All three female cohorts of mice exhibited the same weight gain (Figure 4.1B). However, multiple comparison analysis using Tukey's test showed significant differences between males $Zhx2^{ko}$ and both $Zhx2^{wt}$ and $Zhx2^{het}$ on day 33 only (Figure 4.1A). This difference is transient as all three male cohorts had the same weight after this one time point.

Overall, there was no significant correlation between knocking down Zhx2, the mice survival rate and gaining weight. Although not significant, there was a trend in the direction of a negative correlation between those parameters.

Discussion

In this project, we monitored survival and postnatal weight gain in $Zhx2^{wt}$, $Zhx2^{het}$ and $Zhx2^{ko}$. These data indicate that male $Zhx2^{ko}$ are born at a lower percentage than predicted, although female are born at the expected ratio. We saw no differences in weight gain in female mice, but did observe that male $Zhx2^{ko}$ mice exhibited lower weight at p33 compare to $Zhx2^{wt}$ and $Zhx2^{het}$ littermates.

Our thinking about increased death in genetically modified mice is logical since similar observation has been reported in the literature and it is due to numerous reasons such as disturbance in neonatal physiological functions including respiratory system, malnutrition and homeostasis [150]. In this Chapter, our data have demonstrated that male $Zhx2^{ko}$ mice were compromised 15.9% of the total live males' mice in this study. Interestingly, the percentage was less than our expectation of 25%. These findings support our previous lab observation and it is novel by being in males only, suggesting that the presence of Zhx2 could play a role in producing healthy pups, however, one cannot be certain if there are other factors have participated in this phenotype. Although, the majority of dying pups after birth were $Zhx2^{ko}$ (data not shown), we have not genotyped the newly born pups to verify their sexes. We believed that the new dying pups are mostly males. Further investigations are required to elucidate these findings (Project is continued).

The study period for this project was 6 months and through this time we noticed that 5 dwarf mice had short necks in addition to being developmentally delayed. Three of them were $Zhx2^{ko}$ and two were $Zhx2^{het}$, they comprised 5% of the total number of the off spring. Interestingly, we have not seen dwarf $Zhx2^{wt}$ mice. Therefore, given that Zhx2 regulates Stat5a and Stat5b [Creasy Thesis, 2015], and Stat5 is critical regulator of growth hormone [146], Mups are downregulated in little mice as well as growth hormone [96], and Zhx2 regulate Mups (Previously discussed in Chapter 3), we hypothesized that knocking out Zhx2 may delay mice growth and development through disturbing growth hormone. We recommend doing a larger study that spans at least two years.

On contrast, when we bred male $Zhx2^{ko}$ to female $Zhx2^{ko}$ to examine if knocking out Zhx2 could be lethal or would produce health disorders, our visual observations have shown normal appearances for 95% of the pups and 5% are dwarf, the rate of weight gain was normal as compared to pups which were offspring of $Zhx2^{het}$ male bred to $Zhx2^{het}$ female (Data not shown). Although, we need to monitor more mice, this data suggest that Zhx2 regulation is likely occurring exclusively in male $Zhx2^{het}$ bred to female $Zhx2^{het}$ mice.

Moreover, Lusis *et al* 2009 have identified Zhx2 as a governor of BALB/cJ *Hyplip2* phenotype. [Clinkenbeard Thesis, 2012] has described Zhx2 as a natural hepatic guardian against lipid accumulation. Zhx2 is a regulator of several lipid metabolism genes which might play a role in CVD [Creasy Thesis, 2015]. For all these reasons, we speculate and correlate Zhx2 to cardiovascular disease and weight gain. In fact, genetic factors have an important role in CVD and NAFLD, although, they are governed by many other factors such as food intake, physical activity, smoking, age and environmental. Considering the fact that one of seven deaths caused by coronary heart disease [151], if knocking out Zhx2 could increase mice susceptibility to weight gain, Zhx2 might be an alternative treatment option to promote survival.

All these data led us to logically propose that $Zhx2^{ko}$ are more susceptible to weight gain than $Zhx2^{wt}$ mice. Unexpectedly, our observation has shown that differences in weight gain rates between $Zhx2^{wt}$, $Zhx2^{het}$ and $Zhx2^{ko}$ were not significant, even though, we observed only a slight decrease in weight of few male and female $Zhx2^{ko}$ as compared to $Zhx2^{wt}$ and $Zhx2^{het}$ on day (D)13. Tukey's test has detected significant differences in

gaining weight of male mice on day 33 might be due to the deletion of Zhx2 and the need has been compensated on the following time period due to elevated expression of unknown developmental genes, it could be another Zhx family member or similar function genes. The fact that small females have gained more weight when they are adults could be because female hormones are likely to make them gain more weight than males. In support of this hypothesis, it has been reported that women tend to gain more weight than males due to hormonal and biological differences [152]. I suggest for future studies to place mice on high fat diet and track the weekly measurement of weight gain (Discussed in Chapter 6).

Newborn mice mortality associated with mice genotypes remain substantial, although evidence of sex-related differences in mortality remain equivocal. Results in Chapter 3 revealed regulation of Zhx2 to several salivary glands MUPs, Mice mother behavior will be influenced due to excess or less Mups being secreted into the mice environment, where they activate neuronal sensors in the nasal cavity. This data led us to speculate that $Zhx2^{het}$ and $Zhx2^{ko}$ pups can miss communicate with their mothers if they expressed different levels of Mups proteins (Discussed in details in Chapter 3), and perhaps could be partially neglected by their parents.

In summary, in this project we presented that Zhx2 correlates with early pup's death. Based on our visual observation, we noticed a trend towards positive correlation between the dwarf mice and having heterozygous or knock out Zhx2 status. Finally, we found no significant correlation between Zhx2 and mouse susceptibility to gain weight except in males on day 33.

Table 4.1 Mice survival at p60

Breeding Cycles	**Males**			**Females**		
	$Zhx2^{wt}$	$Zhx2^{het}$	$Zhx2^{ko}$	$Zhx2^{wt}$	$Zhx2^{het}$	$Zhx2^{ko}$
#1	0	4	1	2	2	1
#2	1	3	0	2	4	1
#3	1	2	1	0	1	1
#4	1	2	1	0	1	2
#5	3	11	3	4	8	5
#6	2	1	0	2	2	0
#7	2	0	0	1	1	0
#8	0	1	1	0	4	1
#9	1	2	0	0	0	5
Total 94	11	26	7	11	23	16
Mice %	25%	59%	15.9%	22%	46%	32%

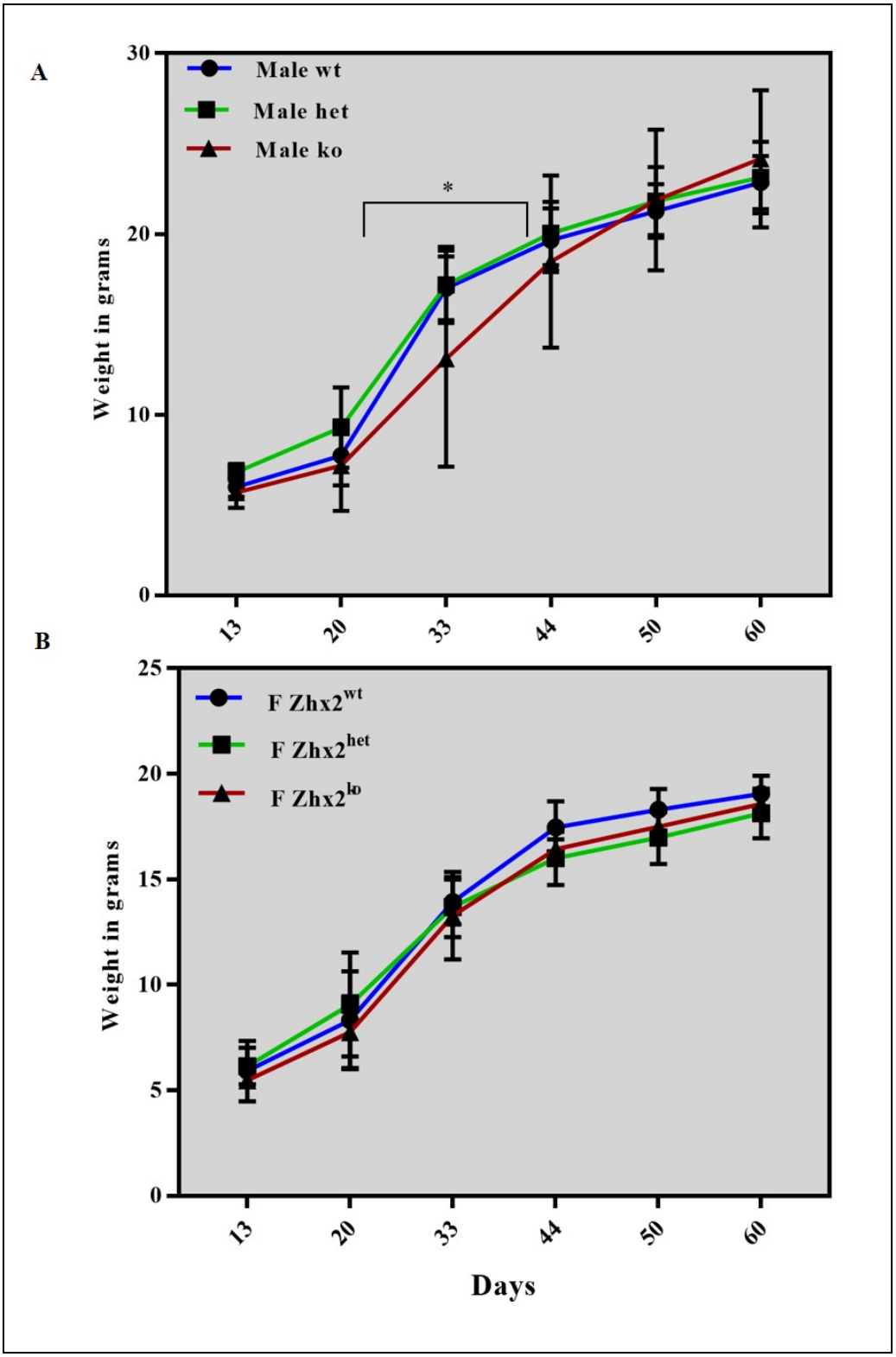
A
Male wt
Male het
Male ko
*
Weight in grams
30
20
10
0
13
20
33
44
50
60
B
F Zhx2wt
F Zhx2het
F Zhx2ko
Weight in grams
25
20
15
10
5
0
13
20
33
44
50
60
Days

Figure 4.1 Comparable weight gain rates were observed in $Zhx2^{wt}$, $Zhx2^{het}$ and $Zhx2^{ko}$ males and female mice cohorts. Males (A) and females (B) were placed on normal diet for 8 weeks and weekly weight measurements have indicated no significant correlation with Zhx2 genetic background of the mice groups except $Zhx2^{ko}$ males on day 33 has shown reduction in gaining weight as compared to the $Zhx2^{wt}$ and $Zhx2^{het}$. Males $Zhx2^{wt}$ n=10, $Zhx2^{het}$ n=10, $Zhx2^{ko}$ n=7, female $Zhx2^{wt}$ n=9, $Zhx2^{het}$ n=10, $Zhx2^{ko}$ n=7

Chapter 5

Zinc finger and homeoboxes (Zhx (family members Zhx1, Zhx2 and Zhx3)): subcellular localization and predicted structural models

Introduction

Proper cell physiological functions require proper protein localization and trafficking. Aberrant protein site between the nucleus and the cytoplasm might result in aberrant cell signaling, which could contribute to numerous health disorders such as cardiovascular disease [153], kidney pathogenesis [126], and cancer [65]. Targeting aberrantly localized proteins has been employed in designing human therapies [153].

Several previous studies have investigated Zhx protein binding affinity and their localization in different cell compartments. For instance, transfected human ZHX1-GFP localized to the nucleus in HEK293 cells [52] and similar results have been reported when the same cell line was transfected with rat ZHX1-GFP [47, 154]. Human ZHX3 can be homodimerized or heterodimerized with ZHX1, ZHX2, NF-YA and localized primarily to nuclei in HEK293 cells [47]. However, different results have been obtained in rodent kidney, including models of kidney disease. In these studies, it appears that ZHX1, ZHX2 and ZHX3 exist as cytoplasmic heterodimers in normal rat kidney podocytes with 80%, 95% and 95%, respectively. In the incidence of kidney Puromycin nephrosis disease, ZHX proteins lose their dimerization and the majority of ZHX3 translocates to the nuclei. Transfected rat ZHX3 tagged with V5 into HEK293 cells localizes to the nucleus; these have been further confirmed using western blot. In general, ZHX protein localization is altered in models of kidney disease, suggesting that these proteins might play a role in glomerular diseases and could serve as future potential prognostic markers in patients, since translocation from normal cellular location has been correlated with the occurrence of the disease [126].

In an attempt to assess ZHX1 localization, one group transfected a ZHX1 (1-873 a.a) full length linked to GFP in HEK293 and observed it in the cells nuclei. Truncated ZHX1 (469-473 a.a), (741-765 a.a) and (861-867 a.a) having NLS, when fused to GFP all

of them have been detected in the nuclei. In contrast, when Zhx1 Zinc finger domains are fused to GFP, this fusion protein is observed in the cytoplasm [52]. The homeodomain 2 (HD2) region of ZHX1 also has a NLS [47], and this domain may be involved in binding NF-YA [45]. Moreover, ZHX1 has been reported to bind several other proteins including the BS69 co-repressor, ataxia-telangiectasia-like protein, Androgen-induced aldose reductase, ATP-IP, Spinocerebellar ataxia type I, Zyxin, Elf-1, and Eleven-nineteen lysine-rich leukemia gene[47]. The ZHX1 core amino acid sequences are conserved between humans and mice despite differences that have been seen in both the C- and N- terminal ends [50]. The rat ZHX1 protein is also conserved, with 92.6% similarity with human and 96.7% with mice [154]. Furthermore, ZHX1 is unique by having 2 NLS, one in the 740-860 a.a region and a second in the C-terminal 830-851 a.a. region [50].

ZHX2 is localized to the nucleus in normal human but is often found in the cytoplasm in HCC. Interestingly, in HCC patients, higher cytoplasmic and decreased nuclear ZHX2 correlates with poor prognosis and decreased overall survival rate. This may be due to enhanced HCC cell proliferation and increased tumor microvascularization. ZHX2 expression plasmids injected into HCC tumor or transfected into cancer cell lines reduced tumor growth and cell proliferation, respectively. Surprisingly, ZHX2 has to reside in the nucleus in order to halt HCC proliferation in vitro and in vivo experiments. In conclusion, liver ZHX2 localization can be employed as a potential prognostic HCC marker, or it could serve as a target for HCC treatment [65]. ZHX2 has two or more NLS, since the full length ZHX2 (1-873 a.a) and truncated forms (1-262 a.a), (263-497 a.a), (263-446 a.a) and (317-446 a.a) tagged with GFP exhibit nuclear localization in HEK293 cells. In contrast, other truncated forms of ZHX2 (317-407 a.a), (408-440 a.a) (441-783) fused to GFP do not localize to the nucleus [46]. Curiously, ZHX2 localization in the brain was different than what has been observed in the liver and HEK-293 cells, but similar to the kidney, since it has been observed in the cytoplasm where it has been shown to bind to the cytoplasmic domain of ephrin-B1 in neuronal progenitor cells (See Chapter 1 for details). Zhx2 cytoplasmic localization appears to be crucial for halting neuronal cell differentiation. However, Ds Red-tagged Zhx2, localized to the nucleus in transfected

COS-7 cells [76]. ZHX2 contains a proline rich region that might enhance its binding affinity [46], and ZHX2 has been reported to bind NF-YA [46].

To investigate which part of ZHX3 determines its cellular localization, HEK293 cells transfected with full-length rat ZHX3 (1-956 amino acids (a.a)) fused to GFP was detected solely in the nucleus. A series of truncated forms of ZHX3 were then generated and each showed different cellular localization. For example, ZHX3(1-303)-GFP and ZHX3(303-555)-GFP where observed in the nucleus, suggesting that ZHX3 contains two or more nuclear localization signals (NLS). However, ZHX3 (555-956)-GFP localized to the cytoplasm, indicating that this region lacks a NLS or contains nuclear export signal (NES). Moreover, ZHX3(242-488) has been hypothesized to bind ZHX1 while ZHX1 (272-432) containing HD1 and HD2 can homodimerize or heterodimerize with ZHX3 [47]. NF-YA binds to ZHX3 via HD1 [47].

These findings support the idea that ZHX proteins are transcription factors and their nuclear location is pivotal for their function. All Zhx proteins have two ZFs and 4 or 5 HDs; ZHX3 also possesses a glutamic acid-rich region located between a.a. 670-710; this is often involved in DNA binding [47]. While more studies are needed, it appears as though ZHX protein localization can be determined by cell type, disease state and species. Due to the notion that different ZHX proteins can possibly bind different targets, and the fact that different cell line might express different proteins, I decided to use bioinformatics tools to find predicted ZHX-interacting proteins.

Bioinformatics

Little is known about Zhx interacting proteins and Zhx tertiary structure. This necessitates efforts to predict the tertiary structure of Zhx proteins in order to reveal possible Zhx-interacting proteins. The iterative threating assembly refinement (I-TASSER) is a computational website described in Nature journal as a reliable method in using sequence, structure and function standards to predict protein tertiary structure and function. This method is based on similarity between the predicted structure and the structure of well-known proteins, since it is reasonable to believe that similarity in structure will reflect

similarity in function. Another reason to choose I-TASSER is that it is rated as one of the best automated method in predicting protein structure by CASP (Community-wide critical assessment protein structure prediction) [155]. Moreover, I-TASSER has TM-align function that will align the target protein sequence to all proteins in the protein data base (PDB) library and find 10 proteins which have shown high homology to the target gene. I-TASSER, through its COACH function, can predict the top 5 proteins that might have affinity to bind target proteins, anticipate the residues that might be involved in the binding and in some cases they provide 3D simulation of the binding [114]. Protein-protein interactions within cells mediate cell signaling pathways that are vital for cell function. Interestingly, the ZDOCK protein-protein docking algorithm server is the highest-resolution computational method which can be used to predict the likelihood that two or more proteins might bind together and identify which domain might be responsible for the proposed binding. M-ZDOCK, another server in ZDOCK website, analyzes the likelihood that target protein can form dimer or trimer with 3D simulation of the final structure [115] .

In summary, ZHX protein localization changes have correlated to numerous diseases and there are conflicting data reporting ZHX protein localization. Therefore, in this Chapter I have investigated ZHX localization in transfected HEK293 cells and primary mouse hepatocytes and have analyzed ZHX structures using bioinformatics tools. These studies could further define the molecular and cellular localization of ZHX proteins and reveal possible binding partners, thus providing information for future clinical targeting of Zhx proteins for therapeutic use.

Results

In this Chapter, I describe localization and predicted biological properties of mouse Zhx1, Zhx2 and Zhx3 (Zhx). In previous studies, our lab along with our collaborator data have demonstrated that ZHX2 is localized in the liver nuclei [65]. Expression vectors for Zhx1, Zhx2 and Zhx3, alone or fused to GFP, were generated. These constructs were transfected alone or in combination in primary mouse hepatocytes, Hep3B cells, HeLa cells and HEK293 cells. Fluorescence imaging of cells, along with 4', 6-diamidino-2-Phenylindale (DAPI) staining of nuclei, was used to determine cellular localization. I

observed that GFP alone localized to the cytoplasm in primary hepatocytes cells (Figure 5.1 A), HEK293 cells (Figure 5.2 A) and HeLa cells (Figure 5.2 B). Similar results were seen in Hep3B (data not shown). Zhx1-GFP was detected in the nuclei of primary hepatocytes (Figure 5.1 B) and co-localized with DAPI in HEK293, although some of these cells exhibited light green fluorescence in the cytoplasm around the nucleus (Figure 5.3 A). Similar results were seen in Hep3B and HeLa cells (data not shown). Zhx2-GFP was highly restricted to the nuclei as all the positive green fluorescent was observed in nuclei of the mouse primary hepatocytes (Figure 5.1 C), co-localized with DAPI in HEK293 (Figure 5.3 B), and in the nuclei of Hep3B and HeLa cells (data not shown). Curiously, all the Zhx3-GFP were observed in the entire cells of primary hepatocytes (Figure 5.1 D) and similar results were seen in HEK293 (Figure 5.3 C), Hep3B and HeLa cells (data not shown). Black dots in the nuclei indicate that Zhx1, Zhx2 and Zhx3 are absent from the nucleolus (Figure 5.3 A-C).

In conclusion, Zhx1-GFP and Zhx2-GFP are localized to the nuclei, while Zhx3-GFP is found throughout the entire cell of transfected primary hepatocytes, HepG2, HeLa cells and HEK293 cells.

Investigate the possibility that Zhx proteins could influence each other localization

Several groups have reported that ZHX proteins can form heterodimers [46, 47, 156]. In an attempt to assess Zhx proteins binding affinity and how the Zhx family members could impact each other subcellular localization, HEK293 cells were co-transfected with Zhx1 or 2 or 3 linked to GFP with Zhx1or 2 or 3 linked to hemagglutinin (HA).

Zhx1-GFP localization is slightly altered when co-transfected with Zhx3-HA

First, HEK293 cells were transfected with Zhx1-GFP plus Zhx1-HA as ZHX1 has been reported to form a homodimer [47]. We found that the majority of positive green cells were localized in the nucleus (Figure 5.4 B). Since ZHX1 has been proposed to bind ZHX2 [156], we investigated whether Zhx2 could alter Zhx1-GFP localization. Therefore, we co-transfected Zhx1-GFP with Zhx2-HA in HEK293 and in all cases, I observed GFP in the nucleus and therefore did not observe any deviations in Zhx1-GFP nuclei localization

(Figure 5.4 C). To determine if Zhx3 might alter Zhx1 nuclear position and since ZHX1 has been proposed to form heterodimer with ZHX3 [47], we co-transfected Zhx1-GFP with Zhx3-HA. We observed that a majority of the cells exhibited nuclear GFP except two cells also showed cytoplasmic staining localization (Figure 5.4 D).

Zhx2-GFP localization is not altered by co-transfection with Zhx1-HA, Zhx2-HA or Zhx3-HA

In order to assess if Zhx2-GFP nuclear localization can be altered by Zhx1, we performed co-transfection of Zhx2-GFP with Zhx1-HA in HEK293 cells. In these co-transfections, Zhx2-GFP always localized to the nuclei (Figure 5.5 B), indicating that Zhx2-GFP localization was not altered by Zhx1-HA. Similarly, when Zhx2-GFP was cotransfected with Zhx2-HA or Zhx3-HA, Zhx2-GFP maintained its nuclear localization (Figure 5.5 C and Figure 5.5D, respectively).

Zhx3-GFP localization was altered by co-transfection with Zhx2-HA, but not by Zhx1-HA or Zhx3-HA

Zhx3-GFP, in HEK293, is found in both the nucleus and cytoplasm. (Figure 5.3 C and 5.6 A). In order to investigate whether other Zhx family members can influence Zhx3-GFP cellular localization, I co-transfected Zhx3-GFP with Zhx1-HA, since Zhx1 has been reported to bind ZHX3 [47]. All the green fluorescence was found in nucleus and cytoplasm in cotransfected cells, indicating that Zhx1 did not influence Zhx3 localization. When Zhx3-GFP was co-transfected with Zhx2-HA, we noticed that green fluorescence was localized to the nucleus in HEK293 cells (Figure 5.6 C) and Hela cells (data not shown). When Zhx3-GFP was co-transfected with Zhx3-HA in HEK293 cells, GFP staining was found in cytoplasm and nucleus (Figure 5.6 D). These data indicate that Zhx2 can alter localization of Zhx3 to the nucleus.

Bioinformatics prediction of mouse Zhx1, Zhx2 and Zhx3 tertiary structure as monomers, homodimers and heterodimers and identification of domains predicted to be involved in the binding

The fact that Zhx3-GFP was localized to the nucleus after co-transfection with Zhx2-HA, along with previous Zhx protein localization data in the literature, led me to use a bioinformatics approach to investigate Zhx protein structures. The I-TASSER prediction website [114] was used to predict Zhx family tertiary structures, and PyMOL software was used to visualize the predicted models (The PyMOL Molecular Graphics System, Version 1.8 Schrödinger, LLC). The highest scored three dimensional (3D) models of Zhx1, Zhx2 and Zhx3 are shown in (Figure 5.7 A-C). I-TASSER also predicted possible proteins that the Zhx family can bind with scores ranked from highest to lowest (data not shown). To identify Zhx protein domains that may be responsible for homodimerization and heterodimerization with each other, ZDOCK was used to predict the binding domains between ZHX proteins. I also used M-ZDOCK to predict the 3D structure of ZHX protein homodimers (Figure 5.8 A-C) and heterodimers (Figure5.9 A-C). http://zhanglab.ccmb.med.umich.edu/I-TASSER/

Prediction of homodimer formation

M-ZDOCK predicts that Zhx1 can form homodimer when ZF1, ZF2 and HD4 of one Zhx1 molecule binds HD1 and HD2 of the other Zhx1 molecule. Moreover, Zhx1 HD5, which is known to be acidic and has higher affinity for binding, has been predicted to be involved in forming the Zhx1-Zhx1 homodimer (Figure 5.8 A). Zhx2 is predicted to form a homodimer when ZF1 of one Zhx2 molecule binds the HD1 of the other molecule and vis versa (Figure 5.8 B). Finally, Zhx3 can form a homodimer through ZF1, ZF2, HD2 and HD3 of both Zhx3 molecules (Figure 5.8 C) and (Table 5.1).

Heterodimer prediction

ZDOCK predicted that ZF1 and ZF2 of Zhx1 is required for its interaction with ZF1 and ZF2 of Zhx2, while HD2 of Zhx1 can bind with Zhx2 HD4 to form the Zhx1-Zhx2 heterodimer (Figure 5.9 A). ZDOCK also predicts that Zhx1 ZF1, HD1, HD2, HD3 could participate in forming Zhx1-Zhx3 heterodimer via docking with ZF1, ZF2, HD1, HD2 and HD3 of Zhx3 (Figure 5.9 B). Finally, Zhx2 HD1, HD2, and HD4 have been

predicted to bind Zhx3 HD1, HD3 and HD4. Interestingly, Zhx3 Zn1, Zn2 and HD5 are not predicted to be involved in binding (Figure 5.9 C) and (Table 5.1).

Discussion

In this Chapter, I reported data regarding Zhx protein localization in different cell lines and mouse primary hepatocytes by use of GFP fusion proteins. This is an ongoing study. Although, the majority of data generated by our lab, our collaborators or independents groups that have discussed the functions and localization of Zhx family are still preliminary, this report provides the initial efforts to monitor the role of protein-protein interactions in understanding Zhx protein localization.

We expected GFP, when tested alone, to be distributed throughout the cells as has been seen in previous studies in HEK293 cells [52]. Our data has indicated that Zhx1-GFP and Zhx2-GFP are localized in the nucleus is not surprising, since similar data with rat proteins have been reported in previous publications [46] [156]. However, our data are novel since we are the first to transfect mouse Zhx proteins and this is the first evidence that mouse Zhx3 is distributed throughout the entire cell, since previous literature indicated that ZHX3 is localized in the nucleus only [47, 53], although my data is similar to rat kidney ZHX3 tissue immunofluorescent staining [126]. It is possible that the GFP in our hybrid GFP-Zhx3 is altering Zhx3 localization. We fused GFP to the N-terminal side of Zhx3, whereas others fused GFP to the C-terminal side of Zhx3 might account for the different results.

The fact that Zhx1 and Zhx2 reside in the nucleus is consistent with their predicted function as transcription factors that bind to the promoter region of target genes to repress or enhance transcription [43, 48]. This hypothesis is supported by studies in our lab and others. The presence of cytoplasmic Zhx3-GFP raises the possibility that Zhx3 might have cytoplasmic functions. Zhx3 has also been proposed to be transcription factor, so we might predict that Zhx3 could shuttle between the nucleus and the cytoplasm and possibly shuttle other proteins with it.

Even though my study is preliminary, we have discussed these results with Dr. Martha Peterson (personal communication) and feel that further studies are justified, particularly since Zhx2 localization appears to be altered in HCC. Current studies being carried out by others are using Zhx proteins fused to fluorescent tagged (mCherry and Tomato). Studies with these will help co-localize Zhx proteins. We are also using confocal microscopy to better image transfected cells.

The fact that Zhx2-GFP to be strictly exists in the nuclei after co-transfection with Zhx1-HA, Zhx2-HA and Zhx3-HA could have two explanations. First, Zhx2-GFP might not bind Zhx1-HA or Zhx3-HA, and the second that there is a binding that is not influencing Zhx proteins normal localization. In general, the binding of our Zhx proteins is still largely elusive.

When we compare Zhx1-GFP and Zhx2-GFP nuclear localization, we see that Zhx1-GFP covers a larger nuclear area than Zhx2-GFP and some of the Zhx1-GFP transfected cells exhibit light green fluorescence in the perinuclear region. These might be explained by at least some Zhx1-GFP being present in the cytoplasm region just around the nucleus. It is not clear whether this means that Zhx1 can shuttle back and forth from the nucleus to the cytoplasm or if such shuttling might be functionally significant. We might speculate that Zhx1 could bind proteins present in the cytoplasm, since it has been hypothesized that Zhx1 binds the co-repressor BS69 [47], which is a nuclear protein but has a cytoplasmic domain and binds target in the cytoplasm [157]. The Yeast two-hybrid system showed that Zyxin could bind ZHX1[47]. Interestingly, Zyxin is a trafficking phosphoprotein that resides mainly in the integrin-rich cytoplasmic area and transport proteins between the nucleus and the cytoplasm and vice versa [158].

The fact that Zhx3-GFP cellular localization has not been altered after Zhx1-GFP co-transfection suggest that that Zhx3-GFP might not bind Zhx1-HA or that such binding is insufficient to move Zhx3-GFP to the nucleus. Staining for HA or repeating the transfection with Zhx1 linked to tomato fluorescent might answer this question (project in progress). Surprisingly, co-transfection of Zhx2-HA with Zhx3-GFP was able to redistribute at least some Zhx3-GFP completely from the cytoplasm to the nucleus. Two

potential mechanisms might explain these results; first, consistent with previous studies indicating that ZHX2 could bind ZHX3, we hypothesize that a direct binding might occur between Zhx3-GFP and Zhx2-HA. The second is that Zhx3 could bind unknown targets in the cytoplasm that sequester the Zhx3 NLS. Zhx2-HA could bind to this unknown target in the cytoplasm and free Zhx3 to enter the nucleus. This hypothesis is supported by a report that found ZHX3 exists as heterodimer in the cytoplasm and upon losing this binding, free ZHX3 can translocate to the nucleus. In contrast to our finding, western blot analysis of HEK293 cells transfected with rat ZHX3-V5 has shown ZHX3 localizes mainly to the nucleus. Similar results were observed after staining the same cells with anti-V5 antibody [53]. Different species could account for our different results since we used mouse Zhx3 and the other study used rat. There is high homology between human, mice and rat Zhx3, but any difference might influence the experiment results.

Recruitment of Zhx3 into the nucleus could potentially promote or impede transcription of target genes of these proteins in the nucleus. These in vitro studies warrant further Zhx1, Zhx2 and Zhx3 localization in various mouse hepatic tissues by immunohistochemistry staining. Such studies might provide insight into the function of Zhx proteins in different tissues and different diseases

As can be seen in figure 5.7 A-C, Zhx1 is structurally more similar to Zhx2 than Zhx3. This prediction is not surprising since ZHX1 amino acid sequence is also more similar to ZHX2 than ZHX3 [156]. Our ZDOCK modelling suggests that HD1 of Zhx1 is critical in forming Zhx1 homodimer and heterodimer with Zhx3. Curiously, Yamada *et al* 2002 has shown similar results via generating multiple ZHX1 constructs and testing them using yeast-two-hybrid system [52].

Our docking sites prediction of Zhx binding sites through ZDOCK is consistent with Kawata *et al* [156] by showing that Zhx1-HD1 binds to Zhx3, Zhx1 HD2 binds Zhx2 and Zhx2 HD1 binds to Zhx3. Moreover, it has been reported that Zhx1 can bind activation domain of NF-YA via HD1 and HD2 [45]. ZDOCK predicted that Zhx1 can homodimerize via HD1 and heterodimerize with Zhx3 by several domains including HD1 and HD2 (Figure 5.9 B), which further support the importance of these domains in Zhx1 binding

affinity and validate ZDOCK and M-ZDOCK as good programs to predict potential interaction domains. On the other hand, Zhx2 HD1 and HD2 have been proposed to be important in Zhx2 binding to NF-YA [46].

In order to validate ZDOCK and M-ZDOCK predictions, we might prepare a series of truncated and mutated Zhx constructs to analyze in tissue culture cells. Of particular importance would be NLS and NES regions that are involved in nuclear-cytoplasmic localization of Zhx proteins.

Table 5.1 Computer prediction of domains participate in forming Zhx homodimer or heterodimer

Binding form	**First protein**	**Second protein**
Zhx1-Zhx1	**Zhx1**	**Zhx1**
Computer prediction	ZF1 and ZF2	HD1
	HD4	HD2
	HD5	
Yeast-two-hybrid [52]	HD1	HD1
Zhx2-Zhx2	**Zhx2**	**Zhx2**
Computer prediction	ZF1	HD1
	HD1	ZF1
Yeast-two-hybrid [46]	HD1	HD1
Zhx3-Zhx3	**Zhx3**	**Zhx3**
Computer prediction	ZF1 and ZF2	ZF1 and ZF2
	HD2	HD2
	HD3	HD3
Yeast-two-hybrid [47]	HD1	HD1
Zhx1-Zhx2	**Zhx1**	**Zhx2**
Computer prediction	HD2	HD4
	ZF1 and ZF2	ZF1 and ZF2
Yeast-two-hybrid [46]	HD1 and HD2	HD1
Zhx1-Zhx3	**Zhx1**	**Zhx3**
Computer prediction	ZF1	ZF1 and ZF2
	HD1	HD1
	HD2	HD2
	HD3	HD3
Yeast-two-hybrid [47]	HD1	HD1
Zhx2-Zhx3	**Zhx2**	**Zhx3**
Computer prediction	HD1	HD1
	HD2	HD3
	HD4	HD4
Yeast-two-hybrid [156]	HD1	HD1

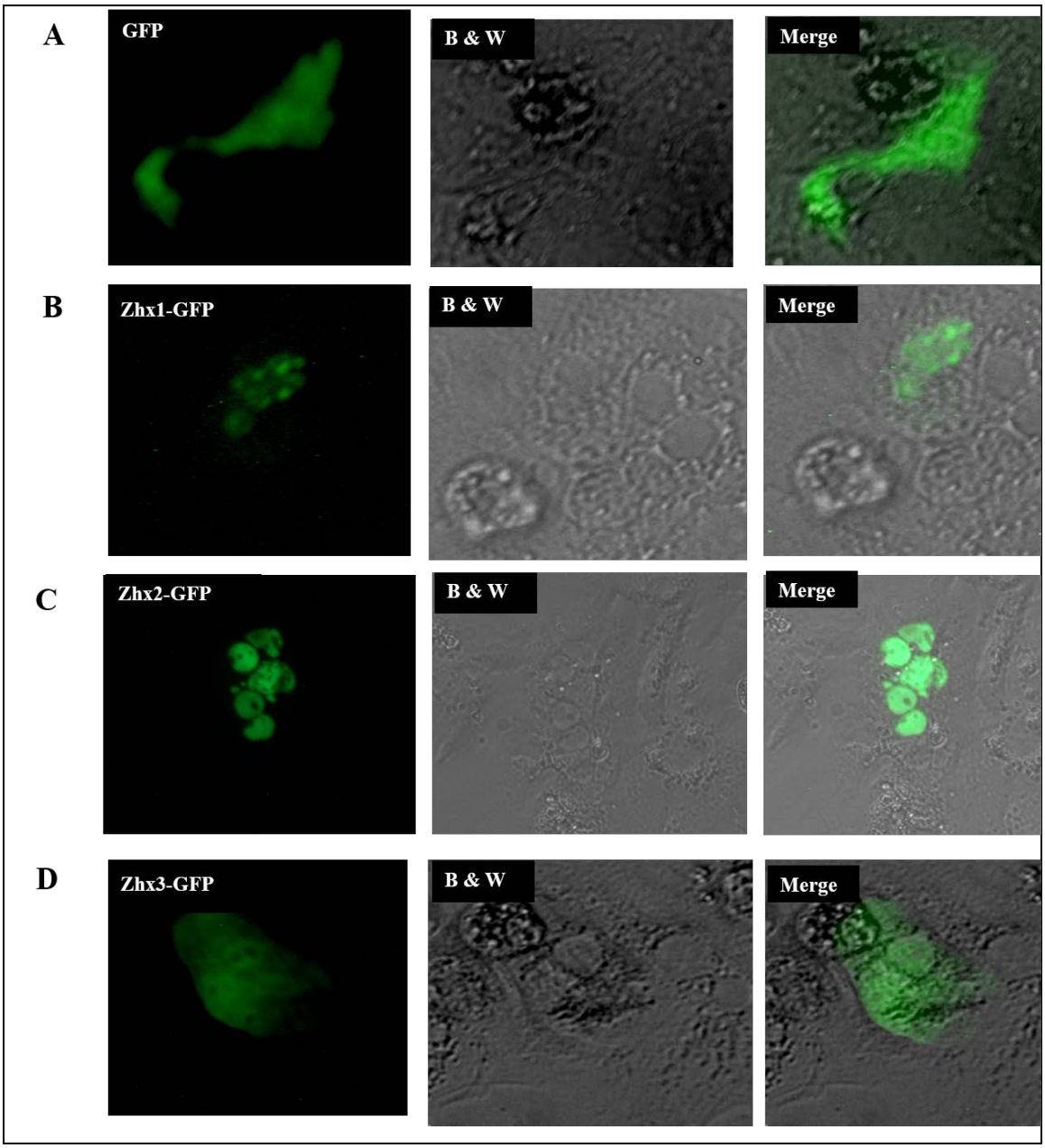
A
GFP
B & W
Merge
B
Zhx1-GFP
B & W
Merge
C
Zhx2-GFP
B & W
Merge
D
Zhx3-GFP
B & W
Merge

Figure 5.1 Nuclear localization of Zhx1-GFP, Zhx2-GFP, and cellular localization of Zhx3-GFP have been observed in mouse primary hepatocytes. $Zhx2^{wt}$ mouse liver was perfused, cells were cultured and 24 hour later transfected with expression plasmids which encode GFP alone, or Zhx1-GFP, Zhx2-GFP or Zhx3-GFP. 48 hours after transfection GFP was seen in the entire cell (A), Zhx1-GFP in the nuclei (B). While Zhx2-GFP was seen solely in the nuclei (C). Zhx3-GFP was observed in both nucleus and the cytoplasm of the cell (D). The left panels are the fluorescence microscopy photographs, the middle are the phase contrast microscopy photographs of the same fields and the right panels are the merge of both pictures.

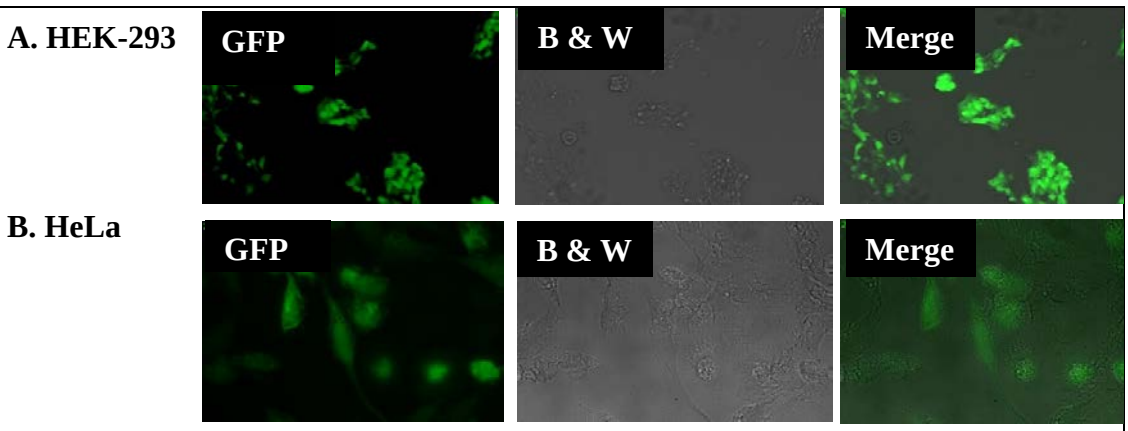

Figure 5.2 Cellular localization of GFP in HEK-293 and HeLa cells. GFP plasmid was transfected into either HEK-293 (A) or HeLa cells (B). GFP was observed in the entire cell 48 hours after transfection in both cell lines. The left panels are the fluorescence microscopy photographs, the middle are the phase contrast microscopy photographs of the same fields and the right panels are the merge of both pictures.

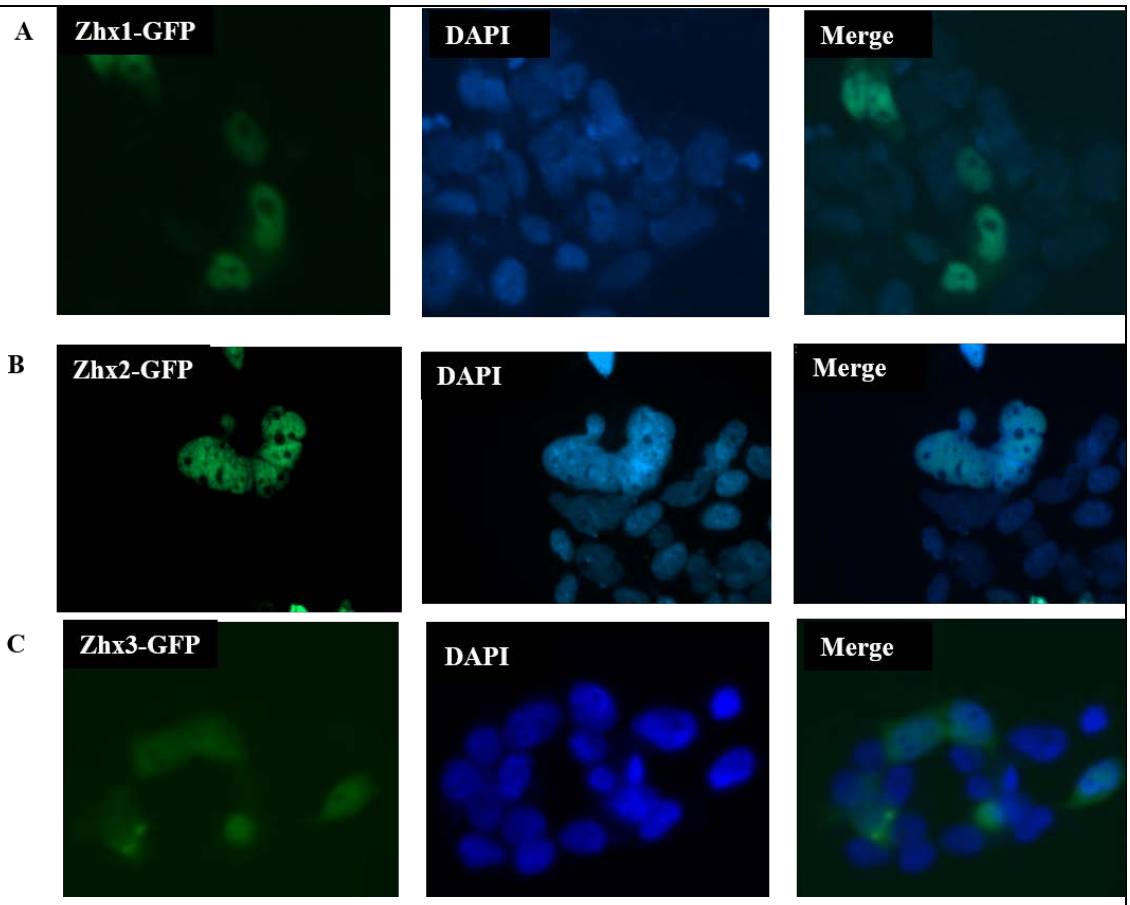

Figure 5.3 Zhx2-GFP and Zhx1-GFP was observed in the nuclei while Zhx3-GFP was seen in the entire cell of HEK-293 cells. Fluorescent microscopical images have shown Zhx1 (green) localized in nucleus with DAPI (blue) and show light green in the cells around the nucleus (A). Zhx2 has been seen only in the nuclei (B). Zhx3 (green) has overcome the nucleus (blue) in the merge cells and show light blue in the nucleus surrounded by green color indicating the presence of Zhx3 in the nucleus and the cytoplasm (C).

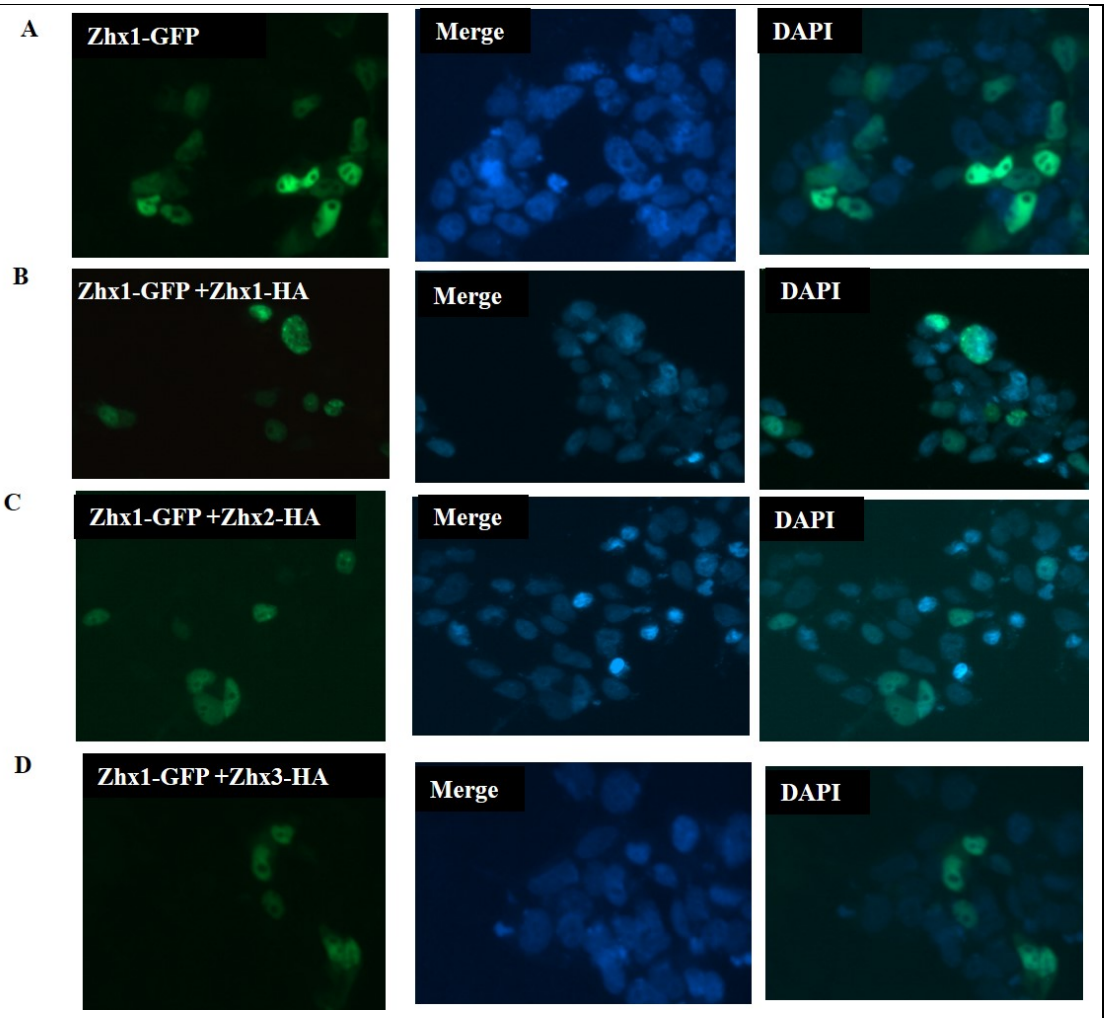

Figure 5.4 Zhx3-HA partially altered Zhx1-GFP localization. Fluorescent microscopically images were shown that Zhx1-GFP to localize in the nuclei of HEK-293 cells whether it transfected alone (A), or co-transfected with Zhx1-HA (B), or with Zhx2-HA (C). Co-transfection with Zhx3-HA has yield nuclear localization except for two cells that showing Zhx1-GFP localizes in the whole cell (D).

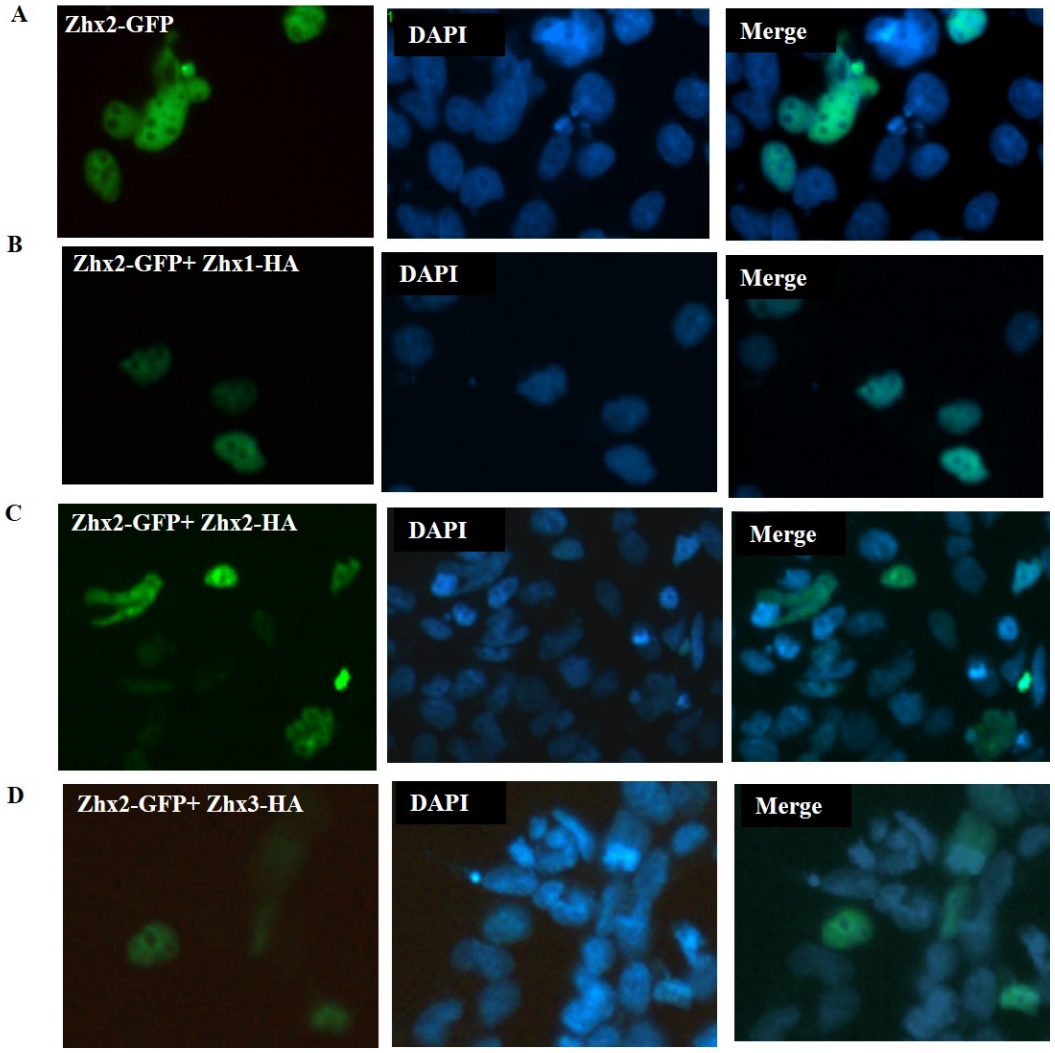

Figure 5.5 Zhx2 nuclear localization was not altered by Zhx1-HA, Zhx2-HA or Zhx3-HA. HEK-293 cells were shown nuclear Zhx2-GFP localization when it transfected alone (A), or co-transfected with Zhx1-HA (B), or Zhx2-HA (C), or with Zhx3-HA (D).

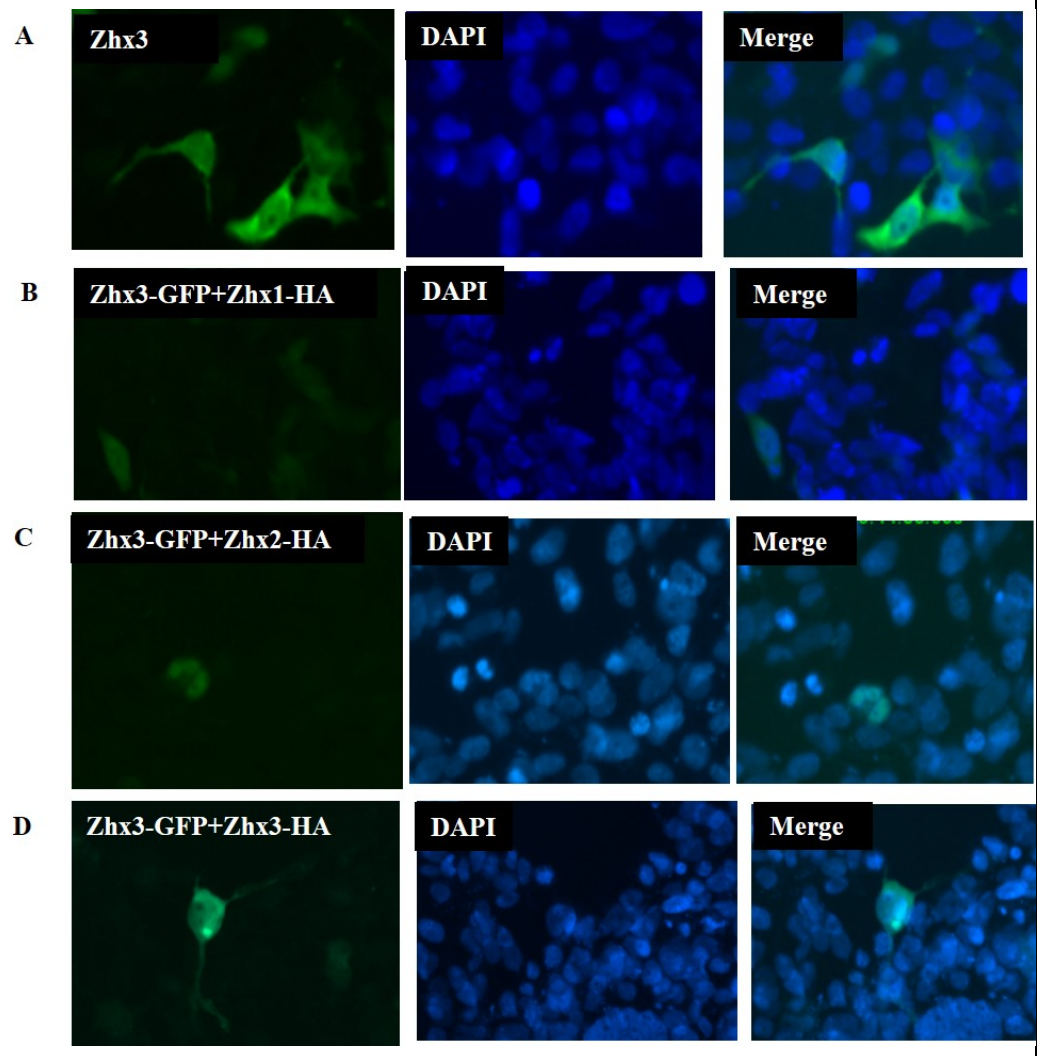

Figure 5.6 Zhx3-GFP whole cell localization was being dramatically altered by Zhx2-HA co-transfection in HEK-293 cells. Zhx3-GFP was observed to be localized in the entire cell when transfected into HEK-293 cells alone (A), or co-transfected with Zhx1-HA (B), or Zhx3-HA (D). Curiously, co-transfection with Zhx2-HA has altered Zhx3 localization to be strictly localized into the nuclei (C).

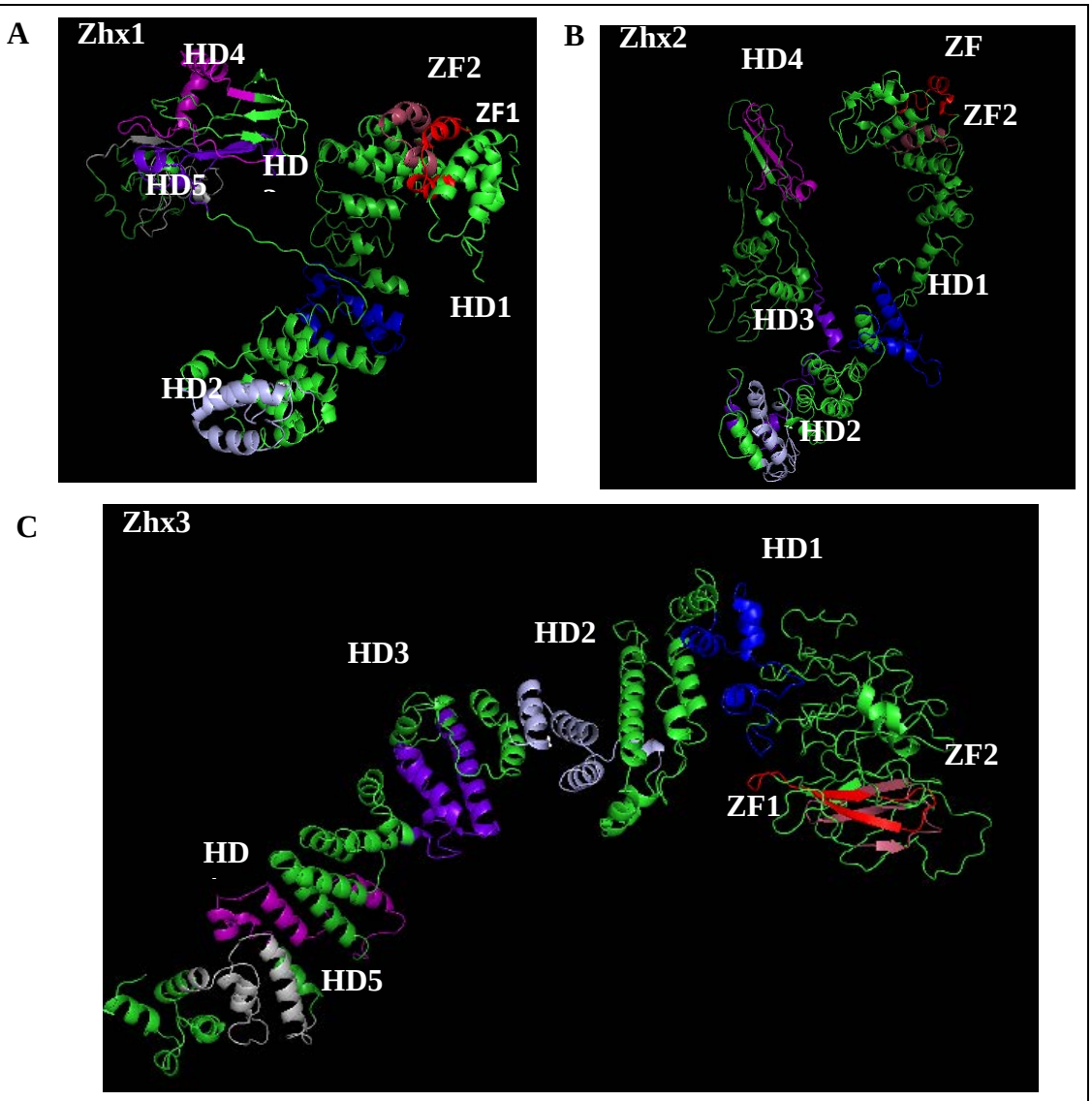

Figure 5.7 3 Dimensional structure prediction of mouse full length Zhx1, Zhx2 and Zhx3 proteins. The sequences were inserted in I-TASSER online server to predict 3 D structure of Zhx1, Zhx2 and Zhx3. Zhx1 and Zhx3 have 2 Zinc finger (ZFs) on the N-terminal and 5 HD on the C-terminal side (A) and (C). Zhx2 tertiary structure has 2 ZFs on the N-terminal and 4 HDs on the C-terminal (B). ZF1 is red, ZF2 is raspberry, Homeodomain (HD) 1 is blue, HD2 is light blue, HD3 is purple blue, HD4 is magenta and HD5 is white.

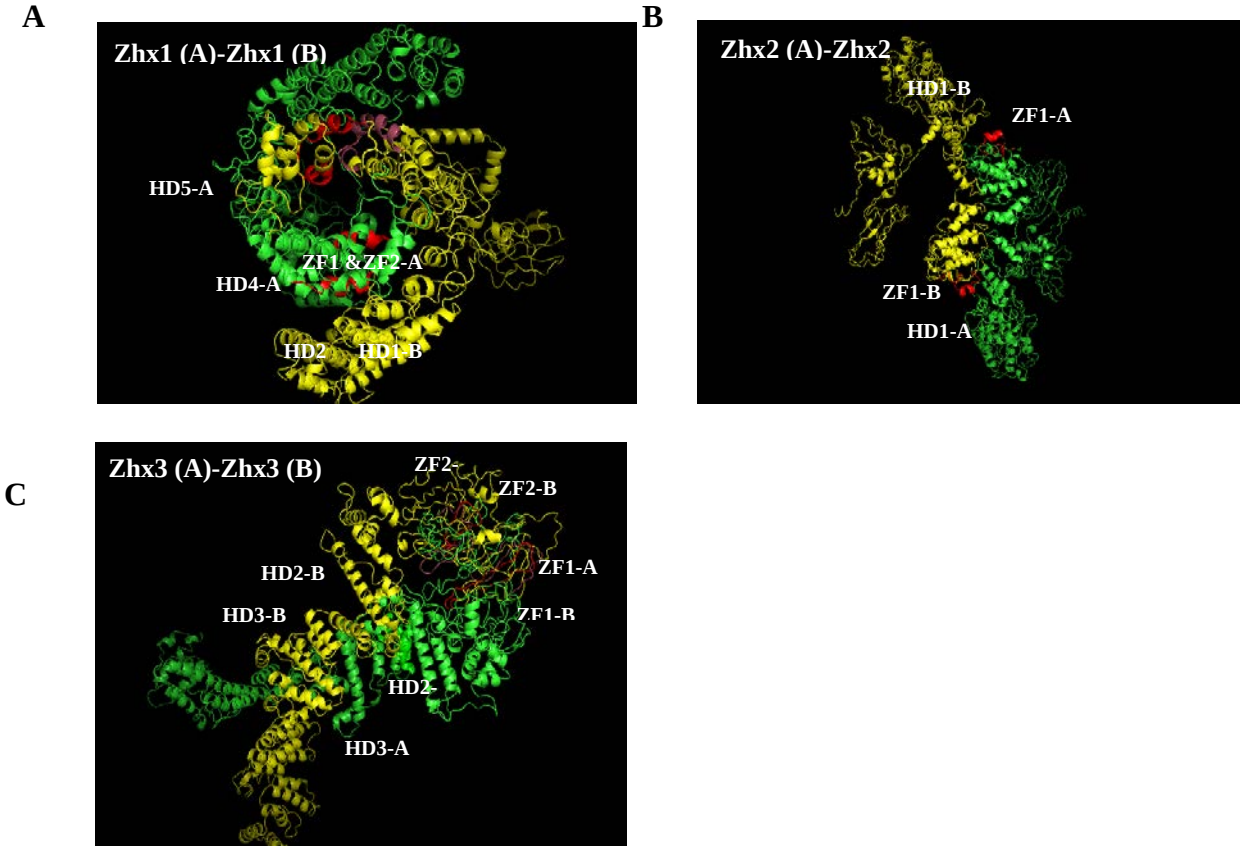

Figure 5.8 Simulation of the predicted Zhx1, Zhx2 and Zhx3 homodimer. Zhx1 (green, molecule A) via ZF1, ZF2, HD4 and HD5 can homodimerize with other Zhx1 molecule (yellow, molecule B) that participate in the binding via HD1 and HD2. ZF1 of Zh2 (green, molecule A) has been anticipated to bind HD1 of Zh2 (yellow, molecule B) and vis versa (B). ZF1 (red), ZF2 (raspberry), HD2 and HD3 of Zhx3 molecule (green) has been predicted to bind ZF1 (red), ZF2 (raspberry), HD2 and HD3 of the second Zhx3 molecule (yellow) to form a homodimer (C).

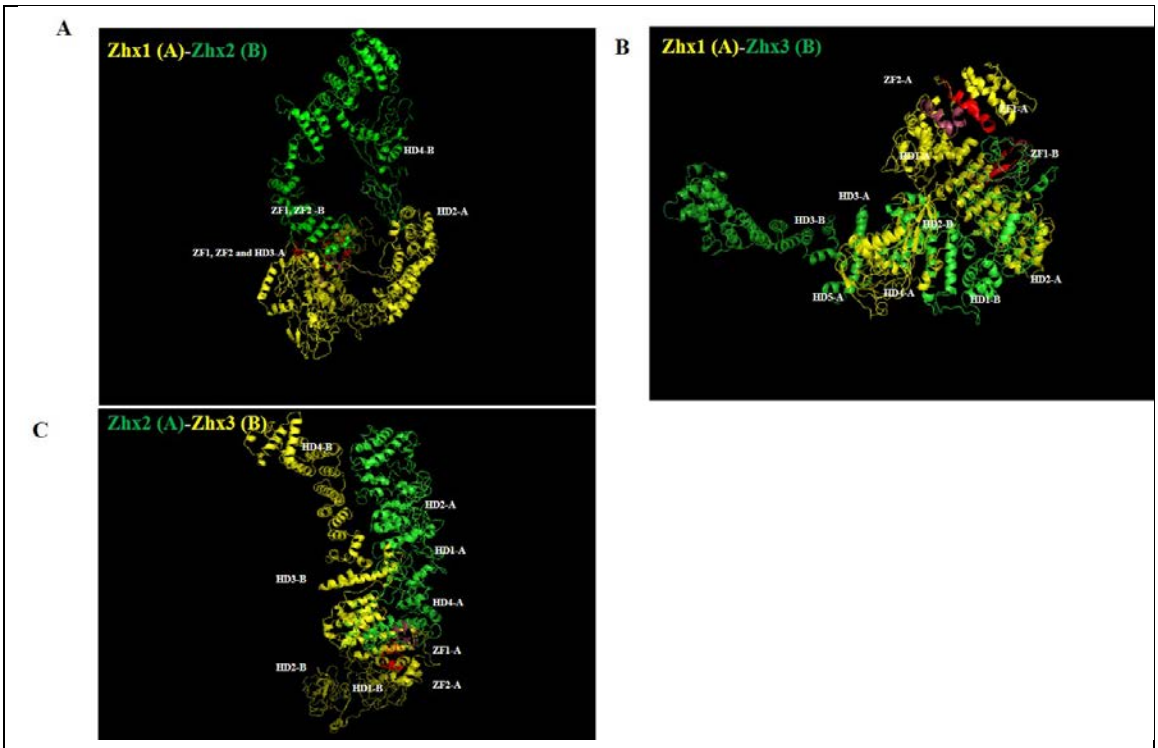

Figure 5.9 Simulation of the predicted mouse Zhx1, Zhx2 and Zhx3 heterodimer. ZF1, ZF2 and HD3 of Zhx1 (yellow) has been predicted to bind Zn1 and Zn2 of Zhx2 (green), while HD2 of Zhx1 can bind HD4 of Zhx2 (A). Zhx1 (yellow) was been predicted to bind Zhx3 (green) through ZF1, ZF2, HD1, HD2, HD3 and HD4. While Zhx3 participate in the binding via ZF1, ZF2, HD1, HD2 and HD3 (B). Zhx2 (green) has been proposed to form a heterodimer with Zhx3 (yellow) via HD1, HD2 and HD4, while Zhx3 participate in the binding via HD1, HD3 and HD4 (C).

Chapter 6

Conclusion and future direction

The hepatic role of Zhx2 has been well documented; however, little was known concerning Zhx2 regulation of target genes in non-hepatic tissues. My dissertation has ignited a greater interest in further exploring the poorly understood role of Zhx2 in non-hepatic tissues. My data reported in Chapter 3 suggest that Zhx2 functions as either a potent transcriptional activator or repressor of several genes with diverse functions including lipid homeostasis, cancer, behavior and a possible correlation with sexually dimorphic gene expression. My dissertation was the first in utilizing the $Zhx2^{ko}$ mice in addressing Zhx2 functions in both hepatic and the non-hepatic tissues.

The Spear lab, along with collaborators, previously demonstrated that Zhx2 negatively regulates AFP, H19 [43], Gpc3 [42] and Lpl and positively regulates Elovl3 [48]. Additionally, in HCC, nuclear localization of Zhx2 proteins correlates inversely with high-grade cancer and has the potency to reduce liver cancer proliferation [65]. Taken together, these data provide clinical evidence that Zhx2 may be novel drug target in liver cancer which may increase survival.

Chapter 3 of this dissertation was the first documentation using RT-qPCR that Zhx2 is expressed ubiquitously, although Zhx2 mRNA levels vary between different organs. I discovered that Zhx2 negatively regulates Mup genes in SG in both males and females and LG in males (I did not examine female LG), including Mup1, MupU, Mup18, Mup24 and Mup25. I will test M MupU in the females SG as it has shown significant reduction by Zhx2 in the males. Building upon these observation, it is plausible to examine Mup gene expression in female lacrimal glands. Further studies should focus on elucidating the mechanism by which Zhx2 controls Mup downregulation in SG and LG. Although Mup genes are not present in human, these data raise the possibility that Zhx2 could be required for salivary glands function in mice. Since Zhx2 and Mup expression in the liver increase after birth, it would be interesting to examine their expression in the SG and LG starting at late embryonic days to p60. It would also be interesting to perfuse the SG to separate it into 3 regions (parotid, submandibular and sublingual) and then investigate Zhx2 and Mup

expression in these regions. Immunohistochemical staining of the SG to investigate Zhx2 and Mup localization could also be performed. Since previous studies reported that MupII (an old term of liver Mup) the mainly expressed liver Mup has been detected in mice mammary glands [97], I hypothesize that mammary gland Mup genes expression will likely either be inversely or positively correlated with the Zhx2 deletion. To test this hypothesis, one would utilize RT-qPCR to analyze mammary glands Mup expression in $Zhx2^{ko}$ and $Zhx2^{wt}$ mice. Moreover, I documented that the Zhx2 deletion did not alter Zhx1 and Zhx3 levels in the SG.

I also demonstrated possible clinical relevance of Zhx2 in regards to human disease as I detected a significant positive and a trend of negative correlation in the mouse liver between Mat1a and Shp, respectively, with Zhx2 (discussed in Chapter 3). Therefore, deletion of Zhx2 in mice is likely to disrupt lipid homeostasis, which would influence the likelihood of cardiovascular disease. Future directions along these lines should focus on elucidating the role of Zhx2 role in CVD. We also hypothesize that $Zhx2^{ko}$ mice could have low plasma methionine level similar to Mat1a knockout mice [33]. To test this hypothesis, we can analyze methionine levels in the plasma of $Zhx2^{ko}$ and $Zhx2^{wt}$ mice. We can also feed mice a high fat diet since we predict that they will get fatty liver similarly to what has been observed in Mat1a knockout mice [33]. I predict that $Zhx2^{ko}$ mice, at 8 months of age, will exhibit spontaneous macrovesicular non-alcoholic steatosis since this result has been seen in Mat1a knockout mice due to elevated liver Cyp2E1 [37]. Indeed, Cyp2E1 might be a future target of Zhx2 and may to be elevated in the liver of $Zhx2^{ko}$ mice. Likewise, Cyp4A10 and Cyp4A14 are predicted to be downregulated in $Zhx2^{ko}$ mice as they have been decreased in Mat1a knock out mice [37]. Since Mat1a knockout mice have enlarged liver as compared to the wild type mice [33], and my data documented that $Zhx2^{ko}$ mice have lower level of Mat1a expression, we will monitor liver to body ratio of the $Zhx2^{ko}$ mice and compare them to the $Zhx2^{wt}$ mice. Since Mat1a is required for VLDL assembly and normal plasma lipid levels [36], I propose that $Zhx2^{ko}$ mice could exhibit altered VLDL composition. To investigate this, blood VLDL from $Zhx2^{ko}$ and $Zhx2^{wt}$ mice will be monitored. The ratio of the lipid in both cohorts could also be compared.

Finally, the molecular switch in gene expression between Mat1a and Mat2a in the liver has led me to predict that Mat2a is a prospective negative Zhx2 target, as it resembles AFP in being expressed in the fetal liver, switch off after birth and reactivated in liver regeneration and HCC [39]. Moreover, Mat2a is expressed in the kidney [39] varies between day night [149]; therefore, studies could investigate Mat2a in the liver and kidney of $Zhx2^{ko}$ and compare them to $Zhx2^{wt}$ mice at the day and night.

The fact that decreased testosterone levels decrease Mup gene expression [96] led me to hypothesize that testosterone could be downregulated in the $Zhx2^{ko}$ mice, but not severely as they have not shown feminine characteristics.

CD36 fatty acid translocase and PPARγ are positively correlated with Zhx2 in $Zhx2^{\Delta hep}$ mice [Creasy, 2015], and Zhx2 is a potential lipid regulator. Therefore, I suggest testing the expression of CD36 and PPARγ in $Zhx2^{ko}$ and $Zhx2^{wt}$ mice. Additionally, Cyp2D6 is a possible negatively-regulated candidate of Zhx2 as it inversely correlates with Shp levels [140]. The Shp partner neuronal PAS domain 2 (Npas2) that play a role in lipid homeostasis since it regulates lipid oscillation could also be studied. Furthermore, orphan receptors ROR and REV-erb correlate with Shp [139], so their levels should also be tested in $Zhx2^{ko}$ mice.

We could also investigate whether there is liver necrosis in $Zhx2^{ko}$ mice via testing GPT, GOT serum levels, in addition to analyzing c-jun and c-fos expression in the liver since these markers are altered in the liver after H19 elevation and Shp downregulation [136]. Moreover, I suggest testing Smad as target of Zhx2 since its expression correlates with H19. Since H19 is expressed after birth in the skeletal muscle [31], I will test Zhx2 regulation of Smad in this tissue, as I believe that skeletal muscle is a good future organ to study Zhx2 regulation of genes.

Studies of kidneys demonstrated a trend towards a positive correlation between Zhx2 and Stat5b in the female but not male kidney as compared to $Zhx2^{ko}$ mice. These data may reach significance with increased mice numbers. Taken together with our previously reported data demonstrating a positive correlation of Zhx2 to both of Stat5a and Stat5b in

the liver of Zhx2$^{\Delta hep}$ mice [Creasy Thesis, 2015], and with the independent investigator reports documented that both of Stat form regulate growth hormone [146], these data suggest that Zhx2 could be associated with kidney developmental delay disorders. Future direction for this study should focus on elucidating the mechanism by which Zhx2 promotes Stat5b expression in the kidney. Moreover, to determine whether Zhx2 is participating in normal kidney function, we could examine podocyte protein-tyrosine phosphatase (GLEPP1) as its expression has been reported to be decreased when there is defect in the kidney function [159]. It has been reported that castrated mice decrease kidney Cyp2a4 concordant with increase Cyp2a4 in the liver [148]. It would be of interest for our study to examine the influence of Zhx2 status on the reciprocal regulation of Cyp2a4 in castrated Zhx2$^{\Delta hep}$ mice.

As mentioned in Chapter 3, I reported a trend toward a positive correlation between Zhx2 and Shp within the male brain. Therefore, I suggest testing Shp in female brain samples. Moreover, we observed a trend, in females only, towards a positive correlation between Zhx2 and Mup18. Since BALB/cJ mice exhibit a small brain size [81], I propose that Zhx2^{ko} mice could have small size brain as will be compared to Zhx2^{wt} mice. To test this hypothesis, we could monitor brain to body weight ratio in the mice cohort (project in progress). Moreover, I hypothesize that Zhx2 could correlate with ephrin-B in the brain since they have been reported to bind each other [76], and miR-4277 since it has been hypothesized to be associated with Zhx2 in Parkinson disease. To validate this assumption, we will quantify their expression in the Zhx2^{ko} and Zhx2^{wt} mice.

Although I did not detect any correlation between Zhx2 and the Zhx2 target gene expression in the small intestine, I suggest testing Mcpt-2 in the small intestine of Zhx2^{ko} and Zhx2^{wt} mice infected or not infected with helminths, since Mcpt-2 has been detected in BALB/cJ mice after parasite stimulation [144].

Since we hypothesized that Zhx2 could bind to its targets promoters to reduce or enhance expression via its two ZF and four HD, I propose that Zhx2 activate Mat1a, Shp, Stat5b, repress H19, repress/or activate Mup1, Mup18 via direct binding to their promoters. We could conduct several assays to test this hypothesis. First, we could amplify and purify

H19, Mat1a, Shp, Stat5b, Mup1, MupU, Mup18 promoter regions from BL/6 mice genomic DNA and clone them into pGEM-TEasy vector (promega) and verify their identity by sequencing. Fragments could then be excised and subcloned into the luciferase vector pGL4.14. Transient transfections could then be performed in HEK-293 or AML-12 cells with Zhx2 and the luciferase reporter plasmids. After cotransfection the cells with Zhx2 and the constructs, we would anticipate the luciferase level will be either elevated for Mat1a and Stat5b constructs or decreased for Shp, H19, Mup1 and Mup18. If the predicted results are obtained, serial promoter deletion constructs could be used to identify a Zhx2 consensus binding site. Targets that show potential Zhx2 binding will further be confirmed utilizing chromatin Immunoprecipitation (ChIP). Alternative methods could also be used to analyze Zhx2 function, including the yeast-2-hybrid system.

If experiments reveal Zhx2 does not directly bind control regions of target genes, an alternative hypothesis is that Zhx2 could regulates targets via posttranslational events. In support of this hypothesis previously, our lab has generated AFP-promoter construct since AFP is the well-known target of Zhx2. Although, BALB/cJ mice, possess mutated Zhx2, have 10-20 fold higher AFP than BALB/c mice (see Chapter 1 for details), AFP promoter-Luc has shown only 2-fold difference after cell line transfection. This puzzling data suggest a post-translational events. Data generated by Dr.Peterson lab (Turcios, L and Peterson, M unpublished data) have detected antisense-AFP further supporting this hypothesis.

BALB/cJ are more susceptible to fibrosis than other mice strains. QTL analysis in a cross between BALB/cJ mice and A/J mice, a fibrosis-resistant mouse strain, has mapped the fibrotic gene (later named Hfib1) to chromosome 15. Interestingly, Zhx2 resides in this area. Therefore, we anticipate that treating $Zhx2^{ko}$ mice with CCl_4 will induce more fibrosis damage than $Zhx2^{wt}$ mice.

In Chapter 4, I reported that male $Zhx2^{ko}$ mice are more vulnerable to die than female $Zhx2^{ko}$ mice early after birth. Since our lab previously documented that Zhx2 regulation of Cyp2a4 was more sever in the livers of males than females, it is conceivable that Zhx2 could promote survival via regulation of genes that are required for male survival

more than female survival. As mentioned in Chapter 4, I hypothesized that the small size of $Zhx2^{ko}$ mice could lead to low growth hormone levels due to downregulation of Ghrhr gene expression, as it documented to be mutated in little mice [160]. Several experiment could be performed to test this hypothesis. First, we could measure the expression of Ghrhr as well as testing insulin like growth factor (Igf1), growth hormone (GH), prolactin (prl), and thyroid stimulating hormone (TSH). Second, we could examine the gene that is mutated in Amber dwarf mice [160]. These markers could help define the molecular differences in small $Zhx2^{ko}$ mice. It would also be interesting to test whether Zhx2 could contribute to insulin homeostasis and diabetes. Glucose and insulin levels could be analyzed in $Zhx2^{wt}$ and $Zhx2^{ko}$ mice with high glucose fluid. Additionally, I propose that ethylmorphine demethylase (EMDase) could be a prospect negative target of Zhx2 in the $Zhx2^{ko}$ males' livers. This enzyme has been reported to be higher in Balb/cJ male mice than females. This sexually biased enzyme has not been seen in CRL:CD1 mice [161]. Since the mice that are dying are males (see Chapter 4 for details), EMDase can have a potential toxic to new born mice. Worth notable, EMDase is active in the guinea pig inner zones of the adrenal cortex [162].

Our collaborator data previously demonstrated that translocation of Zhx2 from the nucleus to the cytoplasm in HCC patients were associated with poor prognosis. In Chapter 5, my *in vitro* analysis identified nuclear localization of Zhx1 and Zhx2 and cytoplasmic localization of Zhx3. In addition, I discovered a possible direct binding between Zhx2 and Zhx3 that shifted Zhx3 to the nucleus. I hypothesize that Zhx2-HA binds Zhx3-GFP and shifted it to the nucleus. To test this, fixed cells can be stained with Anti-HA antibodies. Alternatively, I might use Zhx2 and Zhx3 proteins fused to different fluorescent protein to visualize the binding and use confocal microscopy. Immunoprecipitation followed by western blot could also be used to reveal direct binding. If experiments reveal that proteins do not bind each other, an alternative proposal is that Zhx proteins can influence each other localization via third factors. This hypothesis could be tested using mass spectrometry to discover the direct binding proteins. The same proposed experiments can be done to reveal whether Zhx1 or Zhx2 can form heterodimers. I should note that this is the first report to use computational analysis to study Zhx genes. My bioinformatics search identified several

binding domains that could be involved in forming homodimers and heterodimers. Further insight could be obtained using site-directed mutagenesis, followed by transient transfection, then, co-immunoprecipitation of the predicted binding protein. Future directions for this study will focus on elucidating the molecular mechanisms by which Zhx proteins can influence each other's localization and how these alterations may be relevant to human disease. It would also be of interest to examine the localization of Zhx proteins in different tissues using immunohistochemistry techniques.

In summary, a better understanding of Zhx protein location, function, and biological activity may be employed as unique therapeutic targets. In the future, I highly recommend investigating the molecular functions of Zhx proteins and their proposed targets since they might shed the light for broader role of Zhx genes could be relevant to human disease and develop efficacious and direct drugs application help to heal several types of cancers and diseases.

APPENDEX

LIST OF ABBREVIATION

Abbreviation	Description
a.a	Amino acid
AFP	αfetoprotein
ANOVA	Analysis of variance
ASD	Autism Spectrum Disorder
Apo	Apolipoprotein
B	Brain
CCl_4	Carbon tetrachloride
CFA	Freunds' adjuvants
CNV	Copy number variation
Cyp2a4	Steroid 15α-hydroxylase testosterone
DRG	Dorsal root ganglia
Elovl3	Elongation of very long chain fatty acids like 3
FBS	Fetal bovine serum
FSH	Follicle stimulating hormone
GFP	Green fluorescent protein
GH	Growth hormone
HD	Homeodomain
HDL	High density lipoproteins
HEK293	Human embryonic kidney cells
HeLa	Human cervical cancer
Hep3B	Human hepatoma
HFD	High fat diet
Hnf4a	Hepatocytes nuclear factor 4a
HNF-4α and γ	Hepatic nuclear factors
Igf1	Insulin like growth factor
K	Kidney
Kb	Kilobase

KOMP	Knockout mouse project
L	Liver
LG	Lacrimal gland
LH	Luteinizing hormone
Lpl	Lipoprotein lipase
LXRα	Liver X receptor
Mat1a	Methionine adenosyltransferase 1a
MOE	Main olfactory epithelium
NAFLD	Non-alcoholic fatty liver disease
ND	Normal diet
NES	Nuclear export signal
NLS	Nuclear localization signal
Nr0b2	Neuronal PAS domain 2
ob/ob	Obese mice
PPARα, β, γ1, and γ2	Peroxisome proliferator activated receptors α, β, γ1, and γ2
prl	Prolactin
RXRα	Retinoid X receptor
SG	Salivary gland
SI	Small intestine
SREBP-1c	Sterol regulatory element binding protein-1c
Stat5	signal transducer and activator of transcription 5
TSH	Thyroid stimulating hormone
VLDL	Very low density lipoprotein
VNO	Vomeronasal organ
WT	Wilms tumor
Zhx	Zinc finger protein
Zhx1	Zinc finger and homeoboxes 1
Zhx2	Zinc finger and homeoboxes 2
$Zhx2^{het}$	Heterozygous Zhx2 mice
$Zhx2^{ko}$	Whole body Knock out Zhx2mice

$Zhx2^{wt}$	Wild type Zhx2 mice
$Zhx2^{\Delta hep}$	Hepatocytes specific Zhx2 knock out mice
ZHX3	Zinc finger and homeoboxes 3
Zn	Zinc finger domain

C-terminal GFP tagged of mouse Zhx1 protein. GFP sequence (lower case nucleotides at the C-terminal side).

mdykddddKASRRKSTTPCMVLASEQDPDLELISDLDEGPPILTPVENAK
AESVSSDEEVHGSVDSDNQQNKKVEGGYECKYCTFQTPDLNMFTFHVDSE
HPNVVLNSSYVCVECNFLTKRYDALSEHNLKYHPGEENFKLTMVKRNNQT
IFEQTINDLTFDGSFVKEENTEQGESIDVSSSGISISKTPIMKMMKNKVE
NKRITVHHNSAEGTSEEKENGVKASQEENAESVSSSALESNTSTSTINRV
HPSPASTVVTPTAVLPGLAQVITAVSAQQNSNLLPKVLIPVNSIPTYNAA
LDNNPLLLNTYNKFPYPTMSEITVLSAQAKYTEEQIKIWFSAQRLKHGVS
WTPEEVEEARRKQFNGTVHTVPQTITVIPTHISTGSNGLPSILQTCQIVG
QPGLVLTQVAGTNTLPVTAPIALTVAGVPNQTNVQKSQVPAAQPATDTKP
ATAAVPSSPSVRPEAALVNPDSFGIRAKKTKEQLAELKVSYLKNQFPHDS
EIIRLMKITGLTKGEIKKWFSDTRYNQRNSKSNQCLHLNNDSSATIIIDS
SDETPEPPAAAASQQKQSWNPFPDFAPQKFKEKTAEQLRALQASFLNSSV
LTDEEVNRLRAQTKLTRREIDAWFTEKNKTKALKDEKIEVDESNVGSSKE
EPGESSPGDETVAPKSGGTGKICKKTPEQLHMLKSAFVRTQWPSAEEYDK
LAEESGLARTDIVSWFGDTRYAWKNGNLKWYYYYQSSNSSSLNGLSSLRR
RGRGRPKGRGRGRPRGRPRGGKRMNTWDRVPSLIKFKTGTAILKDYYLKH
KFLNEQDLDELVNRSHMGYEQVREWFAERQRRSELGIELFEENEEEDEVV
DDQEEDEEETDDSDTWEPPRHVKRKLSKSDDgsvskgeelftgvvpilve
ldgdvnghkfsvsgegegdatygkltlkficttgklpvpwptlvttltyg
vqcfsrypdhmkqhdffksampegyvqertiffkddgnyktraevkfegd
tlvnrielkgidfkedgnilghkleynynshnvyimadkqkngikvnfki
rhniedgsvqladhyqqntpigdgpvllpdnhylstqsalskdpnekrdh
mvllefvtaagitlgmdelyk

FLAG-Zhx1-GFP plasmid: Mouse Zhx1 was subcloned from pcDNA to FLAG-CMV-GFP vector using the appropriate restriction sites (Plasmid image: Snap Gene viewer).

C-terminal Flag tagged of mouse Zhx2 protein and the GFP sequence (lower case nucleotides at the C-terminal side).

mdykddddKASKRKSTTPCMVRTSQVLEQDMLEEADRAKDKGAGMPQSDV
TKDSWAAEPEHSSKETEVVEVKSMGENLSKKLQGGYECKYCPYSTQNLNE
FTEHVDMQHPNVILNPLYVCAECNFTTKKYDSLSDHNSKFHPGETNFKLK
LIKRNNQTVLEQSIEATNHVVPITASGPGSSDNDPGVSVGKTPMTKTGKL
KADAKKVPKKPDEAAPENHMEGTARLVTDTAEILARLGSVELLQDSLGHV
MPSVQLPPNINLVPKVPVPLNTTKYNSALDTNATMINSFNKFPYPTQAEL
SWLTAASKHPEEHIRIWFATQRLKHGISWSPEEVEEARKKMFNGTIQSVP
PTITVLPAQLTPTKVSQPILQTALPCQILGQPSLVLTQVTSGSTTVSCSP
ITLAVAGVTNHGQKRPLVTPQAAPEPKRPHIAQVPEPPPKVANTPLTPAS
DRKKTKLQIAHLKASFLQSQFPDDAEVYRLIEVTGLARSEIKKWFSDHRY
RCQRGIVHITSESLAKDQMAITGTRHGRTYHVYPDFAPQKFKEKSQGQLK
TLEDSFLKSSFPTQAEVERLRVETKLSRREIDSWFSERRKLRDSMEQAVL
DSMGSGKKGSDAVAPNGALSRLDQLSGAQLAGSLPSPSSAIVQNQEQVHL
LRSTFARTQWPTPQEYDQLAAKTGLVRTEIVRWFKENRCLLKTGTLSWLE
QYQRHHMSDDRGRDAVSRKVAKQVAESPKNGSEAAHQYAKDPKALSEEDS
EKLVPRMKVGGDPTKDCLAGKPSEATSDRSEGSRDGQGSEENEESGIVDF
VEVTVGEEDAISEKWGSWSRRVAEGTVERADSDSDSTPAEAGQAgsvskg
eelftgvvpilveldgdvnghkfsvsgegegdatygkltlkficttgklp
vpwptlvttltygvqcfsrypdhmkqhdffksampegyvqertiffkddg
nyktraevkfegdtlvnrielkgidfkedgnilghkleynynshnvyima
dkqkngikvnfkirhniedgsvqladhyqqntpigdgpvllpdnhylstq
salskdpnekrdhmvllefvtaagitlgmdelyk

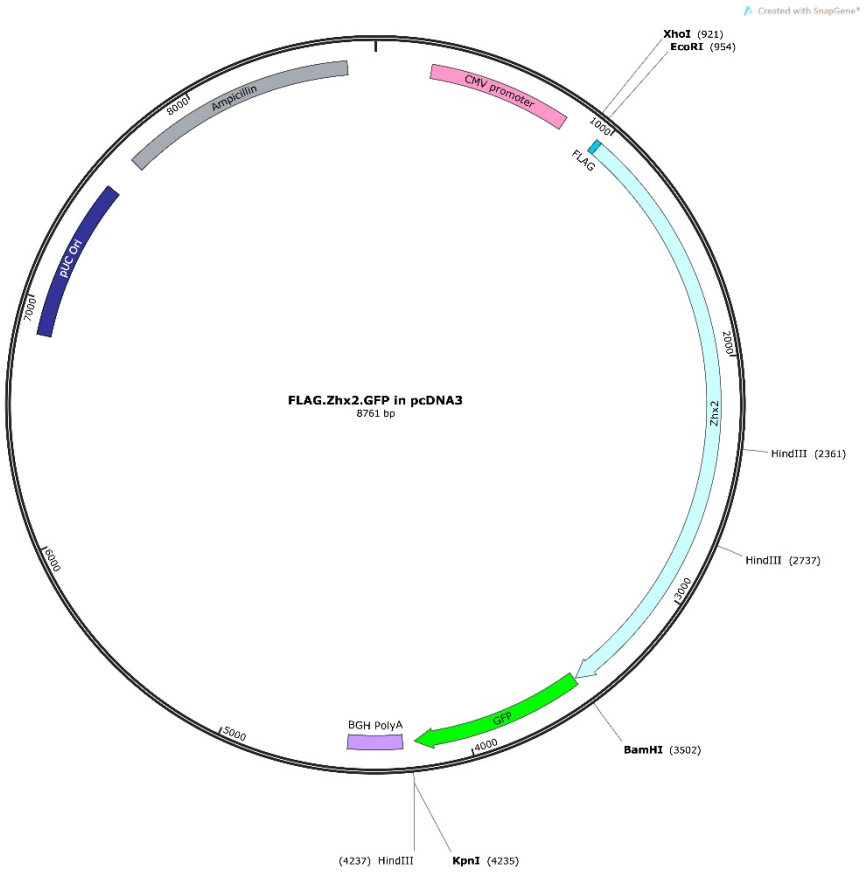

FLAG-Zhx2-GFP plasmid: Mouse Zhx2 was subcloned from pcDNA to FLAG-CMV-GFP vector using the appropriate restriction sites (Plasmid image: Snap Gene viewer).

C-terminal Flag tagged of mouse Zhx3 protein and the GFP sequence (lower case nucleotides at the C-terminal side).

mdykddddKASKRKSTTPCMIPVKTVVLPGASTEPQPVESLPEGPQQDLP
SEAPDASSEAAPNPSSTDGSALANGHRSTLDGYVYCCKECEFRSQDVTHF
IGHMNSEHTDFNKDPTFVCTGCSFLAKNPEGLSLHNAKCHSGEASFLWNV
TKPDNHVVVEQSVPDSASSSVLAGESTTEGTEIIITKTPIMKIMKGKAEA
KKIHMLKENAPNQPGSEALPKPLAGEREVKEGDHTFINGAAPGSQASAKS
TKPPPAANGPLIGTVPVLPAGIAQFLSLQQQPPVHAQHHTHQPLPTSKTL
PKVMIPLSSIPTYNAAMDSNSFLKNSFHKFPYPTKAELCYLTVVTKYPEE
QLKIWFTAQRLKQGISWSPEEIEDARKKMFNTVIQSVPQPTITVLNTPLV
ASAGNVQHLIQATLPGHAVGQPEGTAGGLLVTQPLMANGLQASSSSLPLT
TASVPKPTVAPINTVCSNSASAVKVVNAAQSLLTACPSITSQAFLDANIY
KNKKSHEQLSALKGSFCRNQFPGQSEVEHLTKVTGLSTREVRKWFSDRRY
HCRNLKGSRAMMPGEHGSVLIDSVPEVPFPLASKVPEVTCIPTATSLVSH
PATKRQSWHQTPDFTPTKYKERAPEQLRVLENSFAQNPLPPEEELDRLRS
ETKMTRREIDGWFSERRKKVNTEETKKADGHMPKEEEEGAEQEGRDEELA
NELRVPGENGSPEMFLSHALAERKVSPIKINLKNLRVTEASGKSEFPGMG
VCEPEEDGLNKLVEQPPSKVSYKKTAQQRHLLRQLFVQTQWPSNQDYDSI
MAQTGLPRPEVVRWFGDSRYALKNGQLKWYEDYKRGNFPPGLLVIAPGNR
ELLQDYYMTHKMLCEEDLQTLCDKTQMSAQQVKQWFAEKMGEETRAVADI
SSEDQGPRNGEPVAVHKVLGDAYSELSENSESWEPSAPEASSEPFDTSSP
QSGRQLEADgsvskgeelftgvvpilveldgdvnghkfsvsgegegdaty
gkltlkficttgklpvpwptlvttltygvqcfsrypdhmkqhdffksamp
egyvqertiffkddgnyktraevkfegdtlvnrielkgidfkedgnilgh
kleynynshnvyimadkqkngikvnfkirhniedgsvqladhyqqntpig
dgpvllpdnhylstqsalskdpnekrdhmvllefvtaagitlgmdelyk

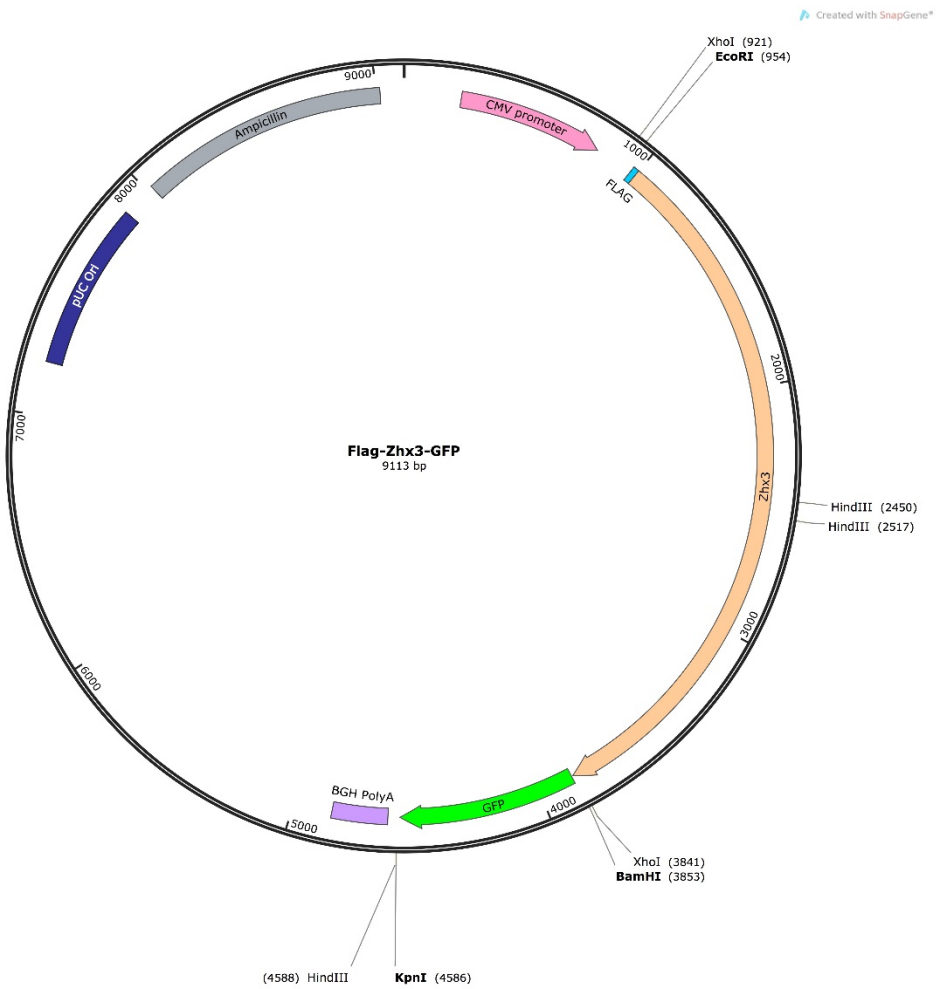

FLAG-Zhx3-GFP plasmid: Mouse Zhx3 was subcloned from pcDNA to FLAG-CMV-GFP vector using the appropriate restriction sites (Plasmid image: Snap Gene viewer).

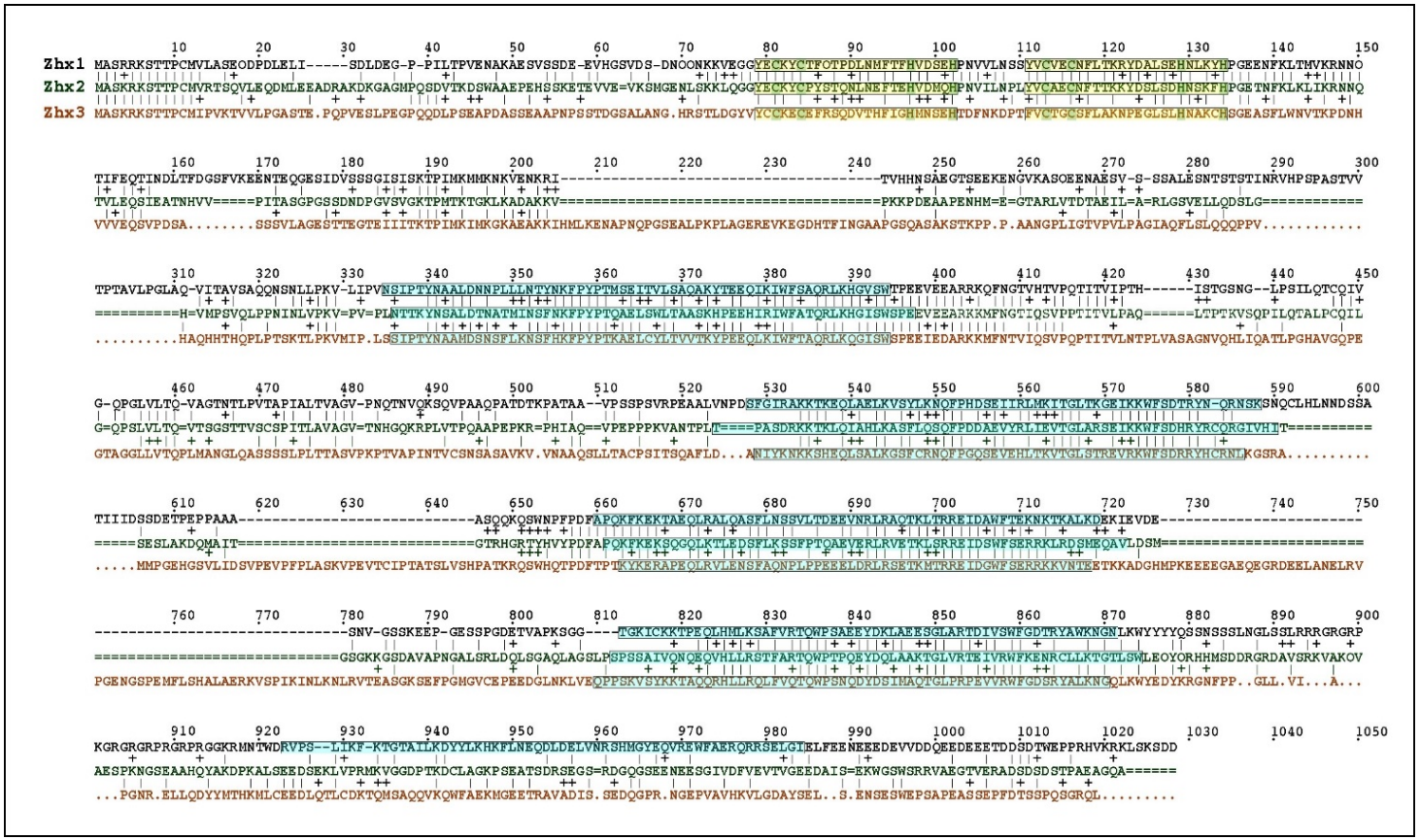

Homology within mouse Zhx1, Zhx2 and Zhx3 proteins showing the two Zinc finger (ZF) highlighted yellow, and four (for Zhx2) or five (Zhx1 and Zhx3) homeodomains (HDs) highlighted blue.

References:

1. Gebhardt, R., *Metabolic zonation of the liver: regulation and implications for liver function.* Pharmacol Ther, 1992. **53**(3): p. 275-354.
2. Nguyen, P., et al., *Liver lipid metabolism.* J Anim Physiol Anim Nutr (Berl), 2008. **92**(3): p. 272-83.
3. Zaret, K.S., *Regulatory phases of early liver development: paradigms of organogenesis.* Nat Rev Genet, 2002. **3**(7): p. 499-512.
4. Berneis, K.K. and R.M. Krauss, *Metabolic origins and clinical significance of LDL heterogeneity.* J Lipid Res, 2002. **43**(9): p. 1363-79.
5. Jump, D.B., et al., *Fatty acid regulation of hepatic gene transcription.* J Nutr, 2005. **135**(11): p. 2503-6.
6. Spear, B.T., et al., *Transcriptional control in the mammalian liver: liver development, perinatal repression, and zonal gene regulation.* Cell Mol Life Sci, 2006. **63**(24): p. 2922-38.
7. Friedman, S.L., *Hepatic stellate cells: protean, multifunctional, and enigmatic cells of the liver.* Physiol Rev, 2008. **88**(1): p. 125-72.
8. Jungermann, K. and N. Katz, *Functional specialization of different hepatocyte populations.* Physiol Rev, 1989. **69**(3): p. 708-64.
9. Warren, A., et al., *T lymphocytes interact with hepatocytes through fenestrations in murine liver sinusoidal endothelial cells.* Hepatology, 2006. **44**(5): p. 1182-90.
10. Herkel, J., et al., *MHC class II-expressing hepatocytes function as antigen-presenting cells and activate specific CD4 T lymphocyutes.* Hepatology, 2003. **37**(5): p. 1079-85.
11. Wisse, E., et al., *Structure and function of sinusoidal lining cells in the liver.* Toxicol Pathol, 1996. **24**(1): p. 100-11.
12. Diesselhoff-den Dulk, M.M., R.W. Crofton, and R. van Furth, *Origin and kinetics of Kupffer cells during an acute inflammatory response.* Immunology, 1979. **37**(1): p. 7-14.
13. Bouwens, L., et al., *Natural cytotoxicity of rat hepatic natural killer cells and macrophages against a syngeneic colon adenocarcinoma.* Cancer Immunol Immunother, 1988. **27**(2): p. 137-41.
14. Theise, N.D., et al., *The canals of Hering and hepatic stem cells in humans.* Hepatology, 1999. **30**(6): p. 1425-33.
15. Lenzi, R., et al., *Histogenesis of bile duct-like cells proliferating during ethionine hepatocarcinogenesis. Evidence for a biliary epithelial nature of oval cells.* Lab Invest, 1992. **66**(3): p. 390-402.
16. Friedman, S.L., et al., *Hepatic lipocytes: the principal collagen-producing cells of normal rat liver.* Proc Natl Acad Sci U S A, 1985. **82**(24): p. 8681-5.
17. Bataller, R. and D.A. Brenner, *Liver fibrosis.* J Clin Invest, 2005. **115**(2): p. 209-18.
18. Tilghman, S.M., *The structure and regulation of the alpha-fetoprotein and albumin genes.* Oxf Surv Eukaryot Genes, 1985. **2**: p. 160-206.

19. Gibbs, P.E., W.F. Witke, and A. Dugaiczyk, *The molecular clock runs at different rates among closely related members of a gene family.* J Mol Evol, 1998. **46**(5): p. 552-61.
20. Naidu, S., M.L. Peterson, and B.T. Spear, *Alpha-fetoprotein related gene (ARG): a new member of the albumin gene family that is no longer functional in primates.* Gene, 2010. **449**(1-2): p. 95-102.
21. Chen, H., J.O. Egan, and J.F. Chiu, *Regulation and activities of alpha-fetoprotein.* Crit Rev Eukaryot Gene Expr, 1997. **7**(1-2): p. 11-41.
22. McLeod, J.F. and N.E. Cooke, *The vitamin D-binding protein, alpha-fetoprotein, albumin multigene family: detection of transcripts in multiple tissues.* J Biol Chem, 1989. **264**(36): p. 21760-9.
23. Belanger, L., S. Roy, and D. Allard, *New albumin gene 3' adjacent to the alpha 1-fetoprotein locus.* J Biol Chem, 1994. **269**(8): p. 5481-4.
24. Deutsch, H.F., *Chemistry and biology of alpha-fetoprotein.* Adv Cancer Res, 1991. **56**: p. 253-312.
25. Perova, S.D., D.A. El'gort, and G.I. Abelev, *[Alpha-fetoprotein in rat serum following partial hepatectomy].* Biull Eksp Biol Med, 1971. **71**(3): p. 45-7.
26. Murray, M.J. and J.C. Nicholson, *alpha-Fetoprotein.* Arch Dis Child Educ Pract Ed, 2011. **96**(4): p. 141-7.
27. Bredaki, F.E., et al., *First-trimester screening for trisomy 21 using alpha-fetoprotein.* Fetal Diagn Ther, 2011. **30**(3): p. 215-8.
28. Zemel, S., M.S. Bartolomei, and S.M. Tilghman, *Physical linkage of two mammalian imprinted genes, H19 and insulin-like growth factor 2.* Nat Genet, 1992. **2**(1): p. 61-5.
29. Dao, D., et al., *Multipoint analysis of human chromosome 11p15/mouse distal chromosome 7: inclusion of H19/IGF2 in the minimal WT2 region, gene specificity of H19 silencing in Wilms' tumorigenesis and methylation hyper-dependence of H19 imprinting.* Hum Mol Genet, 1999. **8**(7): p. 1337-52.
30. Kanwar, Y.S., et al., *Imprinted mesodermal specific transcript (MEST) and H19 genes in renal development and diabetes.* Kidney Int, 2003. **63**(5): p. 1658-70.
31. Dey, B.K., K. Pfeifer, and A. Dutta, *The H19 long noncoding RNA gives rise to microRNAs miR-675-3p and miR-675-5p to promote skeletal muscle differentiation and regeneration.* Genes Dev, 2014. **28**(5): p. 491-501.
32. Kinsell, L.W., et al., *Rate of Disappearance From Plasma of Intravenously Administered Methionine in Patients With Liver Damage.* Science, 1947. **106**(2763): p. 589-90.
33. Lu, S.C., et al., *Methionine adenosyltransferase 1A knockout mice are predisposed to liver injury and exhibit increased expression of genes involved in proliferation.* Proc Natl Acad Sci U S A, 2001. **98**(10): p. 5560-5.
34. Kotb, M., et al., *Consensus nomenclature for the mammalian methionine adenosyltransferase genes and gene products.* Trends Genet, 1997. **13**(2): p. 51-2.
35. Cai, J., et al., *Changes in S-adenosylmethionine synthetase in human liver cancer: molecular characterization and significance.* Hepatology, 1996. **24**(5): p. 1090-7.

36. Cano, A., et al., *Methionine adenosyltransferase 1A gene deletion disrupts hepatic very low-density lipoprotein assembly in mice.* Hepatology, 2011. **54**(6): p. 1975-86.
37. Martinez-Chantar, M.L., et al., *Spontaneous oxidative stress and liver tumors in mice lacking methionine adenosyltransferase 1A.* FASEB J, 2002. **16**(10): p. 1292-4.
38. Salvatore, F., et al., *Quantitative analysis of S-adenosylmethionine and S-adenosylhomocysteine in animal tissues.* Anal Biochem, 1971. **41**(1): p. 16-28.
39. Latasa, M.U., et al., *Hepatocyte growth factor induces MAT2A expression and histone acetylation in rat hepatocytes: role in liver regeneration.* FASEB J, 2001. **15**(7): p. 1248-50.
40. Olsson, M., G. Lindahl, and E. Ruoslahti, *Genetic control of alpha-fetoprotein synthesis in the mouse.* J Exp Med, 1977. **145**(4): p. 819-27.
41. Peyton, D.K., et al., *The alpha-fetoprotein promoter is the target of Afr1-mediated postnatal repression.* Genomics, 2000. **63**(2): p. 173-80.
42. Morford, L.A., et al., *The oncofetal gene glypican 3 is regulated in the postnatal liver by zinc fingers and homeoboxes 2 and in the regenerating liver by alpha-fetoprotein regulator 2.* Hepatology, 2007. **46**(5): p. 1541-7.
43. Perincheri, S., et al., *Hereditary persistence of alpha-fetoprotein and H19 expression in liver of BALB/cJ mice is due to a retrovirus insertion in the Zhx2 gene.* Proc Natl Acad Sci U S A, 2005. **102**(2): p. 396-401.
44. Peterson, M.L., C. Ma, and B.T. Spear, *Zhx2 and Zbtb20: novel regulators of postnatal alpha-fetoprotein repression and their potential role in gene reactivation during liver cancer.* Semin Cancer Biol, 2011. **21**(1): p. 21-7.
45. Yamada, K., H. Osawa, and D.K. Granner, *Identification of proteins that interact with NF-YA.* FEBS Lett, 1999. **460**(1): p. 41-5.
46. Kawata, H., et al., *Zinc-fingers and homeoboxes (ZHX) 2, a novel member of the ZHX family, functions as a transcriptional repressor.* Biochem J, 2003. **373**(Pt 3): p. 747-57.
47. Yamada, K., et al., *Analysis of zinc-fingers and homeoboxes (ZHX)-1-interacting proteins: molecular cloning and characterization of a member of the ZHX family, ZHX3.* Biochem J, 2003. **373**(Pt 1): p. 167-78.
48. Gargalovic, P.S., et al., *Quantitative trait locus mapping and identification of Zhx2 as a novel regulator of plasma lipid metabolism.* Circ Cardiovasc Genet, 2010. **3**(1): p. 60-7.
49. Barthelemy, I., et al., *zhx-1: a novel mouse homeodomain protein containing two zinc-fingers and five homeodomains.* Biochem Biophys Res Commun, 1996. **224**(3): p. 870-6.
50. Yamada, K., et al., *Human ZHX1: cloning, chromosomal location, and interaction with transcription factor NF-Y.* Biochem Biophys Res Commun, 1999. **261**(3): p. 614-21.
51. Mantovani, R., *The molecular biology of the CCAAT-binding factor NF-Y.* Gene, 1999. **239**(1): p. 15-27.

52. Yamada, K., et al., *Functional analysis and the molecular dissection of zinc-fingers and homeoboxes 1 (ZHX1).* Biochem Biophys Res Commun, 2002. **297**(2): p. 368-74.
53. Liu, G., et al., *ZHX proteins regulate podocyte gene expression during the development of nephrotic syndrome.* J Biol Chem, 2006. **281**(51): p. 39681-92.
54. Anders, M.W., *Metabolism of drugs by the kidney.* Kidney Int, 1980. **18**(5): p. 636-47.
55. Knights, K.M., A. Rowland, and J.O. Miners, *Renal drug metabolism in humans: the potential for drug-endobiotic interactions involving cytochrome P450 (CYP) and UDP-glucuronosyltransferase (UGT).* Br J Clin Pharmacol, 2013. **76**(4): p. 587-602.
56. Kurts, C., et al., *The immune system and kidney disease: basic concepts and clinical implications.* Nat Rev Immunol, 2013. **13**(10): p. 738-53.
57. Jemal, A., et al., *Cancer statistics, 2009.* CA Cancer J Clin, 2009. **59**(4): p. 225-49.
58. Altekruse, S.F., K.A. McGlynn, and M.E. Reichman, *Hepatocellular carcinoma incidence, mortality, and survival trends in the United States from 1975 to 2005.* J Clin Oncol, 2009. **27**(9): p. 1485-91.
59. Aravalli, R.N., C.J. Steer, and E.N. Cressman, *Molecular mechanisms of hepatocellular carcinoma.* Hepatology, 2008. **48**(6): p. 2047-63.
60. Imbeaud, S., Y. Ladeiro, and J. Zucman-Rossi, *Identification of novel oncogenes and tumor suppressors in hepatocellular carcinoma.* Semin Liver Dis, 2010. **30**(1): p. 75-86.
61. Llovet, J.M. and J. Bruix, *Molecular targeted therapies in hepatocellular carcinoma.* Hepatology, 2008. **48**(4): p. 1312-27.
62. Moeini, A., H. Cornella, and A. Villanueva, *Emerging Signaling Pathways in Hepatocellular Carcinoma.* Liver Cancer, 2012. **1**(2): p. 83-93.
63. Lv, Z., et al., *Promoter hypermethylation of a novel gene, ZHX2, in hepatocellular carcinoma.* Am J Clin Pathol, 2006. **125**(5): p. 740-6.
64. Shen, H., et al., *ZHX2 is a repressor of alpha-fetoprotein expression in human hepatoma cell lines.* J Cell Mol Med, 2008. **12**(6B): p. 2772-80.
65. Yue, X., et al., *Zinc fingers and homeoboxes 2 inhibits hepatocellular carcinoma cell proliferation and represses expression of Cyclins A and E.* Gastroenterology, 2012. **142**(7): p. 1559-70 e2.
66. Gu, L., M.W. Johnson, and A.J. Lusis, *Quantitative trait locus analysis of plasma lipoprotein levels in an autoimmune mouse model : interactions between lipoprotein metabolism, autoimmune disease, and atherogenesis.* Arterioscler Thromb Vasc Biol, 1999. **19**(2): p. 442-53.
67. Bis, J.C., et al., *Meta-analysis of genome-wide association studies from the CHARGE consortium identifies common variants associated with carotid intima media thickness and plaque.* Nat Genet, 2011. **43**(10): p. 940-7.
68. Tamura, S. and I. Shimomura, *Contribution of adipose tissue and de novo lipogenesis to nonalcoholic fatty liver disease.* J Clin Invest, 2005. **115**(5): p. 1139-42.

69. De Minicis, S., et al., *HCC development is associated to peripheral insulin resistance in a mouse model of NASH.* PLoS One, 2014. **9**(5): p. e97136.
70. Ginsberg, H.N., *Insulin resistance and cardiovascular disease.* J Clin Invest, 2000. **106**(4): p. 453-8.
71. Li, C., et al., *Genetic association and gene-smoking interaction study of carotid intima-media thickness at five GWAS-indicated genes: the Bogalusa Heart Study.* Gene, 2015. **562**(2): p. 226-31.
72. Moen, C.J., et al., *The Hyplip2 locus causes hypertriglyceridemia by decreased clearance of triglycerides.* J Lipid Res, 2007. **48**(10): p. 2182-92.
73. Taraslia, V.K., et al., *Proteomic analysis of normal murine brain parts.* Cancer Genomics Proteomics, 2013. **10**(3): p. 125-54.
74. Miller, J.A., et al., *Transcriptional landscape of the prenatal human brain.* Nature, 2014. **508**(7495): p. 199-206.
75. Tuzi, N.L. and W.J. Gullick, *eph, the largest known family of putative growth factor receptors.* Br J Cancer, 1994. **69**(3): p. 417-21.
76. Wu, C., et al., *ZHX2 Interacts with Ephrin-B and regulates neural progenitor maintenance in the developing cerebral cortex.* J Neurosci, 2009. **29**(23): p. 7404-12.
77. Fekete, R., et al., *Exome sequencing in familial corticobasal degeneration.* Parkinsonism Relat Disord, 2013. **19**(11): p. 1049-52.
78. Chang, M., et al., *Evaluation of phenoxybenzamine in the CFA model of pain following gene expression studies and connectivity mapping.* Mol Pain, 2010. **6**: p. 56.
79. Walker, S. and S.W. Scherer, *Identification of candidate intergenic risk loci in autism spectrum disorder.* BMC Genomics, 2013. **14**: p. 499.
80. Sankoorikal, G.M., et al., *A mouse model system for genetic analysis of sociability: C57BL/6J versus BALB/cJ inbred mouse strains.* Biol Psychiatry, 2006. **59**(5): p. 415-23.
81. Fairless, A.H., et al., *Sociability and brain development in BALB/cJ and C57BL/6J mice.* Behav Brain Res, 2012. **228**(2): p. 299-310.
82. Duncan, R., et al., *Genes that modify expression of major urinary proteins in mice.* Mol Cell Biol, 1988. **8**(7): p. 2705-12.
83. Dow, H.C., et al., *Genetic dissection of intermale aggressive behavior in BALB/cJ and A/J mice.* Genes Brain Behav, 2011. **10**(1): p. 57-68.
84. Barth, R.K., et al., *Developmentally regulated mRNAs in mouse liver.* Proc Natl Acad Sci U S A, 1982. **79**(2): p. 500-4.
85. Finlayson, J.S., et al., *Components of the major urinary protein complex in inbred mice: separation and peptide mapping.* Biochem Genet, 1968. **2**(2): p. 127-40.
86. Derman, E., *Isolation of a cDNA clone for mouse urinary proteins: age- and sex-related expression of mouse urinary protein genes is transcriptionally controlled.* Proc Natl Acad Sci U S A, 1981. **78**(9): p. 5425-9.
87. Finlayson, J.S., et al., *Major urinary protein complex of normal mice: origin.* Science, 1965. **149**(3687): p. 981-2.

88. Kurtz, D.T., *Rat alpha 2u globulin is encoded by a multigene family.* J Mol Appl Genet, 1981. **1**(1): p. 29-38.
89. Ganfornina, M.D., et al., *A phylogenetic analysis of the lipocalin protein family.* Mol Biol Evol, 2000. **17**(1): p. 114-26.
90. Flower, D.R., *The lipocalin protein family: structure and function.* Biochem J, 1996. **318 (Pt 1)**: p. 1-14.
91. Hurst, J.L., et al., *Proteins in urine scent marks of male house mice extend the longevity of olfactory signals.* Anim Behav, 1998. **55**(5): p. 1289-97.
92. Chamero, P., et al., *Identification of protein pheromones that promote aggressive behaviour.* Nature, 2007. **450**(7171): p. 899-902.
93. Hui, X., et al., *Major urinary protein-1 increases energy expenditure and improves glucose intolerance through enhancing mitochondrial function in skeletal muscle of diabetic mice.* J Biol Chem, 2009. **284**(21): p. 14050-7.
94. Shahan, K. and E. Derman, *Tissue-specific expression of major urinary protein (MUP) genes in mice: characterization of MUP mRNAs by restriction mapping of cDNA and by in vitro translation.* Mol Cell Biol, 1984. **4**(11): p. 2259-65.
95. Shaw, P.H., W.A. Held, and N.D. Hastie, *The gene family for major urinary proteins: expression in several secretory tissues of the mouse.* Cell, 1983. **32**(3): p. 755-61.
96. Knopf, J.L., J.F. Gallagher, and W.A. Held, *Differential, multihormonal regulation of the mouse major urinary protein gene family in the liver.* Mol Cell Biol, 1983. **3**(12): p. 2232-40.
97. Shahan, K., et al., *Expression of six mouse major urinary protein genes in the mammary, parotid, sublingual, submaxillary, and lachrymal glands and in the liver.* Mol Cell Biol, 1987. **7**(5): p. 1947-54.
98. Szoka, P.R. and K. Paigen, *Regulation of mouse major urinary protein production by the Mup-A gene.* Genetics, 1978. **90**(3): p. 597-612.
99. Logan, D.W., T.F. Marton, and L. Stowers, *Species specificity in major urinary proteins by parallel evolution.* PLoS One, 2008. **3**(9): p. e3280.
100. Stern, K. and M.K. McClintock, *Regulation of ovulation by human pheromones.* Nature, 1998. **392**(6672): p. 177-9.
101. Boehm, N. and B. Gasser, *Sensory receptor-like cells in the human foetal vomeronasal organ.* Neuroreport, 1993. **4**(7): p. 867-70.
102. More, L., *Mouse major urinary proteins trigger ovulation via the vomeronasal organ.* Chem Senses, 2006. **31**(5): p. 393-401.
103. Amano, O., et al., *Anatomy and histology of rodent and human major salivary glands: -overview of the Japan salivary gland society-sponsored workshop.* Acta Histochem Cytochem, 2012. **45**(5): p. 241-50.
104. Featherstone, J.D., *Prevention and reversal of dental caries: role of low level fluoride.* Community Dent Oral Epidemiol, 1999. **27**(1): p. 31-40.
105. Fox, P.C., *Acquired salivary dysfunction. Drugs and radiation.* Ann N Y Acad Sci, 1998. **842**: p. 132-7.
106. Burlage, F.R., et al., *Parotid and submandibular/sublingual salivary flow during high dose radiotherapy.* Radiother Oncol, 2001. **61**(3): p. 271-4.

107. Ann, D.K., H.H. Lin, and E. Kousvelari, *Regulation of salivary-gland-specific gene expression.* Crit Rev Oral Biol Med, 1997. **8**(3): p. 244-52.
108. Hirayama, M., et al., *Functional lacrimal gland regeneration by transplantation of a bioengineered organ germ.* Nat Commun, 2013. **4**: p. 2497.
109. Zoukhri, D., *Effect of inflammation on lacrimal gland function.* Exp Eye Res, 2006. **82**(5): p. 885-98.
110. Dartt, D.A., *Interaction of EGF family growth factors and neurotransmitters in regulating lacrimal gland secretion.* Exp Eye Res, 2004. **78**(3): p. 337-45.
111. Mowat, A.M. and W.W. Agace, *Regional specialization within the intestinal immune system.* Nat Rev Immunol, 2014. **14**(10): p. 667-85.
112. Knights, D., K.G. Lassen, and R.J. Xavier, *Advances in inflammatory bowel disease pathogenesis: linking host genetics and the microbiome.* Gut, 2013. **62**(10): p. 1505-10.
113. Froh, M., A. Konno, and R.G. Thurman, *Isolation of liver Kupffer cells.* Curr Protoc Toxicol, 2003. **Chapter 14**: p. Unit14 4.
114. Roy, A., A. Kucukural, and Y. Zhang, *I-TASSER: a unified platform for automated protein structure and function prediction.* Nat Protoc, 2010. **5**(4): p. 725-38.
115. Pierce, B.G., et al., *ZDOCK server: interactive docking prediction of protein-protein complexes and symmetric multimers.* Bioinformatics, 2014. **30**(12): p. 1771-3.
116. Wang, X., et al., *Hyplip2, a new gene for combined hyperlipidemia and increased atherosclerosis.* Arterioscler Thromb Vasc Biol, 2004. **24**(10): p. 1928-34.
117. Waxman, D.J., *Regulation of liver-specific steroid metabolizing cytochromes P450: cholesterol 7alpha-hydroxylase, bile acid 6beta-hydroxylase, and growth hormone-responsive steroid hormone hydroxylases.* J Steroid Biochem Mol Biol, 1992. **43**(8): p. 1055-72.
118. Nebert, D.W. and D.W. Russell, *Clinical importance of the cytochromes P450.* Lancet, 2002. **360**(9340): p. 1155-62.
119. Nelson, D.R., *Comparison of P450s from human and fugu: 420 million years of vertebrate P450 evolution.* Arch Biochem Biophys, 2003. **409**(1): p. 18-24.
120. Lindberg, R., et al., *The structure and characterization of type I P-450(15) alpha gene as major steroid 15 alpha-hydroxylase and its comparison with type II P-450(15) alpha gene.* J Biol Chem, 1989. **264**(11): p. 6465-71.
121. Renaud, H.J., et al., *Tissue distribution and gender-divergent expression of 78 cytochrome P450 mRNAs in mice.* Toxicol Sci, 2011. **124**(2): p. 261-77.
122. Johnson, E.F., et al., *Regulation of P450 4A expression by peroxisome proliferator activated receptors.* Toxicology, 2002. **181-182**: p. 203-6.
123. Muller, D.N., et al., *Mouse Cyp4a isoforms: enzymatic properties, gender- and strain-specific expression, and role in renal 20-hydroxyeicosatetraenoic acid formation.* Biochem J, 2007. **403**(1): p. 109-18.
124. Clodfelter, K.H., et al., *Role of STAT5a in regulation of sex-specific gene expression in female but not male mouse liver revealed by microarray analysis.* Physiol Genomics, 2007. **31**(1): p. 63-74.

125. Banes, A.K., et al., *Angiotensin II blockade prevents hyperglycemia-induced activation of JAK and STAT proteins in diabetic rat kidney glomeruli.* Am J Physiol Renal Physiol, 2004. **286**(4): p. F653-9.
126. Clement, L.C., et al., *Early changes in gene expression that influence the course of primary glomerular disease.* Kidney Int, 2007. **72**(3): p. 337-47.
127. Munshi, A., et al., *Lack of association of G779A ZHX-2 gene variant with HbF levels in beta-thalassemia major.* Eur J Haematol, 2011. **86**(6): p. 502-6.
128. Kirschner, K.M., et al., *The Wilms' tumor suppressor Wt1 activates transcription of the erythropoietin receptor in hematopoietic progenitor cells.* FASEB J, 2008. **22**(8): p. 2690-701.
129. Kreidberg, J.A., et al., *WT-1 is required for early kidney development.* Cell, 1993. **74**(4): p. 679-91.
130. Berasain, C., et al., *Expression of Wilms' tumor suppressor in the liver with cirrhosis: relation to hepatocyte nuclear factor 4 and hepatocellular function.* Hepatology, 2003. **38**(1): p. 148-57.
131. Riddle, R.D., et al., *Induction of the LIM homeobox gene Lmx1 by WNT7a establishes dorsoventral pattern in the vertebrate limb.* Cell, 1995. **83**(4): p. 631-40.
132. Burghardt, T., et al., *LMX1B is essential for the maintenance of differentiated podocytes in adult kidneys.* J Am Soc Nephrol, 2013. **24**(11): p. 1830-48.
133. Zou, A., et al., *New Insights into Orphan Nuclear Receptor SHP in Liver Cancer.* Nucl Receptor Res, 2015. **2**.
134. Brendel, C., et al., *The small heterodimer partner interacts with the liver X receptor alpha and represses its transcriptional activity.* Mol Endocrinol, 2002. **16**(9): p. 2065-76.
135. Lee, H.K., et al., *Structure and expression of the orphan nuclear receptor SHP gene.* J Biol Chem, 1998. **273**(23): p. 14398-402.
136. Zhang, Y., et al., *Bcl2 is a critical regulator of bile acid homeostasis by dictating Shp and lncRNA H19 function.* Sci Rep, 2016. **6**: p. 20559.
137. Declercq, J., et al., *Upregulation of Igf and Wnt signalling associated genes in pleomorphic adenomas of the salivary glands in PLAG1 transgenic mice.* Int J Oncol, 2008. **32**(5): p. 1041-7.
138. Aida, K. and M. Negishi, *A trans-acting locus regulates transcriptional repression of the female-specific steroid 15 alpha-hydroxylase gene in male mice.* J Mol Endocrinol, 1993. **11**(2): p. 213-22.
139. Lee, S.M., et al., *Small heterodimer partner/neuronal PAS domain protein 2 axis regulates the oscillation of liver lipid metabolism.* Hepatology, 2015. **61**(2): p. 497-505.
140. Pan, X. and H. Jeong, *Estrogen-Induced Cholestasis Leads to Repressed CYP2D6 Expression in CYP2D6-Humanized Mice.* Mol Pharmacol, 2015. **88**(1): p. 106-12.
141. Remold-O'Donnell, E. and K. Lewandrowski, *Macrophage surface component gp160: sensitivity to plasmin and other proteases.* J Immunol, 1982. **128**(4): p. 1541-4.

142. Costa, R.H., D.R. Grayson, and J.E. Darnell, Jr., *Multiple hepatocyte-enriched nuclear factors function in the regulation of transthyretin and alpha 1-antitrypsin genes.* Mol Cell Biol, 1989. **9**(4): p. 1415-25.
143. Bookout, A.L., et al., *Anatomical profiling of nuclear receptor expression reveals a hierarchical transcriptional network.* Cell, 2006. **126**(4): p. 789-99.
144. Stevens, R.L., et al., *Strain-specific and tissue-specific expression of mouse mast cell secretory granule proteases.* Proc Natl Acad Sci U S A, 1994. **91**(1): p. 128-32.
145. Liu, Y., D. Ma, and C. Ji, *Zinc fingers and homeoboxes family in human diseases.* Cancer Gene Ther, 2015. **22**(5): p. 223-6.
146. Zhang, Y., E.V. Laz, and D.J. Waxman, *Dynamic, sex-differential STAT5 and BCL6 binding to sex-biased, growth hormone-regulated genes in adult mouse liver.* Mol Cell Biol, 2012. **32**(4): p. 880-96.
147. Bonzo, J.A., et al., *Suppression of hepatocyte proliferation by hepatocyte nuclear factor 4alpha in adult mice.* J Biol Chem, 2012. **287**(10): p. 7345-56.
148. Squires, E.J. and M. Negishi, *Tissue-specific regulation of cytochrome P-450 dependent testosterone 15 alpha-hydroxylase.* Can J Physiol Pharmacol, 1990. **68**(6): p. 769-76.
149. Kim, J.S., et al., *Methionine adenosyltransferase:adrenergic-cAMP mechanism regulates a daily rhythm in pineal expression.* J Biol Chem, 2005. **280**(1): p. 677-84.
150. Turgeon, B. and S. Meloche, *Interpreting neonatal lethal phenotypes in mouse mutants: insights into gene function and human diseases.* Physiol Rev, 2009. **89**(1): p. 1-26.
151. Writing Group, M., et al., *Heart Disease and Stroke Statistics-2016 Update: A Report From the American Heart Association.* Circulation, 2016. **133**(4): p. e38-60.
152. Blaak, E., *Gender differences in fat metabolism.* Curr Opin Clin Nutr Metab Care, 2001. **4**(6): p. 499-502.
153. Hung, M.C. and W. Link, *Protein localization in disease and therapy.* J Cell Sci, 2011. **124**(Pt 20): p. 3381-92.
154. Hirano, S., et al., *Rat zinc-fingers and homeoboxes 1 (ZHX1), a nuclear factor-YA-interacting nuclear protein, forms a homodimer.* Gene, 2002. **290**(1-2): p. 107-14.
155. Cozzetto, D., et al., *Evaluation of template-based models in CASP8 with standard measures.* Proteins, 2009. **77 Suppl 9**: p. 18-28.
156. Kawata, H., et al., *The mouse zinc-fingers and homeoboxes (ZHX) family; ZHX2 forms a heterodimer with ZHX3.* Gene, 2003. **323**: p. 133-40.
157. Hateboer, G., et al., *BS69, a novel adenovirus E1A-associated protein that inhibits E1A transactivation.* EMBO J, 1995. **14**(13): p. 3159-69.
158. Nix, D.A. and M.C. Beckerle, *Nuclear-cytoplasmic shuttling of the focal contact protein, zyxin: a potential mechanism for communication between sites of cell adhesion and the nucleus.* J Cell Biol, 1997. **138**(5): p. 1139-47.

159. Clements, K.M., et al., *Maternal socio-economic and race/ethnic characteristics associated with early intervention participation.* Matern Child Health J, 2008. **12**(6): p. 708-17.
160. Amador-Noguez, D., et al., *Gene expression profile of long-lived Ames dwarf mice and Little mice.* Aging Cell, 2004. **3**(6): p. 423-41.
161. Brown, T.R., C.W. Bardin, and F.E. Greene, *Mouse liver N-demethylase activity. Sex differences and androgen responsiveness.* Pharmacology, 1978. **16**(3): p. 159-69.
162. Eacho, P.I. and H.D. Colby, *Regional distribution of microsomal drug and steroid metabolism in the guinea pig adrenal cortex.* Life Sci, 1983. **32**(10): p. 1119-27.

VITA

Minen Al-Kafajy

Educations:

Department of Microbiology, Immunology and Molecular genetics, College of medicine, University of Kentucky

PhD candidate Fall 2011- Present

Department of biology, College of Science, Basra, Iraq

M.Sc. in clinical Immunology November, 2003-August, 2006

College of health and medical technology, Baghdad, Iraq

B.Sc. November, 1997-June, 2001

Professional Experience:

Department of Microbiology, Immunology, and Molecular genetics, College of Medicine, University of Kentucky Lexington, Kentucky, USA.

Research Assistant Fall 2011-Fall 2016

Center for English as a second language (CESL), College of Arts and science, University of Kentucky Lexington, Kentucky, USA.

English certificate Fall 2010-Summer 2011

University of Thi-Qar, Summer College, Thi-Qar, Iraq

Lecturer Assistant January 2008-Present

Shatra hospital, Clinical laboratory analysis, Ministry of health, Thi-Qar, Iraq

November 2001- January 2008

Awards and Scholarships:

Higher Committee for Education development (HCED), Baghdad, Iraq

Fall 2010-Fall 2016

Nominate a recipient for teacher who made a difference prize.

Spring 2016

Center for Center for English as a second language (CESL) Star Student award, College of Arts and science, University of Kentucky Lexington, Kentucky, USA.

Fall 2016

Markey Cancer Center travel awards, College of Medicine, University of Kentucky Lexington, Kentucky, USA.

Spring 2015

Languages:

Arabic and English

Professional affiliation:

American Association For The Advancement Of Science (AAAS).

American Society for Biochemistry and Molecular biology (ASBMB).

Posters:

RNA Nanotechnology meeting, Gordon Research Conferences, Ventura, California. Title: Zhx2: a novel gene regulator in mice. Minen Al-Kafajy, Xin Lu, Jieyun Jiang, Martha L. Peterson and Brett T. Spear.

Spring, 2015

Markey Cancer Research, Lexington, Kentucky. Title: Zhx2: a novel gene regulator in mice. Minen Al-Kafajy, Xin Lu, Jieyun Jiang, Martha L. Peterson and Brett T. Spear.

Spring, 2015

Microbiology Immunology, and Molecular genetics department retreat, Lexington, Kentucky. Title: Zhx2: a novel gene regulator in mice. Minen Al-Kafajy, Xin Lu, Jieyun Jiang, Martha L. Peterson and Brett T. Spear.

Spring, 2015

Markey Cancer Research, Lexington, Kentucky. Title: Zhx2 regulate genes in mouse hepatic and non-hepatic tissue and influence cellular Zhx3 localization. Minen Al-Kafajy, Martha L. Peterson and Brett T. Spear.

Spring, 2016

Microbiology Immunology, and Molecular genetics department retreat, Lexington, KY. Title: Zhx2 regulate genes in mouse hepatic and non-hepatic tissue and influence cellular Zhx3 localization. Minen Al-Kafajy, Xin Lu, Jieyun Jiang, Martha L. Peterson and Brett T. Spear. Spring, 2016

Presentation:

Microbiology Seminars RNA transcript as a miRNA decoy; a non-canonical function in cancer.

Fall, 2013

Microbiology Seminars Zhx2 regulation of target genes in the liver and non-hepatic tissues: Insight from BALB/c mice substrains.

Spring, 2015

Expression of Zinc fingers and homeoboxes 2 (Zhx2) and Zhx2 target genes in multiple tissues of wild-type and Zhx2 knockout mice

Fall, 2016